

**UCSF**

**UC San Francisco Electronic Theses and Dissertations**

**Title**

Candida albicans morphology and commensal fitness in the mammalian gut

**Permalink**

<https://escholarship.org/uc/item/9gc348tz>

**Author**

Penumetcha, Pallavi

**Publication Date**

2018

Peer reviewed|Thesis/dissertation

Candida albicans morphology and commensal fitness in the  
mammalian gut

by

Pallavi Penumetcha

DISSERTATION

Submitted in partial satisfaction of the requirements for the degree of

DOCTOR OF PHILOSOPHY

in

Biomedical Sciences

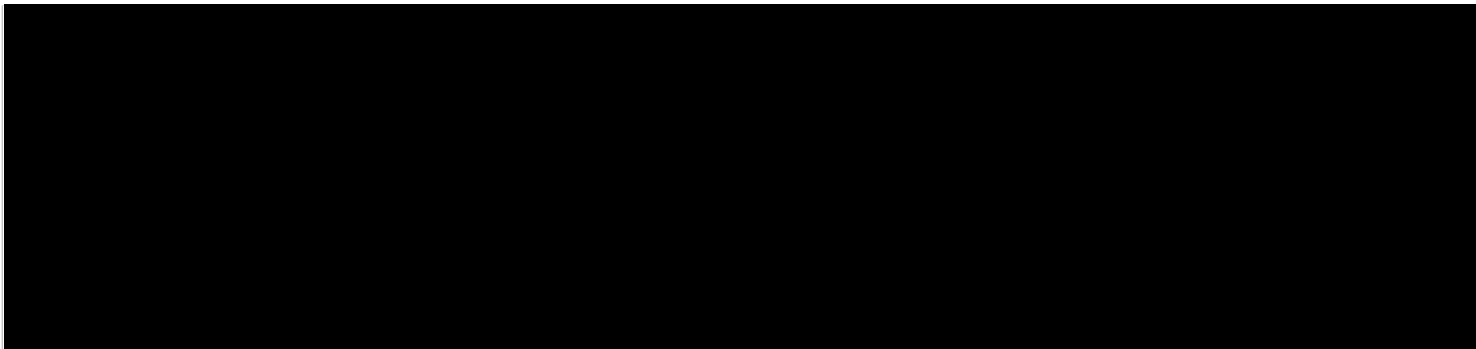
in the

GRADUATE DIVISION

of the

UNIVERSITY OF CALIFORNIA, SAN FRANCISCO

Approved:



Committee in Charge

Copyright 2018  
by  
Pallavi Penumetcha

## **ACKNOWLEDGEMENTS**

I would first like to thank Suzanne Noble for being a patient and knowledgeable mentor. I have learned so much from being under your guidance. I have also received immeasurable support from the members of my thesis committee: Anita Sil, Shaeri Mukherjee and Susan Lynch. I thank each of you for your intellectual guidance and words of encouragement. I would also like to thank the other members of the Noble Lab for your expertise and collaborative nature. Specifically, I would like to thank Brittany Gianetti and Nina Abon who were not only exceptional scientists, but also the truest of friends. To the multitude of friends and family who have supported me throughout this journey, I, quite simply, would not have made it here with you all. I am so unbelievably lucky to have each and every one of you in my life. Finally, to the two people who have been the ultimate pillars of support, my parents. Amma and Nannagaru, all of the good things in my life are because of your inherent patience, kindness and willingness to let me explore, learn and grow. Thank you for giving me the ultimate gift of family and friends that I can always count on.

## **PUBLICATIONS AND CONTRIBUTIONS**

-*Chapter I* contains text written by myself with editing input from Suzanne Noble.

-*Chapter II* contains texts and figures from a manuscript that has been “accepted in principle” by Cell Host and Microbe. Jessica Witchley, Suzanne Noble and myself conceived experiments, Jessica and I contributed equally the experimental work, figure construction and are co-first authors on the manuscript. Jessica performed the experiments for Figures 1, 2 and 5, and I performed the experiments for Figures 3, 4 (NanoString was performed by Aaron Mitchell’s lab at Carnegie Mellon), and 6. Suzanne wrote the manuscript with editing input from Jessica and myself. The FISH protocol was developed with the help of Carolina Tropini (Sonnenburg Laboratory) and Katharine Ng (Huang Laboratory) at Stanford University. Susan Lynch’s lab at UCSF also helped with aspects of developing the FISH assay. Supplementary Tables and Figures can be found in the published manuscript.

-*Chapter III* contains text and figures from a manuscript that is in preparation, written by myself with input from Jessica Witchley and Suzanne Noble. Jessica Witchley conducted experiments in Figure 3.2 and Table 3.1. Cedric Brimacombe made important initial observations that informed the direction of the project. I conceived, designed and performed the remainder of the experiments. Andrew Koh’s laboratory at the University of Texas Southwestern performed the microbial qPCR in Figure 3.2C.

-*Chapters IV, V and VI* contain data and text conceived, performed and written by myself, with input and guidance from Suzanne Noble.

# ***Candida albicans* morphology and commensal fitness in the mammalian gut**

Pallavi Penumetcha

## **ABSTRACT**

While *C. albicans* has largely been studied as a pathogen, its primary role is a commensal of the gastrointestinal tract. Overall, the fungal components of the GI microbiome are less well studied than the bacterial members, despite fungi making up a significant portion of the commensal microbiota. Understanding *C. albicans*' role in the GI niche will provide important insights into fungal GI commensalism.

My studies investigate the role that filamentation plays in gut commensalism. *C. albicans* filamentation has previously been characterized as an important part of the pathogenic lifestyle of the fungus, but the role of hyphae in GI commensalism is unclear. We show that the *C. albicans* filamentation program is detrimental to commensal colonization, as mutants of pro-filamentation transcription factors are hyperfit in the gut. Interestingly, however, we find that hyphae are present throughout the gut. Because hyphae themselves are not detrimental to commensalism, we hypothesize that expression of hyphal specific genes mediates regulation of the commensal population. Indeed, we find that mutants of hyphal specific cell surface proteins, like Sap6, are hyperfit in the GI tract, suggesting that cell type specific markers, rather than cell shape, mediate commensal fitness.

We also find that *C. albicans*' interactions with other members of the microbiota, namely *Lactobacilli*, are important mediators of commensal fitness. Our lab previously discovered a novel phenotypic form of *C. albicans*, termed GUT cells, which are specialized for commensalism. Surprisingly, mice naturally colonized with high levels of

*Lactobacillus spp.* antagonize the GUT cell commensal advantage. GUT cells, which are normally less responsive to classic filamentation cues as compared to white cells, filament robustly in the presence of *Lactobacillus* species *in vitro*. As we know that filamentation is detrimental to commensal, we hypothesized that *Lactobacillus*-GUT cell interactions reverse the competitive advantage of GUT cells. Indeed, we find that pre-colonizing mice with high levels of *Lactobacillus*, antagonizes recovery of GUT cells from GI tract.

Taken together, these studies help us understand how *C. albicans* phenotypic transitions and interactions with other members of the gut microbiota influence commensal colonization in the mammalian GI tract.

# TABLE OF CONTENTS

<b>CHAPTER I: INTRODUCTION.....</b>	<b>1</b>
<b>CHAPTER II: A TRADEOFF THAT CONTROLS THE BALANCE BETWEEN GUT COMMENSALISM AND INVASIVE INFECTION BY <i>CANDIDA ALBICANS</i>.....</b>	<b>7</b>
Abstract.....	7
Introduction.....	7
Results.....	11
Discussion.....	22
Methods.....	27
<b>CHAPTER III: <i>LACTOBACILLUS PLANTARUM</i> COUNTERACTS GASTROINTESTINAL COMMENSAL ADVANTAGE OF <i>CANDIDA ALBICANS</i> GUT CELLS.....</b>	<b>58</b>
Abstract.....	58
Introduction.....	58
Results.....	62
Discussion.....	71
Methods.....	74
<b>CHAPTER IV: HYPHAL SPECIFIC CELL SURFACE PROTEINS AND THEIR ROLE IN GI COMMENSALISM.....</b>	<b>94</b>
Methods.....	96
<b>CHAPTER V: DETERMINING THE GI COMMENSAL NICHE OF <i>C. ALBICANS</i> GUT CELLS.....</b>	<b>103</b>
Methods.....	107



<b>CHAPTER VI: CONCLUSIONS.....</b>	<b>112</b>
<b>REFERENCES.....</b>	<b>115</b>

## LIST OF TABLES

Table 2.S1-Strains used in this chapter.....	56
Table 3.1-Summary of mRNA-seq data for mice co-colonized with <i>C. albicans</i> and <i>L. plantarum</i> .....	92
Table 3.S1. <i>C. albicans</i> strains used in this chapter.....	93
Table 3.S2. Bacterial species used in this chapter.....	93
Table 4.S1. Strains used in this chapter.....	102
Table 5.S1 Strains used in this chapter.....	111

## LIST OF FIGURES

Figure 2.1. Activators of <i>C. albicans</i> filamentation inhibit commensal fitness in the mammalian gut.....	38
Figure 2.2. <i>efg1</i> , <i>brg1</i> , <i>rob1</i> , <i>tec1</i> and <i>ume6</i> mutants exhibit enhanced commensal fitness, but a <i>UME6</i> -overexpression strain has reduced fitness.....	39
Figure 2.3. <i>C. albicans</i> colonizes the gut as mixed population of yeasts and hyphae....	41
Figure 2.4. NanoString reveals induction of hypha-associated and pH-responsive genes in the gut.....	43
Figure 2.5. mRNA-seq reveals that a subset of hypha-associated genes are controlled by Ume6 in the gut.....	45
Figure 2.6. Hypha-associated secreted and cell surface proteins inhibit GI commensalism.....	47
Figure 2.S1. Validation of commensalism phenotypes of transcription factor mutants using independent isolates.....	49
Figure 2.S2. Assessment of competitive fitness of strains recovered directly from the host.....	50
Figure 2.S3. <i>ume6</i> and <i>sap6</i> mutants colonize the mammalian GI tract to similar levels as WT.....	51
Figure 2.S4. <i>ume6</i> is defective for filamentation <i>in vitro</i> but <i>sap6</i> displays normal filamentation.....	52
Figure 2.S5. Propagation within the host GI tract suppresses the filamentation defect of <i>tec1</i> but not <i>efg1</i> , <i>brg1</i> , or <i>rob1</i> .....	54

Figure 2.S6. <i>SAP6</i> expression is downregulated in commensally propagated <i>efg1</i> , <i>brg1</i> , <i>rob1</i> , and <i>tec1</i> mutants.....	55
Figure 3.1. GUT cells have a reduced response to classic filamentation cues <i>in vitro</i> and <i>in vivo</i> .....	78
Figure 3.2. Commensal fitness advantage of GUT cells is lost in mice with high abundance of <i>Lactobacillus spp.</i> .....	80
Figure 3.3. GUT cells are not recovered from Hollister mice colonized with <i>Lactobacillus plantarum</i> .....	82
Figure 3.4. GUT cells are filamentous were co-cultured with <i>L. plantarum</i> .....	83
Figure 3.5. GUT cells do not filament when co-colonized with <i>L. plantarum</i> .....	84
Figure 3.6. GUT cell filamentation is dependent on <i>L. plantarum</i> lactate dehydrogenase genes.....	85
Figure 3.S1. GUT cells display low levels of filamentation in all compartments of the GI tract.....	87
Figure 3.S2. <i>L. plantarum</i> is the most resistance <i>Lactobacillus spp.</i> to streptomycin....	89
Figure 3.S3. <i>Lactobacillus</i> -induced GUT cell filamentation is specific to certain species of <i>Lactobacilli</i> .....	90
Figure 3.S4. <i>Lactobacillus</i> -induced GUT cell filamentation is dose-dependent on the amount of <i>L. plantarum</i> present.....	91
Figure 4.1. Hyphal cell surface proteins predominate as negative regulators of commensalism.....	98
Figure 4.2. <i>ALS3</i> is a negative regulator of GI commensalism, but <i>ECE1</i> 's role remains unclear.....	100

Figure 5.1. *Wor1p* expression and GUT cell formation appears to be sequential along the GI tract.....109

Figure 5.2. BirA\* promiscuously biotinylates proteins in *C. albicans*.....110

## CHAPTER I: INTRODUCTION

*C. albicans* is the most common human fungal pathogen, but primarily colonizes the human body as a commensal in approximately 70% of humans<sup>1</sup>. Its remarkable phenotypic plasticity allows it to colonize a wide variety of niches in humans such as the gastrointestinal (GI) tract<sup>2</sup>, oropharyngeal cavity<sup>3</sup>, skin<sup>4</sup> and vagina<sup>5</sup>. Here, we focus on the role that phenotypic plasticity plays in *C. albicans*' colonization of its primary commensal reservoir, the GI tract.

*C. albicans*' status as a prominent and prevalent member of the human gastrointestinal tract necessitates understanding its primary role as a commensal. Most work in the field has focused on *C. albicans*' role as a pathogen because of its rank among the top four most common cause of invasive bloodstream infections in US hospitals<sup>6</sup>. *C. albicans*' role as a quiescent commensal, however, may be just as important given its potential in maintaining GI mucosal health.

In humans, the contribution of the mycobiome (fungal commensals) to the gut commensal population, has been greatly overshadowed by the microbiome (bacterial commensals). Extensive studies of the bacterial microbiome have revealed the importance of these organisms in various aspects of human health, most notably development of the mucosal immune system<sup>7</sup>. While fungi compose a minority of the organisms in our GI tract and many of them are un-culturable, their significantly larger size compared to bacteria surely makes them a large portion of the overall microbial biomass in the gut<sup>8</sup>.

Indeed, improving culture and sequencing methods have revealed that a diverse population of fungi exists in the GI tract: anywhere from 60-85 fungal genera have been

isolated from the healthy human gut<sup>3,9</sup>. Among these, *C. albicans* is the most commonly detected<sup>10</sup>. While better sequencing technology has increased our understanding of the composition of fungal gut commensals, relatively few studies have investigated whether or not these organisms play a commensal role akin to their bacterial counterparts. Recent reports have, however, shown that fungi, like bacteria are involved in maintaining and promoting GI health. *C. tropicalis*, *C. albicans*' close cousin, plays a role in developing secondary lymphoid organs of mice.<sup>11</sup> *C. albicans* itself has been shown to promote development of the Th17 compartment of gastrointestinal mucosal immune system in mice<sup>12</sup>, similar to certain bacterial species. Therefore, understanding fungal commensalism is critical for gaining a holistic picture of gastrointestinal homeostasis and *C. albicans* commensalism merits further study.

*C. albicans*' success as both a commensal and a pathogen is likely due to its phenotypic plasticity. Fungi, in general, are known for existing in a great diversity of morphological forms, ranging from the micrometer-sized intracellular pathogens of the microsporidia family, to the multi-kilometer *Armillaria ostoyae*, a tree pathogen that is among the largest living organisms in the world<sup>13,14</sup>. Unlike many other fungal pathogens, such as *Histoplasma capsulatum*, *Aspergillus* species and *Cryptococcus neoformans*, which have environmental niches, *C. albicans* has only been isolated from mammalian hosts<sup>1</sup>. Therefore, its phenotypic plasticity underscores its unique adaptation to survive in multiple niches within the human host.

Of the nine described phenotypic forms of *C. albicans*, four are essential to this work and described below. *C. albicans*' standard phenotype is round to oval shaped yeasts, which form white-domed colonies on plates. White phase yeasts are unicellular

and found in multiple niches as commensal organisms, but are also found in the peripheral organs and the bloodstream in mouse models of disseminated disease<sup>15</sup>. Until recently, white cells were thought to be the commensally specialized cell type. Previous studies in our laboratory, however, found that a different “yeast-like” morphotype of *C. albicans*, termed GUT cells, are actually specialized for commensalism<sup>16</sup>. GUT cells exist as elongated yeasts and form darker, flatter colonies on plates. These cells are hypercompetitive in one to one competitions with wild-type in a mouse model of GI commensalism, and exhibit a reorganized metabolism primed for survival in the gut. GUT cells were first identified in *C. albicans* that constitutively expresses the transcription factor *Wor1* after passage through the mammalian GI tract. Both high levels of *Wor1* expression and host signals are required for the GUT switch to take place, but *Wor1* stabilizes this phenotype outside of the body, in the absence of host signals.

Another yeast-like phenotype is the opaque cell, which, like the GUT cell, has an elongated cell shape that forms dark colonies on plates. Unlike GUT cells, however, opaque cells contain pimple-like structures on their cell surface<sup>17</sup>, are specialized for mating<sup>18</sup> and are commensals of the skin<sup>1</sup>. This transition occurs in response to low temperature (25°C), the presence of *N*-acetylglucosamine and acidic pH<sup>19</sup>.

Finally, the third common phenotypic transition results in filamentous hyphae. In response to signals such as high temperature (37°C), presence of serum and an alkaline pH<sup>19</sup>, round yeast transition to multicellular structures whereby daughter cells remain attached to parent cells and elongate to form tube like structures. These cells are thought to be specialized for virulence both because of their physical structure (the



elongated cell structure is thought to allow hyphae to penetrate epithelial cell layers,) and their expression of multiple genes associated with virulence such as adhesins (HWP1, HYR1 and ALS3)<sup>20,21</sup>, proteases (SAP6)<sup>22</sup> and a recently described toxin (ECE1)<sup>23</sup>. Mutants of hyphal promoting transcription factors are defective in filamentation *in vitro* and are less virulent in animals models of pathogenesis<sup>24</sup>.

As phenotypic plasticity is a critical part of the *C. albicans*' lifestyle, understanding the role that phenotypic transitions play in commensal colonization is crucial for understanding how the GI commensal population is maintained. Previous studies investigating the phenotypic form of *C. albicans* in the mammalian gut have concluded that it primarily colonizes in the yeast form<sup>25,26</sup>. Interestingly, however, RNA analysis has revealed that genes associated with hyphal development are also upregulated in this niche<sup>27</sup>. These two seemingly disparate conclusions have been rationalized with the idea that yeasts may express these stereotypically "hyphal" genes in the gut because they may be beneficial for commensal interactions with the host. The majority of these studies, however, only assay a portion of the gut (i.e. small intestines and cecum), when the GI tract is made up of numerous highly specialized environmental niches that have the potential to generate a great diversity of phenotypes. Therefore, holistic studies along the length of the gut are necessary to truly understand how *C. albicans*' morphotypes, and associated phenotype specific gene expression, affects the commensal population.

In addition to *C. albicans*' self-regulation of morphogenesis in different environmental conditions, other members of the microbiome are also critical to this process. It is well known that prolonged antibiotic exposure in humans can lead to

candidiasis<sup>28</sup>, and that antibiotic treatment in mice allows for *C. albicans* colonization<sup>29</sup>, which mice are naturally resistant to. These observations clearly demonstrate that bacterial-fungal interactions are important mediators of commensal colonization. In the gastrointestinal tract, the relationships between *C. albicans* and a variety of bacterial species have primarily been characterized as bi-directionally antagonistic. For example, exposure to *B. thetaioamicron* or *B. producta* eliminates any colonizing *C. albicans* in the gut<sup>30</sup>, and colonization with *C. albicans* post antibiotic treatment prevents resurgence of *Lactobacillus spp.* that were present prior to antibiotic administration<sup>31</sup>. Not only are bacterial species antagonistic towards colonization, but multiple bacteria species commonly found in the GI tract such as *E. faecalis*, *E. coli*, and *Salmonella spp.* have evolved mechanisms to inhibit hyphal formation, or kill filaments<sup>32</sup>. The ability to affect hyphal morphogenesis is not limited to gut associated bacterial species, but has also been observed with *S. maracens*<sup>33</sup>, *P. aeruginosa*<sup>34</sup>, *B. cenocepacia*<sup>35</sup>, and *S. mutans*<sup>36</sup>. Bacterial species are clearly important mediators of *C. albicans* morphogenesis and commensal colonization, but all of these studies have been performed with the white phenotypic form of *C. albicans*, and not the GI-adapted GUT cell. To truly understand how bacteria influence *C. albicans* GI commensalism, it is necessary to elucidate how bacteria affect GUT cells.

The mammalian gastrointestinal tract is a complex environment that contains multiple microenvironments within it. *C. albicans*' abundance in this niche suggests that it has evolved unique mechanisms to promote persistent commensal colonization. Understanding how *C. albicans* establishes and maintains its presence in its primary commensal reservoir is critical to better understand the commensal role of fungi in the

gut. In the studies presented here, we seek to understand how morphology specific gene expression and interactions with other members of the commensal microbiome influences maintenance of the gastrointestinal commensal population of *C. albicans*.

## CHAPTER II: A TRADEOFF THAT CONTROLS THE BALANCE BETWEEN GUT COMMENSALISM AND INVASIVE INFECTION BY *CANDIDA ALBICANS*

### ABSTRACT

*Candida albicans* is a human gut commensal and an opportunistic pathogen. The ability to transition from yeasts to invasive hyphae is a central virulence attribute, but it is unclear how these two cell types function during commensal growth. Using FISH to visualize *C. albicans* in a murine gut colonization model, we observed the co-occurrence of yeasts and hyphae throughout the gastrointestinal tract. Forward genetic analysis revealed that major transcriptional activators of yeast-to-hypha morphogenesis have unexpected activity as potent inhibitors of commensalism. *In vivo* FISH, transcriptomic, and genetic analyses indicate that the morphogenesis program inhibits commensal fitness, not through control of cell shape as expected from *in vitro* studies, but by activating expression of a hypha-specific pro-inflammatory secreted protease and a hyphal cell surface adhesin. These results reveal a tradeoff between fungal programs supporting commensalism and virulence within the commensal niche in which selection against hypha-specific markers limits the disease-causing potential of this ubiquitous commensal-pathogen.

### INTRODUCTION

As the most common fungal pathogen of humans, *Candida albicans* is responsible for hundreds of millions of symptomatic infections each year<sup>6,37,38</sup>. Disease syndromes range from treatable infections of skin and mucous membranes to highly

morbid, invasive infections of the blood and internal organs<sup>6,38</sup>. However, the vast majority of *C. albicans*-host interactions are asymptomatic, as this fungus is a normal component of the human gut microbiota. Most individuals are colonized in childhood, and the infecting clones are thought to persist quiescently over a lifetime<sup>39</sup>.

Colonization may even confer benefits to the host, as experimental studies in gnotobiotic mice have shown that monoassociation with *C. albicans* is sufficient to stimulate development of the mucosal immune system, as has previously been shown for selected bacterial species<sup>12</sup>. How *C. albicans* mediates such diverse interactions with its hosts is an area of ongoing investigation.

Decades of study have highlighted the central role of yeast-to-hypha morphogenesis in *C. albicans* pathogenesis<sup>1</sup>. Whereas the yeast form predominates under standard *in vitro* culture conditions, introduction of this organism into animal models of disease or exposure to host-associated cues in the laboratory triggers a transition to hyphae. In contrast to yeasts, highly elongated hyphal cells remain attached after cell division and produce multicellular, branching, filamentous networks. Hyphae are naturally invasive and penetrate through agar-based media *in vitro* and epithelial and endothelial barriers within the host. Hyphae also express cell type-specific virulence factors such as degradative enzymes (for example, the Sap family of secreted aspartyl proteases), cell surface adhesins (for example, Als3, Hwp1, and Hyr1), and the pore-forming toxin, Candidalysin<sup>21-23,40-42</sup>. Yeast-to-hypha morphogenesis is controlled by an environmentally-responsive gene regulatory cascade, the hyphal gene regulatory network. Mutants defective in this network display defects in multiple animal models of virulence<sup>24</sup>.

While hyphae are clearly important for *C. albicans* disease, roles for hyphae and yeasts in commensalism are less well defined. The mammalian digestive tract is replete with signals that trigger yeast-to-hypha morphogenesis in the laboratory, such as hypoxia<sup>43,44</sup>, hypercarbia<sup>43,45</sup>, and N-acetylglucosamine<sup>46</sup>. Consistent with the presence of hyphae in this niche, investigators have detected expression of certain hypha-associated genes in animal models of gut colonization<sup>25,27</sup>. However, based on direct visualization of organisms washed from the intestines of colonized mice, two groups reported that yeasts compose more than 90% of the commensal fungal population<sup>26,25</sup>. A third group recently analyzed the abundance of yeast-like vs. hypha-like shapes in sectioned intestines of mice colonized with *C. albicans*<sup>47</sup>. These authors observed a substantial population of hypha-like shapes (~70%) in conventionally reared animals, whereas yeast-like shapes predominated (~90%) in gnotobiotic animals after monoassociation with *C. albicans*. To date, no study has quantified the relative number of *C. albicans* yeasts and hyphae *in situ* (e.g. by FISH or immunostaining) or their relationships to host anatomy.

To gain insight into commensal interactions between *C. albicans* and mammalian hosts, we performed competitive infections of ~650 *C. albicans* homozygous gene disruption mutants in a mouse model of stable gastrointestinal colonization. Null mutants affecting four transcriptional activators of the hyphal gene regulatory network displayed hypercompetitive phenotypes, suggesting an unanticipated role for the morphogenesis program in limiting commensal fitness. A newly engineered mutant affecting Ume6, a 'master regulator' of filamentation, also outcompeted wild-type *C. albicans* in the commensal model, whereas a Ume6-overexpression strain was itself

outcompeted by wild type. To determine whether the fitness advantage of morphogenesis pathway mutants correlates with altered cell morphology, we developed a fluorescence *in situ* hybridization (FISH) technique to visualize *C. albicans* in host tissues. Wild type was found to colonize the gut as a mixed population of yeasts and hyphae, with yeasts predominating in proximal segments (stomach and small intestines) and hyphae predominating more distally. Surprisingly, the *ume6* deletion mutant was morphologically indistinguishable from wild type in this host niche, in contrast to its strong filamentation defect under *in vitro* conditions. These results indicate that at least one fungal morphogenesis factor can substitute for Ume6 in commensally propagated strains, and argues that cell morphology *per se* is not responsible for the hypercommensal phenotype of Ume6. Using mRNA-Seq to determine the transcriptomes of commensally-propagated wild-type and *ume6* strains, we identified ~50 hypha-associated genes that require Ume6 for normal expression in this niche. Remarkably, disruption of one of these genes, encoding a hypha-specific secreted aspartyl protease that is known to elicit pro-inflammatory host responses from host immune cells (Sap6<sup>48-51</sup>), suffices to confer a commensal fitness advantage resembling that of cells lacking Ume6, whereas overexpression of *SAP6* confers a reduced fitness phenotype. Thus, expression of Sap6 and other hypha-specific genes, an asset for tissue invasion, is a liability for successful commensalism. We propose that this antagonistic relationship is central to the balance achieved by *C. albicans* between commensal and pathogenic infection of mammals.

## RESULTS

### Identification of four *Candida albicans* mutants with enhanced commensal fitness

We previously reported the construction of two libraries of *C. albicans* homozygous gene disruption strains, which together comprise more than 650 unique mutants<sup>52,53</sup>.

Because the *C. albicans* genome is diploid, two selectable markers (*Candida dubliniensis HIS1* and *Candida maltosa LEU2*) were used to replace the two alleles of each target ORF. In addition, each mutant was barcoded with one of 48 oligonucleotide sequences to allow for quantitation of individual strains in pools of up to 48. The number of barcodes was selected based on the maximum number of strains that can be co-infected in a mouse tail vein model of virulence without stochastic loss.

To facilitate screens of larger pools of mutants, we recently developed a protocol to sequence short regions of genomic DNA that abut the *C.d.HIS1* selectable marker. Because this marker replaces the disrupted ORF in each mutant, the neighboring genomic sequences are distinct and can serve as functional ‘barcodes.’ As described in the Methods, genomic sequences of interest are amplified by linear PCR, following by high-throughput sequencing. The relative abundance of each mutant in a pool is calculated from the abundance of its ORF-flanking sequences among all the sequencing reads.

We used this method to quantify the competitive fitness of ~650 *C. albicans* mutants in a mouse model of persistent gastrointestinal (GI) commensalism (Figure 2.1). Mutants and an isogenic wild-type control strain (SN250) were propagated individually in liquid culture (YPD fungal medium), then pooled and washed in sterile saline. The pooled inoculum was introduced directly into the digestive tract of three



immunocompetent BALB/c mice by gavage. Because the commensally colonized animals remain healthy, serial analysis of feces could be used to monitor the progress of the competition. Yeasts from the inocula (“I”) and following recovery from feces after 3-5 and 10 days of colonization (“R”) were plated on Sabouraud agar (with ampicillin and gentamicin), and sequencing libraries were prepared from genomic DNA as described above. The competitive index of each strain was defined as the  $\log_2$  function of relative strain abundance in the recovered pool compared to the inoculum. The results of our initial screen (“Screen 1”) are presented in Figures 2.1, 2.1, and Table 2.S1. Figure 2.1 depicts the competitive index of every strain in a single, representative animal. Here, the *efg1* mutant (shown in red) outcompeted every other mutant (gray) as well as wild-type *C. albicans* (WT, black). As shown in Figure 2.1, the hypercompetitive phenotype of *efg1* was reproduced in all three colonized animals. The emergence of *efg1* as a dominant strain was not unexpected, as enhanced fitness phenotypes of *efg1* have previously been observed in smaller studies<sup>16,54,55</sup>. To identify additional commensalism factors, we repeated the screen using an inoculum prepared without the *efg1* mutant. As shown in Figure 2.1 and Table 2.S2 (“Screen 2”), the second screen identified two additional hyperfit mutants, *brg1* and *rob1*. This result was unexpected because previous screens of the mutant collection in a disseminated infection model had identified only loss-of-fitness mutants<sup>47,53</sup>. Unfortunately, the presence of hyperfit strains distorts the abundance of other strains in pooled infections and precludes the ability to identify mutants with attenuated fitness. We reasoned that, if Efg1, Brg1, and Rob1 were the only gain-of-fitness mutants present in our library, then co-infection with the remaining strains might identify ones with loss-of-fitness phenotypes (suggestive of

pro-commensalism functions of the disrupted genes). As shown in Figure 2.1 and Table 2.S3, however, a third screen (“Screen 3”) of all of the mutants except for *efg1*, *brg1*, and *rob1* identified *tec1* as a fourth hyperfit mutant. The identification of four mutants with gain-of-fitness phenotypes suggests that there are far more negative regulators of *C. albicans* commensalism than of virulence.

### **Transcriptional activators in the filamentation program inhibit commensalism in the gut**

Remarkably, all four mutants identified in our gut commensalism screens affect transcription factors with previously described roles in *C. albicans* filamentation<sup>43,52,56-59</sup> and virulence<sup>57,59,60</sup>. As depicted in Figure 2.1, Efg1, Rob1, Brg1, and Tec1 all activate genes associated with filamentation<sup>43,58,61,62</sup>. In addition, Efg1, Brg1, and Tec1 have been shown to promote filamentation indirectly via the ‘master regulator’, Ume6<sup>58,61,63</sup>. Mutants lacking *EFG1*, *BRG1*, *ROB1*, *TEC1*, or *UME6* are defective for filamentation *in vitro*<sup>52,56,57,59,60,64</sup>, and *efg1*, *brg1*, *tec1*, and *ume6* also display virulence defects in the mouse tail vein model of disseminated infection<sup>57,59,60,64</sup>.

Our independent identification of four activators of filamentation in a gut colonization screen suggested a possible, unanticipated role for this program in the regulation of commensal fitness. To validate these results, we retested two independent isolates of each mutant in 1:1 competitions with wild type in the murine GI commensalism model (Figure 2.2). The competitive fitness of each strain was evaluated over a ≥25-day time course using qPCR with primers specific to each strain. As shown in Figure 2.2 and Figure 2.S1, the enhanced commensalism phenotypes

were reproduced in every case. To validate the use of stool samples as a proxy for strain abundance in the host digestive tract, we also analyzed samples obtained directly from animals after euthanasia. As shown for *brg1*, *rob1*, and *tec1* in Figure 2.S2, results obtained using tissues, luminal contents, or entire segments (tissue plus contents) recovered from different GI compartments closely mimic results obtained using feces.

As a final test, we generated mutants affecting Ume6, which was not represented in the original mutant collection. Ume6 is the terminal transcriptional activator in the hyphal gene regulatory network (Figure 2.1) and is therefore considered to be most specific to morphogenesis. When competed 1:1 against wild-type *C. albicans*, *ume6* gene disruption mutants exhibit enhanced fitness in the GI commensalism model (Figure 2.2 and Figure 2.S1), similar to the phenotype of other filamentation pathway mutants. In contrast, a *UME6*-overexpression strain (*UME6*<sup>OE</sup>) exhibits reduced fitness (Figure 2.2 and Figure 2.S1). Of note, competition experiments expose differences that are difficult to appreciate when strains are evaluated in isolation. For example, wild type and *ume6* strains colonize the GI commensalism model to similar levels when tested individually (Figure 2.S3), in contrast to their pronounced differences when evaluated in competition. Taken together, these findings indicate that the well-characterized *C. albicans* filamentation program inhibits commensal fitness in the mammalian gut.

### ***C. albicans* colonizes the gastrointestinal tract as a mixed population of yeasts and hyphae**

Given previous reports that *C. albicans* yeast forms predominate in the murine digestive tract<sup>25,26</sup>, we hypothesized that the enhanced fitness of filamentation pathway mutants may derive from a block to morphogenesis. In other words, if yeasts are superior to hyphae in colonization of this niche, then yeast-locked mutants might outcompete strains that transition reversibly between the two cell types. To visualize fungal morphology within the mouse GI tract, we adapted a fluorescence *in situ* hybridization (FISH) protocol<sup>65,66</sup> that was originally developed for gut bacteria. Ten days after colonization with *ume6* or an isogenic wild-type strain, animals were euthanized, and gut compartments (stomach, small intestines, cecum, and large intestines) were fixed in methacarn, a solution that preserves the architecture of the mucus layer. Histological sections were hybridized to a Cy3-coupled DNA oligonucleotide against *C. albicans* 28S rRNA, which is distributed throughout the fungal cytoplasm. Sections were also stained with 4',6-diamidino-2-phenylindole (DAPI) to visualize host epithelial cells as well as FITC-coupled lectins (UEA-1 from *Ulex europaeus* +/- WGA-1 from *Triticum vulgare*) to visualize mucus. Examples of staining with this technique are presented in Figure 2.3, with fungal cells in the murine cecum shown in the left panel and cells propagated *in vitro* shown on the right. Results for wild-type *C. albicans* in different compartments of the mammalian gut are presented in Figure 2.3 and 2.3. Similar to previous reports<sup>25,26</sup>, we observed a preponderance of yeasts in the stomach (~60% yeasts, ~40% hyphae) and small intestines (~80% yeasts, ~20% hyphae; Figure 2.3). However, hyphae were enriched

more distally, forming more than half of the fungal population of the cecum (~40% yeasts, ~60% hyphae) and large intestines (~40% yeasts, ~60% hyphae). In retrospect, the conflicting observations reported by previous investigators regarding *C. albicans* cell morphology in the murine gut can be at least partially explained by their focus on different GI compartments (distal ileum in<sup>25</sup> vs. large intestines in<sup>67</sup>). Our results suggest that yeasts and hyphae are present throughout the gut, with hyphae present in greater numbers in the distal regions that are enriched for known hypha-inducing signals such as hypoxia<sup>44</sup>, hypercarbia<sup>45</sup>, and N-acetylglucosamine<sup>46</sup>.

Results for the *ume6* mutant are also shown in Figure 2.3. Surprisingly, and in contrast to our prediction, *ume6* colonizes the gut with morphology that is virtually indistinguishable from that of wild type. Yeasts predominate in the stomach (~60% yeasts, ~40% hyphae) and small intestines (~80% yeasts, ~20% hyphae), whereas hyphae are more highly represented in the cecum (~45% yeasts, ~55% hyphae) and large intestines (~40% yeasts, ~60% hyphae). The preserved ability of *ume6* to undergo the yeast-to-hypha transition within the GI tract contrasts with its reported defects under most *in vitro* hypha-inducing conditions<sup>64</sup>.

To rule out a strain-specific difference in our *ume6* isolate, we tested this strain and a wild-type control in four different hypha-inducing media under standard atmospheric or hypha-inducing anaerobic conditions. Cell morphology was evaluated after propagation in liquid media, and colony morphology was evaluated after propagation on agar-containing plates. As shown in Figure 2.S4 (upper panels), the *ume6* strain forms filamentous structures under most of the hypha-inducing conditions; however, these structures are short and misshapen compared to the true hyphae

formed by wild-type *C. albicans*. Likewise, colonies formed by the *ume6* mutant (Figure 2.S4, lower panels) fail to invade the agar substrate and contain fewer surface wrinkles (which reflects the ratio of filaments to yeasts within the colony). Thus, our isolate reproduces the previously reported *in vitro* defects of *ume6*.

To determine whether the filamentation defects of *efg1*, *brg1*, *rob1*, and *tec1* are also suppressed within the commensal environment, we used FISH to visualize fungal cell morphology in animals individually colonized with these strains. In contrast to our results with *ume6*, we found that the filamentation defects of *efg1* and *rob1* are maintained in the murine gut, with almost pure populations of yeasts observed in every evaluated compartment (Figure 2.S5). On the other hand, *brg1* forms some hyphae, particularly in the large intestines, and *tec1* colonizes with an almost wild-type proportion of hyphae. It is unclear why the *in vitro* filamentation defects of *ume6* and *tec1* are suppressed within the mammalian gut environment, but we speculate that a signal or combination of signals in this niche may activate a compensatory mechanism in the fungus.

Overall, the FISH experiments reveal that 1) *C. albicans* hyphae and yeasts are both capable of colonizing the mammalian GI tract; 2) filamentation can occur even in the absence of Ume6 within this niche; and, therefore, 3) Ume6 most likely exerts its inhibitory effect on commensal fitness by a mechanism other than cell morphology.

## **NanoString analysis reveals stable induction of *C. albicans* hypha-specific genes throughout the host GI tract**

If fungal cell morphology *per se* does not determine commensal fitness, we reasoned that differences in gene expression must be responsible for the enhanced fitness of *ume6*, *efg1*, *brg1*, *rob1*, and *tec1*. To determine fungal transcript levels in commensally growing strains, we utilized the NanoString nCounter platform<sup>68</sup>, which can quantify even low abundance fungal transcripts amid excess RNAs from the host, as well as co-colonizing bacteria, archaea, viruses, etc. We first examined gene expression in wild-type *C. albicans*, comparing results obtained in different GI compartments over a 10-day time course (Figure 2.4, Table 2.S4). Animals were euthanized after 1, 4, or 10 days of colonization (3 animals per time point), and total RNA was prepared individually from the contents of stomachs, small intestines, ceca, and large intestines. 182 previously reported NanoString primer sets were used to profile fungal transcripts that encode proteins associated with filamentation, pH-related processes, nutrient acquisition and metabolism, adhesion and cell wall structure, the cell cycle, stress response, and other processes<sup>69</sup>.

We obtained high quality results for fungal gene expression in the stomach, cecum, and large intestines, but there was insufficient fungal RNA in samples from the small intestines to perform the analysis. Overall, gene expression in commensally propagated *C. albicans* appeared stable over time and was surprisingly similar among different GI compartments (Table 2.S4). Hypha-associated genes and pH-related processes were enriched among genes exhibiting five-fold or greater differences in the gut compared to standard *in vitro* growth conditions (Table 2.S4,  $p=3.0 \times 10^{-6}$  for hypha-

associated genes,  $p=1.1 \times 10^{-3}$  for pH-related genes). Shown in Figure 2.3 and 2.3 are heatmaps depicting all significantly ( $p < 0.05$ ) regulated genes in these two categories. Of note, a small subset of genes was differentially expressed in the stomach compared to other gut compartments. An example is *PHR2*, which encodes a glycosidase that is active in low pH environments (Figure 2.3)<sup>70</sup>.

To determine whether this gut-associated pattern of fungal gene expression requires Ume6, we compared NanoString profiles of wild-type vs. *ume6* strains after 10 days of propagation in the murine commensalism model ( $n = 3$  animals per strain). Analysis was performed as above, with independent analysis of RNA recovered from stomachs, ceca, and large intestines. Apart from the absence of *UME6* expression in the null mutant, however, we observed no significant differences in gene expression between the two strains (Table 2.S5).

### **mRNA-seq reveals a subset of hypha-specific genes that requires Ume6 during gut colonization**

A disadvantage of NanoString is that the relatively high cost of custom primers limits the number of transcripts that can be monitored. To obtain a more global view of gene expression in commensally propagated strains, we turned to mRNA-Seq, which can theoretically quantify any cellular transcript that is expressed above a certain threshold. Paired colonization experiments were performed with wild type and *ume6* ( $n=5$  animals/strain), followed by RNA recovery from large intestines after 10 days; this is the GI compartment in which *UME6* is maximally expressed by wild-type strains (Witchley and Noble, unpublished observations using mRNA-Seq). For comparison, the



strains were also propagated *in vitro* under standard (YPD liquid, 30°C, n=3 cultures) and hypha-inducing conditions (YPD liquid plus 10% bovine serum, 37°C, n=3 cultures). At least 35 million mRNA-Seq reads mapping to the *C. albicans* genome were generated for each strain under every condition (Figure 2.5).

Overall, mRNA-Seq detected expression of 5169 *C. albicans* genes or roughly 85% of the predicted genome under at least one experimental condition (Table 2.S6). Compared to growth under standard *in vitro* conditions, 2201 genes were regulated by two-fold or more in wild-type strains recovered from host large intestines (log2 fold change  $\geq 1$  or  $\leq -1$  and  $p < 0.05$ ; Table 2.S6; these include all of regulated transcripts previously detected using NanoString. GO-term analysis of the 1238 upregulated genes was unrevealing, whereas the 963 downregulated genes were associated with relatively broad categories such as “oxoacid metabolic process” ( $p = 2.68 \times 10^{-19}$ ), “response to stimulus” ( $p = 9.53 \times 10^{-13}$ ), and “RNA export from nucleus” ( $p = 1.53 \times 10^{-08}$ ). Prompted by the significant regulation of hypha-associated genes captured in our NanoString dataset, we focused on a set of 334 genes that are upregulated under at least five independent *in vitro* hypha-inducing culture conditions<sup>71</sup> and represented in our dataset (Table 2.S6). 205 genes in this category, including *UME6*, were upregulated by  $\geq 2$ -fold in the gut, a significant overrepresentation ( $p = 9.69 \times 10^{-52}$ , hypergeometric test).

To identify Ume6-dependent transcripts that might impact commensal fitness, we compared the transcriptomes of wild-type and *ume6* strains recovered directly from the mouse digestive tract. In addition to *UME6* itself, 409 genes were differentially expressed by 2-fold or more in *ume6* compared to a commensally propagated wild-type

strain ( $p < 0.05$ , Table 2.S6). To narrow this number to a smaller set of candidates that would be suitable for testing in animals, we focused on 52 genes that are associated with the yeast-to-hypha transition (Figure 2.5 and Table 2.S6<sup>71</sup>). A volcano plot of results for all 334 hypha-associated genes in wild type vs. *ume6* is presented in Figure 2.5, with differences in gene expression plotted on the x-axis and the significance of these changes plotted on the y-axis. From this analysis, *SAP6* and *HYR1* emerged as the two best-characterized genes that combine strong and significant dependence on Ume6, with *SAP6* expression reduced by 15-fold ( $p = 2.1 \times 10^{-6}$ ) and *HYR1* by 10-fold ( $2.0 \times 10^{-6}$ ) in the null mutant compared to wild type. Sap6 is a hypha-specific secreted aspartyl protease that is required for virulence in a mouse corneal infection model<sup>72</sup>. Hyr1 is a GPI-anchored hyphal cell wall protein<sup>73</sup>.

To test the hypothesis that downregulation of *SAP6* and/or *HYR1* contributes to the enhanced commensal fitness of *ume6*, we performed competition experiments between *sap6* and *hyr1* null mutants and wild-type *C. albicans*. As shown in Figure 2.6, *sap6* strongly outcompetes wild type in the mouse GI colonization model, reminiscent of *ume6* itself (Figure 2.2), whereas *hyr1* exhibits a weaker gain-of-fitness phenotype (Figure 2.6). The superior commensal fitness of *sap6* is also supported by its (slightly) increased titers in the cecum and feces of colonized animals (Figure 2.S3). Restoration of a single copy of *SAP6* to the *sap6Δ/sap6Δ* gene disruption mutant partially suppresses its enhanced fitness phenotype (Figure 2.6). By contrast, a *SAP6*-overexpression strain (*SAP6*<sup>OE</sup>) exhibits reduced commensal fitness (Figure 2.6), similar to the phenotype of *UME6*<sup>OE</sup> (Figure 2.2).

To exclude potential effects of *SAP6* on yeast-to-hypha morphogenesis, we examined the morphology of the null mutant under *in vitro* hypha-inducing conditions and in the murine gut colonization model. Under all tested *in vitro* conditions, *sap6* cell and colony morphology is indistinguishable from that of wild type (Figure 2.S4), as has been reported for a different *sap6* strain<sup>74</sup>. Similarly, *sap6* colonizes each compartment of the mammalian gut with similar proportions of yeasts and hyphae (Figure 2.6) as wild type (Figure 2.3). These results confirm that the presence or absence of the Sap6 gene product, rather than cell morphology, determines *C. albicans* fitness in the gut. Finally, we asked whether decreased expression of *SAP6* might contribute towards the enhanced commensal fitness of *efg1*, *rob1*, *tec1* and *brg1*. Animals were individually colonized with each strain, and RT-qPCR was used to quantify the level of *SAP6* mRNA in cells recovered from the large intestines or feces. Whereas *SAP6* is expressed to variable levels by commensally propagated wild-type *C. albicans*, gene expression is significantly downregulated in each of the hyperfit mutants (Figure 2.S6). These results demonstrate that the hypha-associated gene, *SAP6*, is a potent inhibitor of *C. albicans* fitness in its primary commensal niche.

## DISCUSSION

The rules governing microbial colonization of mammalian hosts are poorly understood, particularly in the case of fungal commensals. In this study, we identified five *C. albicans* transcription factors that decrease the fitness of this fungus in a murine colonization model. Iterative screens were required to identify the gain-of-fitness strains, since each competitive infection was dominated by one or two mutants with the

strongest phenotype/s, and no loss-of-fitness mutants were recovered. The identification of multiple *C. albicans* mutants that outperform wild type within the commensal niche raises the question of why an organism would encode factors that inhibit its own fitness.

Prior to this study, the roles played by *C. albicans* yeasts and hyphae in the host GI tract have been controversial. In particular, two observations have been difficult to reconcile: 1) *C. albicans* colonizes the GI tract primarily in the yeast form<sup>25,26</sup>; and 2) certain genes associated with hyphae, including ones encoding virulence factors, are expressed in this niche<sup>27</sup>. To clarify these observations, we developed a FISH protocol for direct visualization of wild-type *C. albicans* in a murine gut colonization model. Our detailed, quantitative analysis of fungal morphology in fixed tissues provides clear evidence for the presence of both yeasts and hyphae throughout the GI tract. The differences in relative abundance of the two cell types in different gut compartments can be rationalized in light of known triggers of yeast-to-hypha morphogenesis. For example, under *in vitro* conditions, acidic pH promotes yeast morphology by inhibiting a Rim101-dependent pro-filamentation signaling pathway<sup>75-78</sup>, whereas hypoxia, hypercarbia, and N-acetylglucosamine promote hypha formation via the Ofd1-, cAMP-, and Ras1/Cst1 MAPK-dependent signaling pathways, respectively<sup>43,79-84</sup>. If these signals function similarly in the host, then the acidic environment of the stomach may promote a predominance of yeasts in this compartment, whereas higher concentrations of CO<sub>2</sub> and N-acetylglucosamine (part of the bacterial cell wall and host mucin) and lower concentration of O<sub>2</sub> in the cecum and large intestines may induce a predominance of hyphae in the distal gut.

Given the well-documented filamentation defects of *ume6* mutants under a variety of *in vitro* culture conditions (Figure 2.S4<sup>64,85</sup>), the ability of this strain to form hyphae within the murine GI commensalism model came as a surprise. The striking difference of this mutant's behavior in the gut vs. in the laboratory implies that at least one host-associated signal for hypha formation is absent from existing *in vitro* assays. Further, at least one fungal activator of filamentation must compensate for the absence of Ume6 within the commensal niche. The presence of hyphae in all examined gastrointestinal compartments and the existence of redundant mechanisms to support hypha formation in this environment suggest that hyphae must play an important role during commensal colonization. Whether this role is required for interactions with host cells, utilization of nutrients, resistance to stress, and/or interactions with co-colonizing microorganisms and viruses remains to be determined.

Our finding that the hyperfit *ume6* mutant maintains wild-type cell morphology (that is, a mix of yeasts and hyphae) in the mouse GI tract argues that cell shape *per se* does not determine fitness in this niche. Transcriptomic analysis of commensally propagated wild-type and *ume6* strains revealed that Ume6 is required for normal induction of 52 hypha-associated genes. Remarkably, disruption of one of these genes, encoding the secreted aspartyl protease Sap6, is sufficient to confer an enhanced fitness phenotype that phenocopies that of the *ume6* mutant, whereas overexpression of *SAP6* produces a reduced fitness phenotype resembling that of *UME6*<sup>OE</sup>. The strong, reciprocal commensal phenotypes of *sap6* and *SAP6*<sup>OE</sup> belie the common assumption that defects caused by secreted factors should be complemented by other strains in pooled assays. In this case, we surmise that dispersal of *C. albicans* within the host

permits differential selection of cells in areas of higher or lower local concentrations of Sap6 protein. In addition to *SAP6*, we identified a second *UME6* regulatory target, *HYR1*, with a (more subtle) effect on commensal fitness. The slight gain-of-fitness phenotype of the *hyr1* mutant suggests that altered expression of multiple genes may contribute to the net phenotype of *ume6*.

While this manuscript was under revision, another group published an *in vivo* evolution experiment in which serial passage of wild-type *C. albicans* through a murine commensal model resulted in strains with enhanced commensal fitness<sup>86</sup>). Interestingly, sequencing of gut-adapted strains revealed convergent acquisition of mutations in the *FLO8* gene across multiple independent evolution experiments. *FLO8* encodes a transcription factor in the hyphal gene regulatory network (Cao et al., 2006), like Efg1, Brg1, Rob1, Tec1, and Ume6. Based on our results, we speculate that the hyperfit phenotype of these *flo8* mutants may result at least partially from decreased expression of *SAP6*.

Sap6 belongs to a family of ten *C. albicans* secreted and cell surface-associated aspartyl proteases with documented roles in virulence<sup>87,88</sup>. Individual members of the superfamily differ in pH optima, substrate specificity, and expression pattern, with certain Sap proteins expressed constitutively, whereas others are expressed only under specific environmental conditions or in a particular cell type. For example, Sap4, Sap5, and Sap6 are expressed exclusively by hyphae. Individual Sap proteins are thought to facilitate nutrient acquisition, tissue invasion, and/or immune evasion within particular host niches. Interestingly, Sap6 is one of two family members that elicit pro-inflammatory cytokine responses from host innate immune cells<sup>51</sup>. Specifically,

exposure of cultured murine dendritic cells and macrophages to recombinant Sap6 protein (or a catalytically inactive variant) is sufficient to activate the NLRP3 inflammasome, resulting in secretion of IL-1b, among other cytokines<sup>50</sup>.

Based on the observations reported here as well as information from the literature, we propose a model in which colonizing *C. albicans* and the mammalian host engage in intense, bidirectional communication within the commensal niche. *C. albicans* senses a variety of signals (pH, O<sub>2</sub>, CO<sub>2</sub>, nutrient abundance, and N-acetylglucosamine, among others) whose strength and composition vary by host compartment. In response to changes in these signals, the fungus substantially remodels its cell morphology and pattern of gene expression, converting from a yeast-dominated population in the proximal gut to a hypha-dominated population more distally. On the host side, yeasts may be tolerated or even supported, as this cell type is relatively innocuous in this niche. Hyphae, however, are potentially dangerous, and we propose that this cell type is monitored by sensing of cell type-specific gene products such as Sap6 and Hyr1. When these markers exceed a threshold level, a localized antifungal immune response may be triggered to limit the threat. Thus, mutants such as *ume6*, *sap6*, and *hyr1*, which produce lower levels of key hypha-specific proteins, proliferate undetected by the host and can outcompete wild-type *C. albicans* in mixed infections, although presumably they would be less fit in certain situations. If correct, our model implies that active curation of the fungal microbiota by the host helps to limit the risk of opportunistic infection.

## METHODS

### Mice

All procedures involving animals were approved by the UCSF Institutional Animal Care and Use Committee. We used a previously described mouse model of *C. albicans* commensalism<sup>16,89</sup>, with minor modifications. 8–10 week (18-21 gram) wild-type, female BALB/c mice from Charles River Laboratories were provided with autoclaved water containing 5% glucose and antibiotics (penicillin 1500 un/ml and streptomycin 2 mg/ml) for 7-8 days prior to gavage with 10<sup>8</sup> CFUs of *C. albicans*, and antibiotic water was continued throughout the experiments. All animals were singly or doubly housed depending on experiment and provided autoclaved distilled water and autoclaved mouse chow (PicoLab).

### Strains

Genetic screens for *C. albicans* commensalism factors were performed with the Noble<sup>53</sup> and Homann<sup>52</sup> collections of isogenic, barcoded, homozygous deletion mutants. Both libraries are available from the Fungal Genetics Stock Center (<http://www.fgsc.net/>). All other strains are described in Table 2.S7. *ume6* (SN1478 and SN1479) were generated using a previously described fusion PCR technique<sup>53</sup>. Plasmids used to construct strains *UME6*<sup>OE</sup> (SN1557 and SN1558), *SAP6*<sup>OE</sup> (SN1798), and *sap6/SAP6* (SN1796) are described in Table S6. All other plasmids and primers used in this study are listed in Table 2.S8 and Table S9, respectively. *C. albicans* strains were routinely propagated on liquid or solid YPD medium at 30°C. Filament-inducing conditions consisted of YP supplemented with 10% bovine serum (Gibco), Spider medium, Lee's glucose pH 6.8,



and Lee's GlcNAc (N-acetylglucosamine) pH 6.8, as well as propagation under anaerobic conditions generated using a BD Anaerobe Gas Generator Pouch with Indicator.

### *Method Details*

#### **Mouse Model of GI commensalism**

Screens were performed with >650 *C. albicans* homozygous knockout mutants<sup>52,53</sup> and an isogenic wild-type control (SN250). Each strain was individually propagated to mid log growth in 1 ml liquid YPD in 96-well culture dishes at 30°C, prior to pooling into a mixed inoculum. Following washes and resuspension of cells in sterile 0.9% saline, cell density was determined using a hemocytometer, and 10<sup>8</sup> CFUs of each inoculum was gavaged into 2-4 animals. To minimize microbial transfer among cage mates, only one to two animals were housed per cage. Inoculum and stool samples obtained after 3-5 and 10 days of colonization were plated onto Sabouraud agar (BD) with ampicillin 50 mg/mL and gentamicin 15 mg/mL and incubated for 2 days at 30°C. CFUs were washed from plates with sterile water and collected by centrifugation. Cell pellets were stored at -80°C prior to isolation of genomic DNA.

Colonization with single strains (for NanoString and RNA-Seq analysis) or 1:1 mixtures of wild type and mutants (*efg1*, *brg1*, *rob1*, *tec1*, and *hyr1* from mutant libraries, and newly constructed *ume6* (SN1478, SN1479), *UME6*<sup>OE</sup> (SN1557 and SN1558), *sap6* (SN1664), and *SAP6*<sup>OE</sup> (SN1798)) were performed as for the screens. Animals used for mRNA-Seq were individually housed.

For experiments involving direct evaluation of fungal populations in the host digestive tract, each GI segment was dissected immediately following euthanasia of the animal. Fungal CFUs were recovered by plating luminal contents, tissue homogenates, or both onto Sabouraud agar (BD) containing ampicillin 50 mg/mL and gentamicin 10 mg/mL.

For strain competitions in the GI commensal model, the paired student's t-test was used to assess the difference in abundance between strains at each time point for significance.

### **Determination of Competitive Index**

To determine the fitness of individual mutants in the commensalism screens, reads from each sequencing library were mapped to the *Candida albicans* genome (candidagenome.org, Assembly 21) using bowtie<sup>90</sup>. Reads were assigned to a given mutant based on proximity (within 200 bp) of the genomic sequence to the start or end of ORFs targeted in the deletion collections<sup>52,91</sup>. Strain abundance was calculated as the ratio of the sequencing reads for a given mutant to the total number of reads for all strains present in the same pool. Mutants with fewer than 100 reads in the inoculum library were eliminated from further analysis. Competitive index was defined as the log<sub>2</sub> transformed ratio of the abundance of each mutant strain in feces (recovered, R) to its abundance in the inoculum (I).

To assess the commensal fitness of mutants in 1:1 competition with wild type, genomic DNA was extracted from *C. albicans* recovered from feces at the time points indicated in the figures. Strain abundance was determined by qPCR (SYBR Green;

Bio-Rad), using strain-specific primers (Table 2.S9) and a Roche LightCycler 480 instrument. The paired student's t-test was used to assess the significance of observed differences.

### **Preparation of screen sequencing libraries**

Genomic DNA from plated inocula and fecal pellets was isolated as previously described<sup>16,89</sup>. Feces from one animal per cage was prepared for sequencing. A linear amplification-based method modified from<sup>92</sup> was used for selective amplification of genomic sequences flanking the *Candida dubliniensis HIS1* selectable marker<sup>53</sup>, which replaces the disrupted ORF in each mutant. Briefly, 5-20 mg aliquots of genomic DNA were used in individual AluI, BfaI, DpnII, RsaI, and TaqI (New England Biolabs) digests overnight. Following heat inactivation of the restriction enzymes, digests of a given sample were pooled and precipitated to concentrate the DNA, and gel-free size selection was performed using a SeraMag bead mix (prepared as in<sup>93</sup> to capture DNA of ~200-1000 bp. 1 mg of DNA was used for linear amplification by AccuPrime Taq (Invitrogen) with biotinylated primer SNO1774 for 100 cycles. Single-stranded biotinylated DNA was captured using streptavidin-coated beads provided in the Dynabeads kilobaseBINDER kit (Invitrogen) overnight and a second adapter ligation was performed with Circligase II (Epicentre) using primer SNO1775 the next day. PCR using AccuPrime Taq and Illumina primers 1 (SNO1777) and 2 (barcoded; SNO1776, SNO1819-1829 or SNO1949-1960) was performed for 15 cycles. PCR products were separated from primers using SeraMag bead mix. 2100 Bioanalyzer (Agilent) traces were used to quantify library abundance and size distribution. Multiplexed libraries for

sequencing were pooled based on Bioanalyzer traces. Sequencing (50 bp-single end) was performed using a custom sequencing primer SNO1830 at the University of California Berkeley QB3 Vincent J. Coates Genomics Sequencing Laboratory (GSL) on an Illumina HiSeq2000 or HiSeq4000, which are supported by NIH S10 Instrumentation Grants S10RR029668, S10RR027303 and OD018174.

### **Imaging of *Candida albicans in vivo***

BALB/c mice were singly or doubly housed and colonized with wild type (SN250, n=6), *ume6* (SN1478, SN1479, n=9), *sap6* (m886, n=3; SN1664, n=3), *efg1* (SN1011, n=2), *brg1* (SN1106, n=3), *rob1* (SN1439, n=3), or *tec1* (SN1441, n=3) as described above. After 10 days, animals were euthanized, and segments of the digestive tract (stomach, jejunum, ileum, cecum, and large intestines) were fixed in a methacarn solution (60% methanol, 30% chloroform, 10% glacial acetic acid) at room temperature for at least three hours.

Fixed tissues were processed in 100% methanol (twice for 35 minutes each), 100% ethanol (twice for 25 minutes each), and xylenes (histological grade, Sigma-Aldrich; twice for 20 minutes each), followed by transfer to melted paraffin wax (Sigma) for two hours at 70°C. Preparation of paraffin blocks was performed by the UCSF Cancer Center Immunohistochemistry and Molecular Pathology Core, and 4 µm or 8 µm sections were prepared by Nationwide Histology (Veradale, WA).

Fluorescence *in situ* hybridization (FISH) was performed as previously described<sup>66</sup> and summarized here. Slides were de-paraffinized in xylenes (twice at 60°C), followed by a 5 minute incubation in 100% ethanol at room temperature.

Hybridization was performed in a hybridization buffer (20 mM Tris-HCl pH 7.4, 0.9 M NaCl, 0.1% SDS and 1% formamide) with a fungal 28S rRNA DNA oligonucleotide that is coupled to Cy3 (5'-Cy3-CTCTGGCTTCACCCTATTC-3'; Integrated DNA Technologies) for three hours at 50°C. Slides were washed for 15 minutes at 50°C in wash buffer (20 mM Tris-HCl pH 7.4, 0.9 M NaCl) followed by two washes in PBS, pH 7.4 at room temperature. Samples were counterstained with DAPI (for epithelial cell nuclei) and FITC-conjugated UEA-1 (for mucin; Sigma), for 45 minutes at 4°C. Because staining of mucin in the small intestine and cecal specimens was less efficient, FITC-conjugated WGA-1 (Sigma) was added for counterstaining of these sections. Slides were washed twice in PBS, pH 7.4 at room temperature and then mounted with Vectashield (Vector Laboratories). Sections were imaged on the Keyence microscope model BZ-X700 or High Speed Spinning Disk Confocal microscope (Yokogawa W1). Yeasts and hyphae were quantified manually using the cell counter plug-in for Fiji (ImageJ)<sup>94</sup>. Statistical significance was determined by the unpaired student's t-test.

### **Sample collection and analysis for NanoString**

BALB/c mice were colonized with a single *C. albicans* strain (wild-type strains SN250 or SN425, *ume6* mutant SN1479), as described above. Three animals were colonized with each strain per experimental time point and housed individually. Samples of the inocula were flash frozen in liquid nitrogen and stored at -80°C. At designated time points, animals were euthanized, and the digestive tract was dissected aseptically. Whole GI segments (tissue + contents) were analyzed together. GI specimens were flash frozen in liquid nitrogen and stored at -80°C.

RNA extraction was performed as previously described<sup>68</sup> and summarized here. Tissue samples were homogenized in buffer RLT (Qiagen) with 1%  $\beta$ -mercaptoethanol ( $\beta$ -ME) with a gentleMACS dissociator (Miltenyi Biotec). Phenol:chloroform:isoamyl alcohol (25:24:1) was added to the homogenate along with zirconia beads (0.5mm) (Research Products International) and vortexed on a mini-beadbeater (Biospec Products). The aqueous phase was collected and washed on an RNeasy spin column (Qiagen), followed by elution in water.

The NanoString nCounter Analysis System was used with a previously described set of fluorescent probes for hybridization and detection<sup>69</sup>). Briefly, hybridization buffer combined with the codeset of interest is combined with 5  $\mu$ l of total RNA and incubated at 65°C overnight. Samples were then loaded onto the prep station and incubated under the high sensitivity program for 3 hours. Following the prep station, samples were read using the NanoString digital analyzer with the high resolution option. Measured counts for individual transcripts were normalized to the average of all transcripts in the sample. Heatmaps were generated using the results for *C. albicans* in the digestive tract compared to inoculum grown to  $OD_{600}=1.0$  in liquid YPD maintained at 30°C. Raw counts below 20 were excluded from further analysis.

The linear fit model generated by *limma* using NanoString probe counts was used to determine the significance of expression differences between different conditions in the NanoString dataset. The Fisher's exact test was used to determine the significance of functional category enrichment among genes regulated by five-fold or more. Genes were assigned pH-related, nutrient acquisition and metabolism, adhesion and cell wall structure, cell cycle, stress response, and/or "other" categories based on

gene descriptions in the Candida Genome Database<sup>95</sup>. Hypha-associated genes were defined as genes that are upregulated under at least five different *in vitro* hypha-inducing conditions in the recent study by Azadmanesh *et al*<sup>71</sup>.

### **Sample collection and analysis for mRNA-seq**

Colonization of animals and recovery of experimental samples were performed as described above for the NanoString experiments, with the exception that only samples of luminal contents were evaluated.

RNA extraction for mRNA-seq was performed as previously described in<sup>96</sup>, with modifications. Dow Corning vacuum grease was used for phase separation, instead of phase-lock tubes. Three to five additional acid phenol:chloroform (Ambion) followed by three to five buffer saturated phenol:chloroform:isoamyl alcohol (Ambion) extractions were added to eliminate endogenous RNases. Following precipitation and resuspension of pellets in RNase-free water, RNA was further purified using the MEGAclean transcription clean-up kit (Ambion). DNase I (NEB) treatment was performed on 10 ug RNA for 10 minutes at 37 C, then 0.5 M EDTA was used to inactivate DNase I at 75 C for 10 min. Following DNase treatment, a final acid phenol-chloroform extraction was performed. RNA was then precipitated and resuspended in RNase-free water. *In vitro* and *in vivo* samples were treated identically.

NEBNext Ultra Directional RNA Library Prep Kit for Illumina in combination with NEBNext Poly(A) mRNA Magnetic Isolation Module and NEBNext Multiplex Oligos for Illumina were used to generate mRNA-seq libraries. The protocol provided by NEB was followed precisely using 1 µg total RNA and 13 cycles in the final PCR, with the

exception that Ampure XP bead mix was replaced with Sera-Mag Speed Beads (GE Healthcare) in DNA binding bead mix<sup>93</sup>. Library fragment size was determined using High Sensitivity DNA chips on a 2100 Bioanalyzer (Agilent). Library quantification was performed by qPCR with a library quantification kit from KAPA Biosystems (KK4824) on a Roche LightCycler 480. Sequencing was performed on the UCSF Center for Advanced Technology HiSeq4000.

To determine significant changes in RNA expression, reads were mapped to the current haploid *C. albicans* transcriptome (Assembly 21, candidagenome.org) and transcript abundances were then evaluated using kallisto<sup>97</sup>. Statistical comparisons of transcript abundances between different conditions were performed on estimated counts using the linear fit model generated by *limma* with strain, environmental condition and sequencing run as factors in the design matrix as previously described<sup>98</sup>. Data in heat maps where individual biological replicates are shown were made using transcript per million mapped reads (tpm) values generated by kallisto.

GO-term analysis of processes enriched among upregulated and downregulated gene sets was performed using the CGD Gene Ontology Term Finder<sup>95</sup>.

### **qRT-PCR of *in vivo* SAP6 expression**

Mice were housed two per cage, treated with antibiotics and inoculated with either wild type (ySN250), *efg1* (ySN1011), *brg1* (ySN1106), *rob1* (ySN1439), and *tec1* (ySN1441). After 10 days. For wild type, the GI tracts were used for CFU/organ studies and so fresh feces were substituted for RNA extraction. For the mutants, half of the large intestine contents were snap frozen and stored at -80°C.



RNA was prepared as described for mRNA-seq with the exception that after initial RNA extraction, for RNA purification, homemade RNA binding bead mix (1 mM trisodium citrate, 2.5 M NaCl, 20% PEG 8000, 0.05% Tween 20, pH 6.4) was used following the protocol provided for RNAClean XP mix (Beckman Coulter). RNA was eluted in RNase-free water and DNase I treated. Again, RNA was purified using RNA binding bead mix. One  $\mu\text{g}$  of RNA was reverse-transcribed using SuperScript III with random hexamers. 1  $\mu\text{L}$  of cDNA was used per 10  $\mu\text{L}$  qRT-PCR reaction with either primers to the housekeeping gene *PMA1* (SNO3478 and SNO3479) or to the gene of interest *SAP6* (SNO3202 and SNO3203) in triplicate.

For qPCR analysis, Roche Lightcycler 480 was used with the following program: initial melting occurred at 94°C for 30 seconds, followed by 40 cycles of annealing at 94°C for 10 seconds then extension at 60°C for 60 seconds with fluorescent measurements taken at the end of each extension. Melt curves (60°C-94°C) with continuous acquisition were generated to verify single product amplification. Ct values were generated using software provided with the Lightcycler. To produce  $\Delta\Delta\text{Ct}$  values for individual biological replicates, the following steps were taken. The average of the three technical replicates was taken and standard deviation (SD) calculated in Excel. For each biological sample,  $\Delta\text{Ct}_{\text{SAP6-PMA1}}$  (average Ct *SAP6* – average Ct *PMA1*) and standard deviation ( $\text{SD}_{\text{SAP6-PMA1}}$ ) were calculated  $((\text{SD}_{\text{SAP6}})^2 + (\text{SD}_{\text{PMA1}})^2)^{0.5}$ . To normalize data to the average wild-type value for graphical representation, the average of all wild-type  $\Delta\text{Ct}$  values was taken and then subtracted from each  $\Delta\text{Ct}$  value. The fold change from the average wild-type value is represented as  $2^{-\Delta\Delta\text{Ct}}$ . Standard deviation representing technical variation was calculated from  $2^{-\Delta\text{Ct}}$ ,  $2^{-\Delta\Delta\text{Ct}+\text{SD}}$ , and  $2^{-\Delta\Delta\text{Ct}-\text{SD}}$  in Excel.

For comparison of *SAP6* expression between wild type and transcription factor mutants, average Ct values ( $Ct_{avg}$ ) and  $\Delta Ct_{avg, SAP6-avg, PMA1}$  for each biological sample were calculated then the average  $\Delta Ct_{(avg, SAP6-avg, PMA1), strain}$  and  $SD_{(avg, SAP6-avg, PMA1), strain}$  value within each group (WT, *efg1*, *brg1*, *rob1*, or *tec1*) determined in Excel.  $\Delta\Delta Ct$  values were calculated as  $\Delta Ct_{(avg, SAP6-avg, PMA1), strain} - \Delta Ct_{(avg, SAP6-avg, PMA1), wild\ type}$ . Significance of the fold change between biological replicates of wild type and transcription factor mutants was calculated by GraphPad Prism using the one-tailed Mann-Whitney U test.

### *Quantification and Statistical Analysis*

Statistical parameters and statistical test type (value of n, statistical significance, dispersion and precision measures) are reported in the figure legends and method details. Significance is defined as  $p < 0.05$ . All *in vivo* GI competitions were assessed by a paired Student's t test. Quantification of hyphae vs. yeast *in vivo* was assessed by an unpaired student's t test. Fisher's exact test was used for NanoString gene ontology term analysis. t tests were performed using GraphPad Prism 6.0 and 7.0. The significance of differences among NanoString and mRNA-seq expression data was determined using *limma*.

### *Data and Software Availability*

Raw data for the commensalism screens (Accession #X) and RNA-seq data (Accession #Y) are available at the GEO website (<https://www.ncbi.nlm.nih.gov/geo/>).

## FIGURES

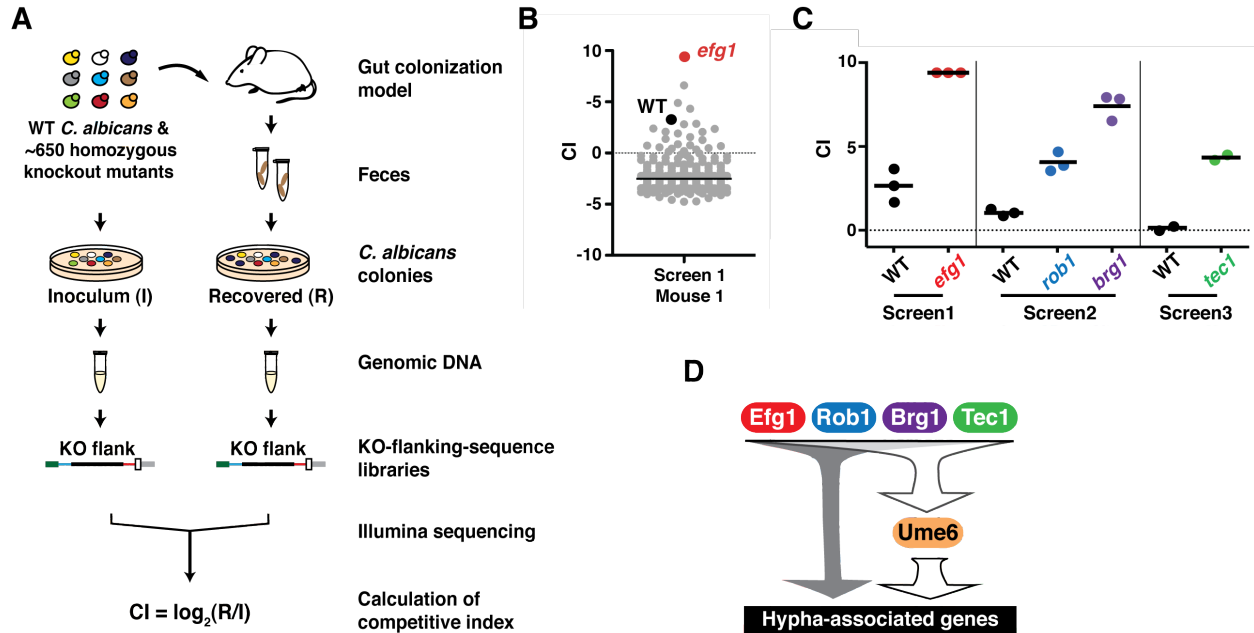


**Figure 2.1. Activators of *C. albicans* filamentation inhibit commensal fitness in the mammalian gut.** A) Schematic of the gastrointestinal commensalism screens. Pools of ~650 homozygous gene deletion mutants and wild-type *C. albicans* (WT, SN250) were gavaged into BALB/c mice ( $n = 2$  or  $3$  animals per inoculum). *C. albicans* in the infecting inoculum and in fecal samples obtained after 3-5 and 10 days of colonization were plated on Sabouraud agar. Sequencing libraries were prepared from segments of genomic DNA that flank the disrupted ORF in mutants or the *C.a.LEU2* gene in WT, as described in the Methods. The competitive index (CI) of each strain was determined as the  $\log_2$  function of  $(R/I)$ , based on sequencing read counts in samples recovered from the host (R) vs. the inoculum (I). See also Tables S1, S2, and S3. B) Competitive indices of all strains recovered from one animal colonized for 10 days with the entire mutant library. The *efg1* mutant is shown in red, WT in black, and all other mutants in gray. C) Competitive indices of four hypercompetitive mutants and WT discovered in three commensalism screens. The inoculum in Screen 1 included every mutant in the library; in Screen 2, all mutants except for *efg1*; in Screen 3, all mutants except for *efg1*, *brg1*, and *rob1*. For a given strain, each data point indicates the result in a different animal. D) Cartoon of the regulatory network controlling yeast-to-hypha morphogenesis. Efg1, Brg1, Rob1, Tec1, and Ume6 are transcriptional activators of genes required for filamentation, as well as genes that are upregulated in hyphae compared to yeasts. Efg1 has been shown to act upstream of Ume6 by genetic epistasis analysis and ChIP-Seq<sup>99,100</sup>. Brg1 and Tec1 have been shown to bind upstream of Ume6 by ChIP-Seq<sup>58,101</sup>. Rob1 has not been characterized with respect to Ume6.

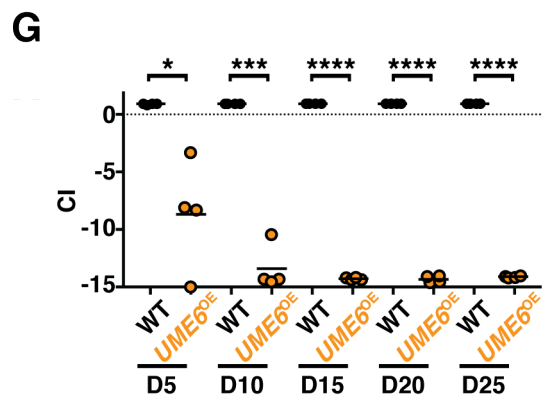
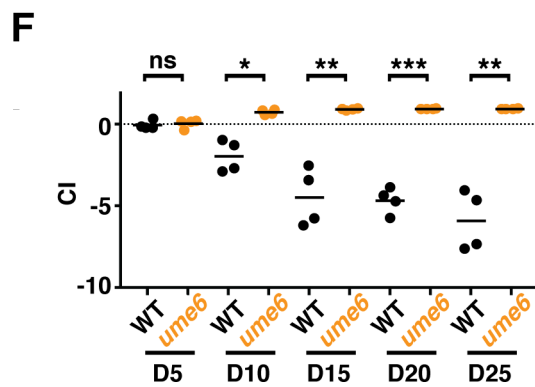
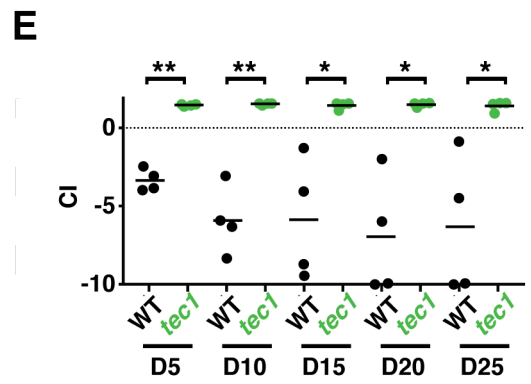
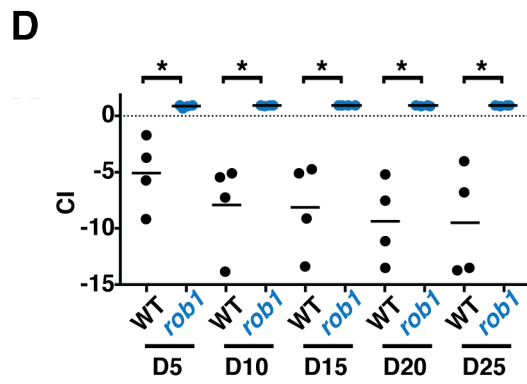
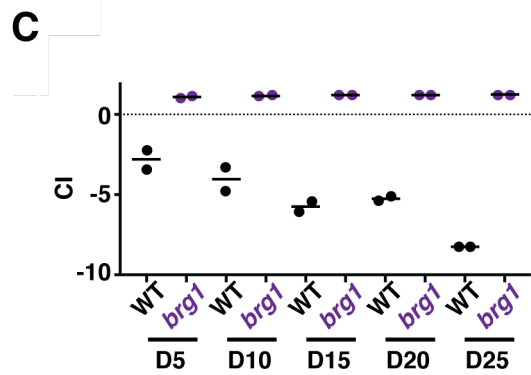
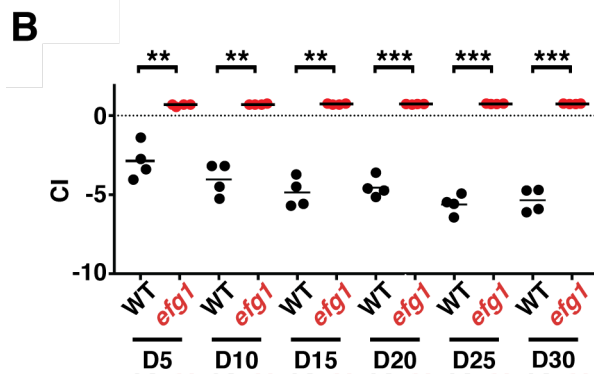
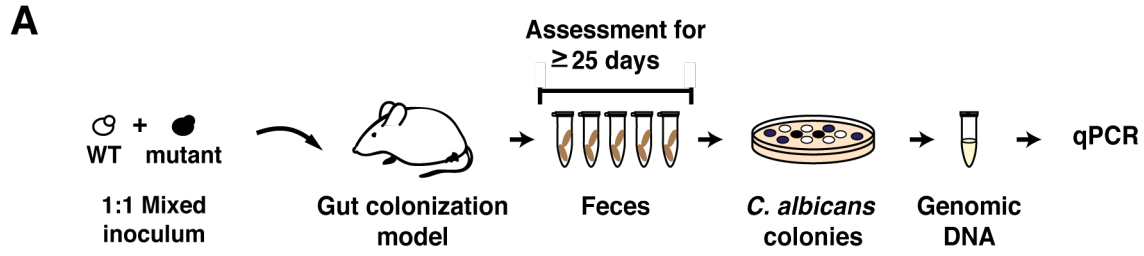


**Figure 2.2. *efg1*, *brg1*, *rob1*, *tec1*, and *ume6* mutants exhibit enhanced commensal fitness, but a *UME6*-overexpression strain has reduced fitness.**

A) Schematic of competition experiments. Mice were gavaged with a 1:1 mixture of WT and a commensalism mutant, and fecal samples were collected every five days for  $\geq 25$ -days. The relative abundance of WT vs. mutant in the inoculum (I) and recovered (R) samples was determined by qPCR, using primers specific to each strain's DNA barcode. B-G) Results are presented for competitions between: (B) WT (ySN226) and *efg1* (ySN119), (C) WT (ySN425) and *brg1* (ySN1180), (D) WT (ySN250) and *rob1* (ySN1440), (E) WT (ySN250) and *tec1* (ySN1442), (F) WT (ySN250) and *ume6* (ySN1479), (G) WT (ySN1556) and *UME6*<sup>OE</sup> (ySN1558). Note that each mutant was compared to a WT strain containing matched auxotrophic markers. Significance was determined using the paired student's t-test: n.s. not significant, \*  $p < 0.05$ , \*\*  $p < 0.01$ , \*\*\*  $p < 0.001$ , and \*\*\*\*  $p < 0.0001$ . Additional results are presented in Figures 2.S1, 2.S2, and 2.S3.

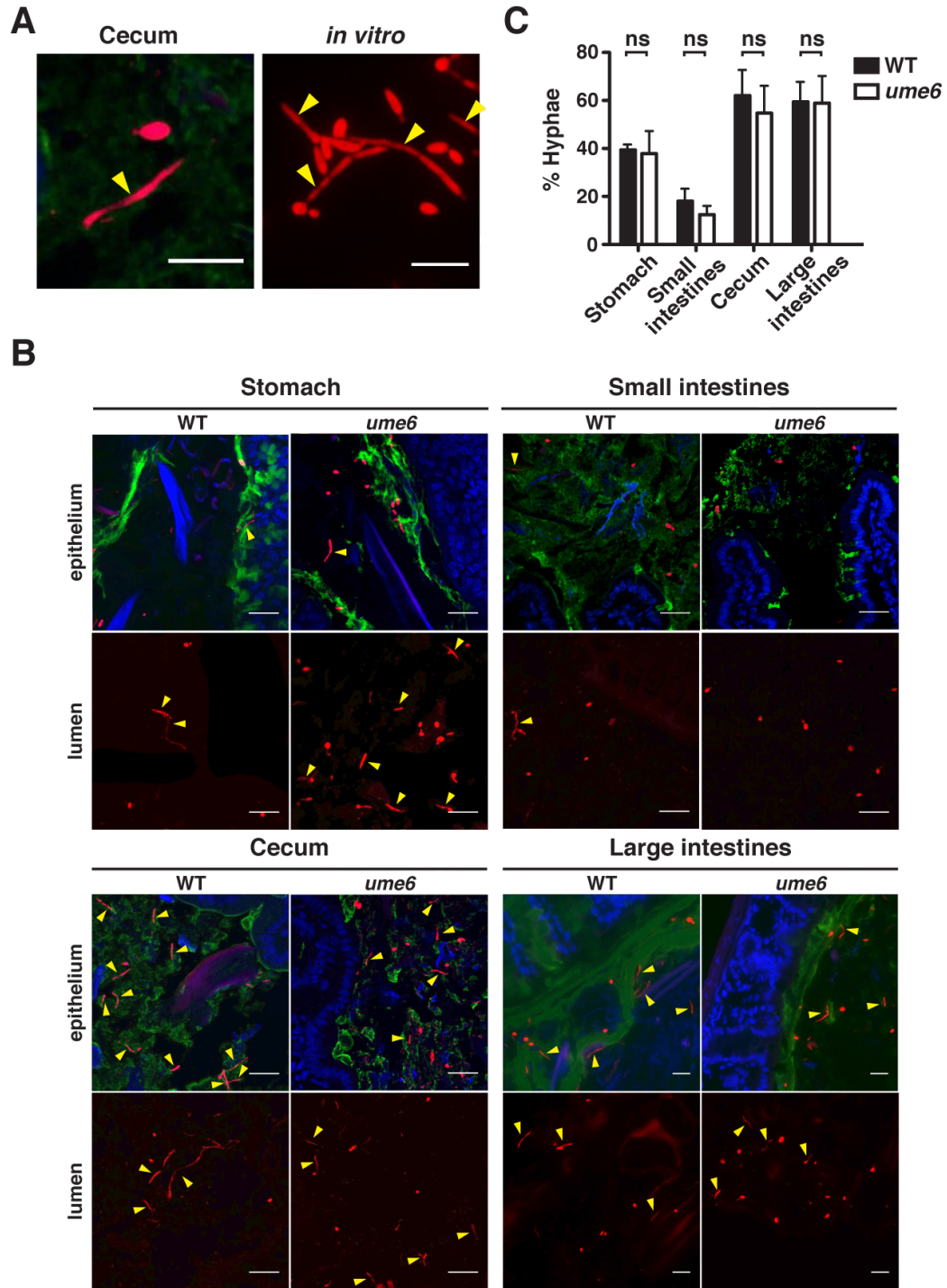
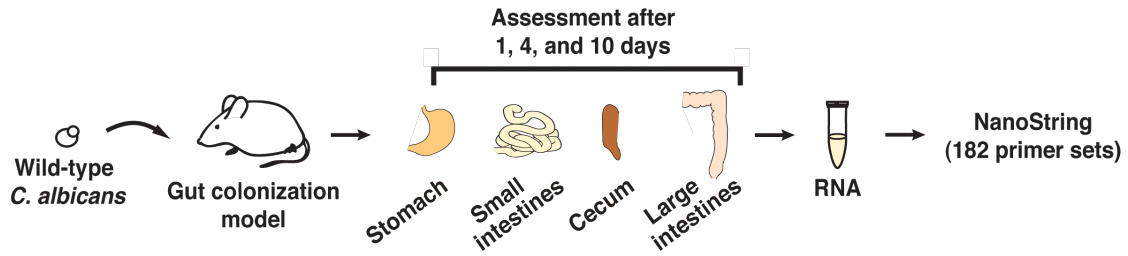


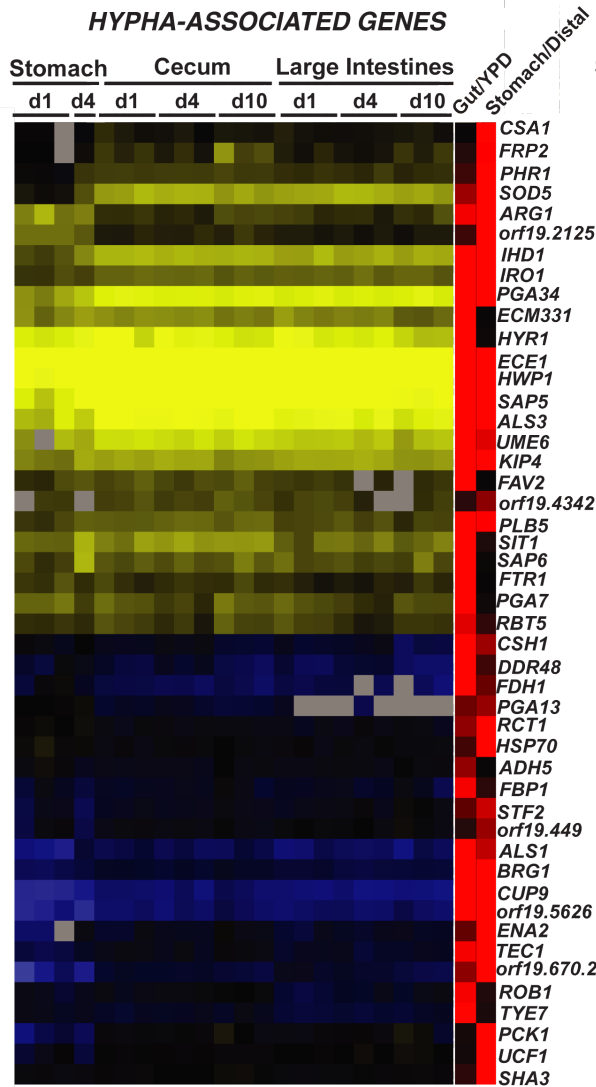
**Figure 2.3. *C. albicans* colonizes the gut as a mixed population of yeasts and hyphae.**

A. Appearance of *C. albicans* yeasts and hyphae in the mouse cecum (left) compared to cells propagated *in vitro* (right). FISH was used to visualize wild-type *C. albicans* (SN425 or SN250) in cecal tissue after 10 days of colonization or after 2 hours in liquid spider medium at 37°C. Hyphal cells are marked with yellow arrowheads, and the scale bar indicates 15 µm. B. WT (SN250) and *ume6* (SN1479, SN1478) strains were visualized in the designated GI compartments after 10 days of colonization. A Cy3-coupled fungal-specific oligonucleotide (red) was used to visualize *C. albicans*, a FITC-coupled lectin (UEA-1 +/- WGA-1) to detect mucus I (green), and DAPI to detect nuclei within host epithelial cells (blue). Scale bar indicates 20 µm. C. Quantification of *C. albicans* yeasts and hyphae in different GI compartments. Morphology was scored in 30 fields of view per GI compartment per animal colonized with WT (n=6 animals) and *ume6* (n=9 animals). Data represent the mean ±SEM. Statistical significance was determined using the unpaired student's t-test. Please see Figure 2.S4 to view *ume6* morphology under *in vitro* hypha-inducing conditions, and Figure 2.S5 to view the morphology of other transcription factor mutants in the gut.

**A**



**B**



**C**

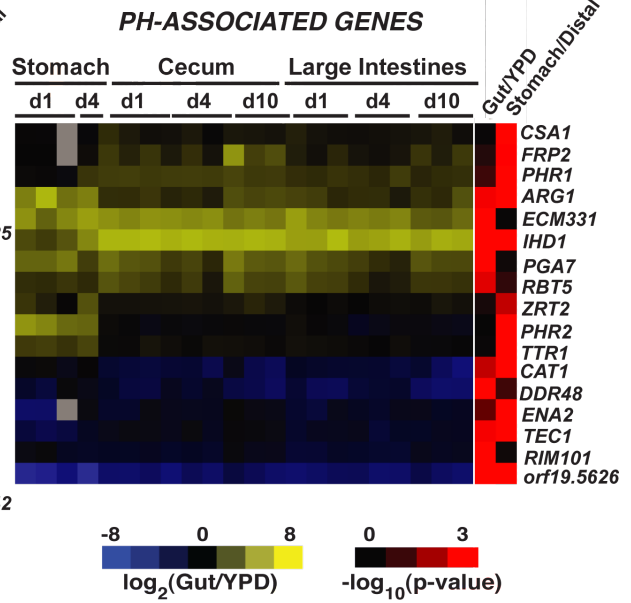




**Figure 2.4. NanoString reveals induction of hypha-associated and pH-responsive genes in the gut.**

A. Schematic of experiment. Animals were colonized with wild-type *C. albicans* (ySN425) for 1, 4 and 10 days prior to dissection of stomachs, ceca, and large intestines. Total RNA was extracted and analyzed with 182 NanoString primer sets. B. Heatmap of expressed hypha-associated genes. Yellow indicates upregulation relative to the inoculum and blue indicates downregulation. The final column indicates the significance of differences in relative gene expression in the gut vs. under laboratory conditions, expressed as  $-\log_{10}(\text{p-value})$ . Significance was determined using a linear fit model. C. Heatmap of expressed pH-associated genes. The final two columns indicate the relative significance of differences in gene expression in the GI commensalism model vs. *in vitro* (left) and in the stomach vs. more distal regions of the GI tract (right).

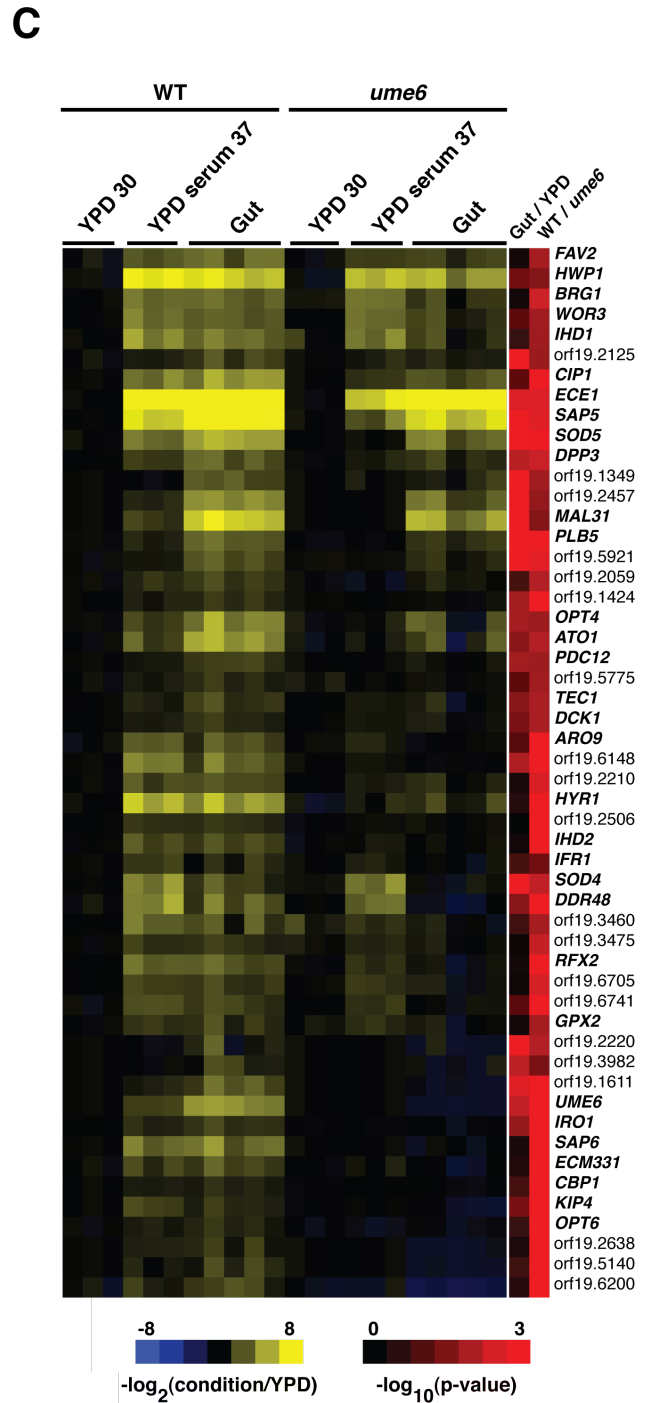
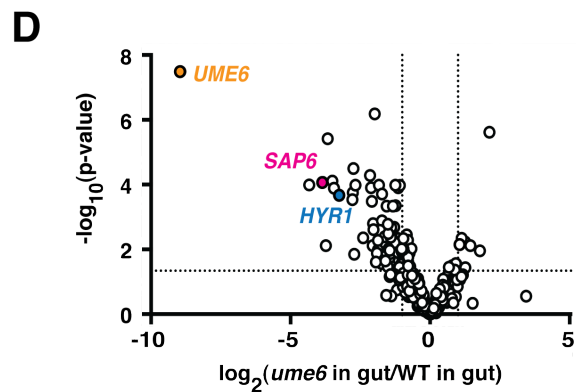
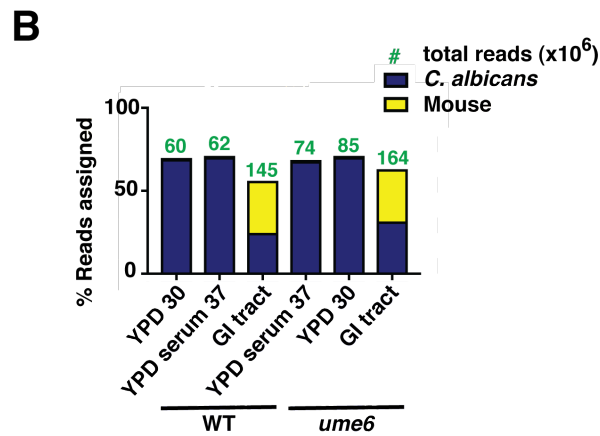
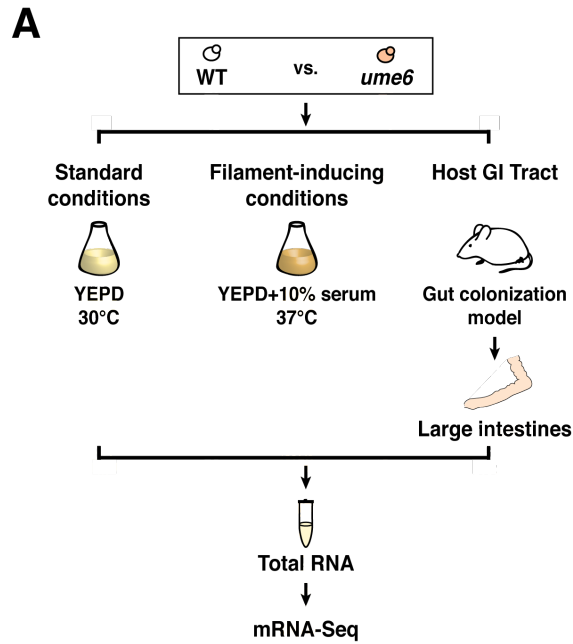


**Figure 2.5. mRNA-Seq reveals that a subset of hypha-associated genes are controlled by Ume6 in the gut**

A. Schematic of mRNA-Seq experiment. PolyA RNA was recovered from WT *C. albicans* (ySN250) and *ume6* (ySN1479) after propagation under standard *in vitro* conditions (YPD, 30°C; n=3 cultures), filament-inducing conditions (YPD+10% serum, 37°C; n=3 cultures), or for 10 days within the GI commensalism model (n=5 animals). Library preparation and sequencing were performed as described in the Methods. B. Heat map of hypha-associated gene expression under *in vitro* vs. *in vivo* conditions. Plotted values represent the  $\log_2$  function of the tpm under each labeled condition divided by the tpm under standard *in vitro* conditions (YPD, 30°C). The final column represents the  $-\log_{10}$ (adjusted p-value) of differences between *ume6* and WT in the GI tract. C. Analysis of sequencing depth and coverage. Bar graph represents the percentage of total reads that align to *C. albicans* vs. mouse transcriptomes. The green numbers denote the number of reads (in millions) of the indicated strain under the indicated condition. D. Volcano plot depicting the  $\log_2$  transformed ratio of relative gene expression of hypha-associated genes versus significance for commensally propagated *ume6* versus WT. Aside from *UME6* itself, *SAP6* and *HYR1* are the most strongly downregulated genes with known or predicted functions in the *ume6* mutant.

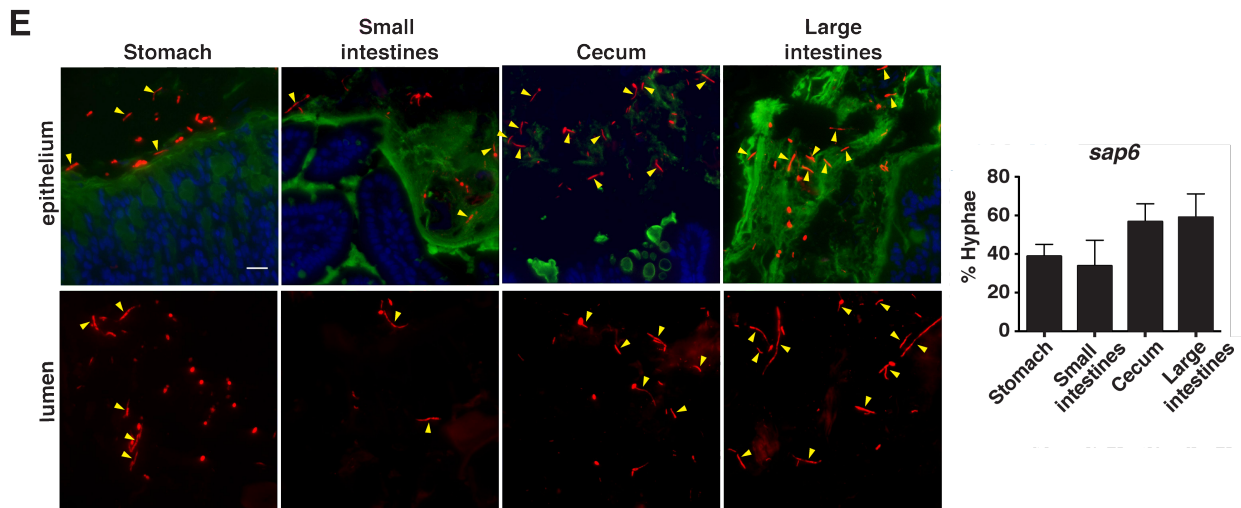
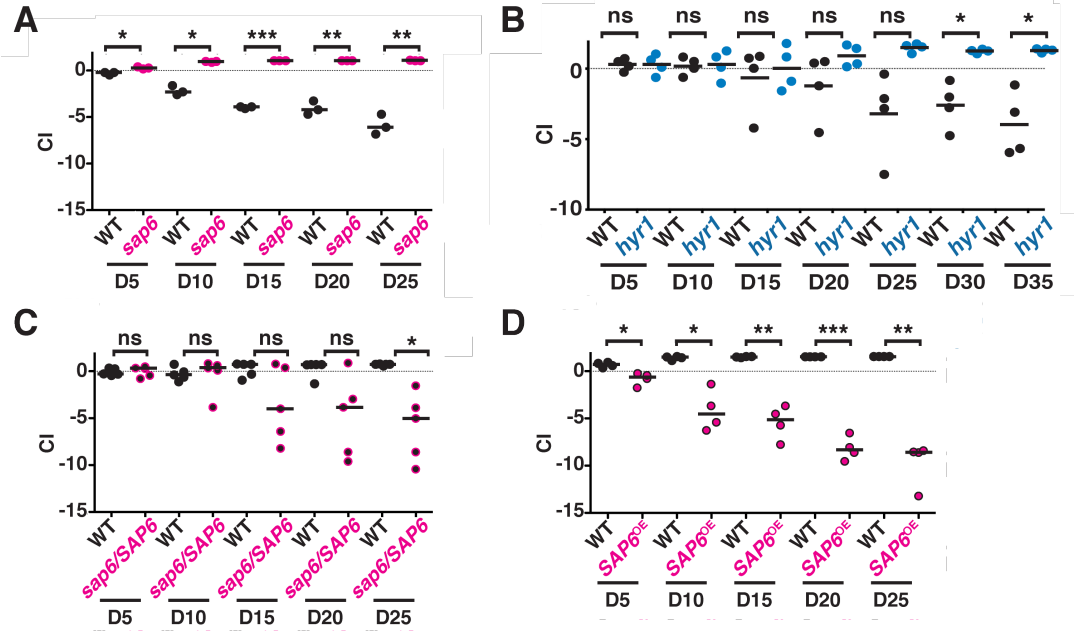


**Figure 2.6. Hypha-associated secreted and cell surface proteins inhibit GI commensalism.**

A-D. Mutants affecting *SAP6* and *HYR1* exhibit altered commensal fitness in the murine GI colonization model. Competitive fitness was determined in one-to-one competition against wild-type *C. albicans*, as in Figure 2.2 A) WT (SN250) vs. *sap6* (SN1664); B) WT (SN250) vs. *hyr1* (SN511); C) WT (SN250) vs. *sap6*+*SAP6* gene addback strain (SN1796, note that one copy of *SAP6* was restored to a strain lacking two alleles of the functional ORF); D) WT (SN235) v. *SAP6*<sup>OE</sup> (SN1798). The paired student's t-test was used to determine significance, with ns indicating not significant, \*p<0.05, \*\*p<0.01, \*\*\*p<0.001. E. The *sap6* mutant exhibits normal morphology in the gut. FISH was used to visualize the *sap6* mutant (SN1664 and m886) in stained sections of the murine GI tract, as in Figure 2.3. Representative images of the large intestines (epithelium and gut lumen) are shown on the left, with yellow arrows indicating hyphae. The plot on the right indicates the mean percentages ( $\pm$ SEM) of hyphae in the stomachs, small intestines, ceca, and large intestines of six animals following ten days of colonization. Red: *C. albicans*, green: mucus layer, blue: epithelium. Scale bar is 20  $\mu$ m. *SAP6* levels in other transcription factor mutants are shown in Figure 2.S6.

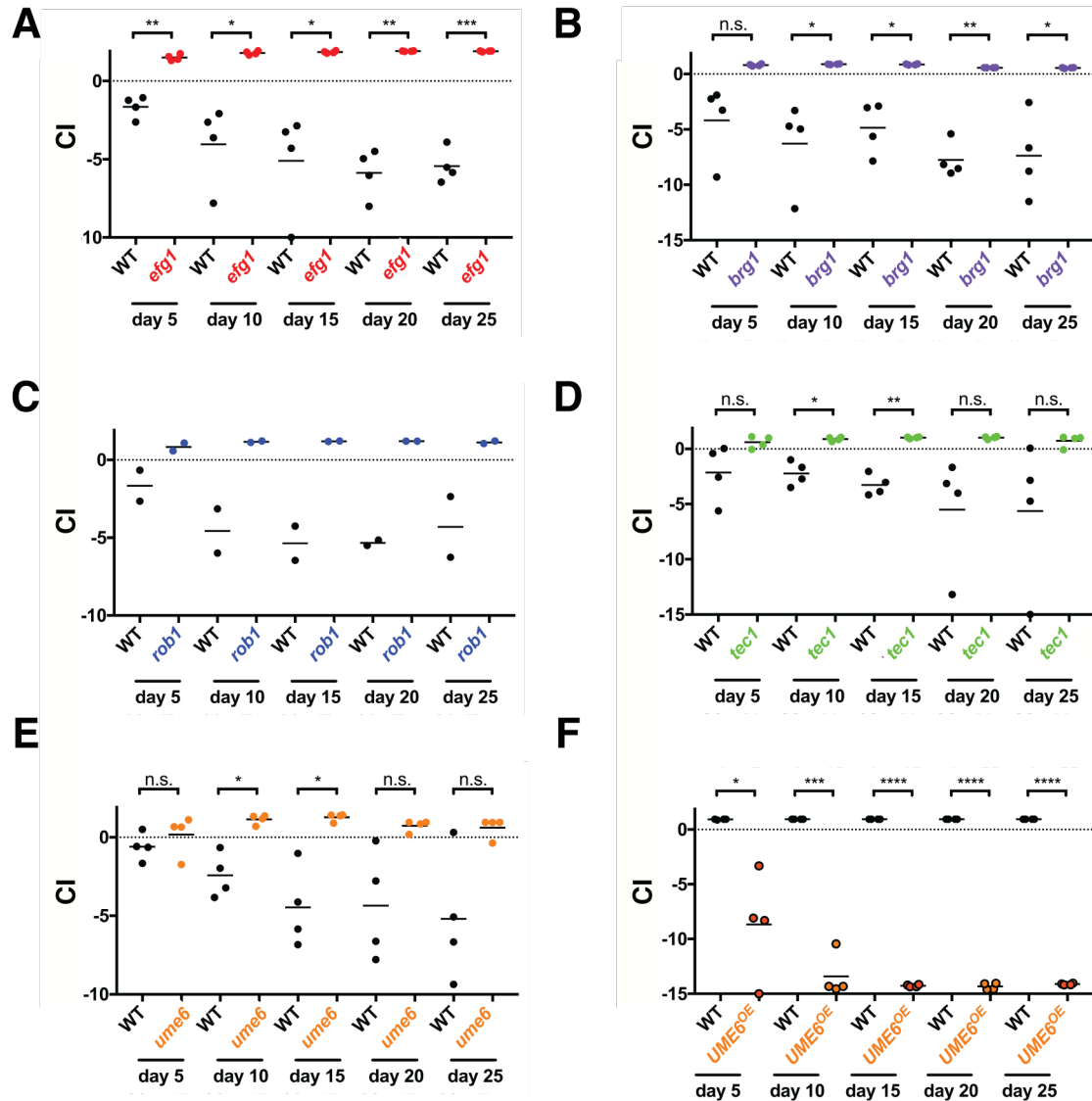


**Figure 2.S1. Validation of commensalism phenotypes of transcription factor mutants using independent isolates.** One-to-one commensal competitions with wild-type *C. albicans* were performed with independent isolates of each mutant depicted in Figure 2. Paired student's t-test: n.s. indicates not significant, \*  $p < 0.05$ , \*\*  $p < 0.01$ , \*\*\*  $p < 0.001$ , and \*\*\*\*  $p < 0.0001$ .

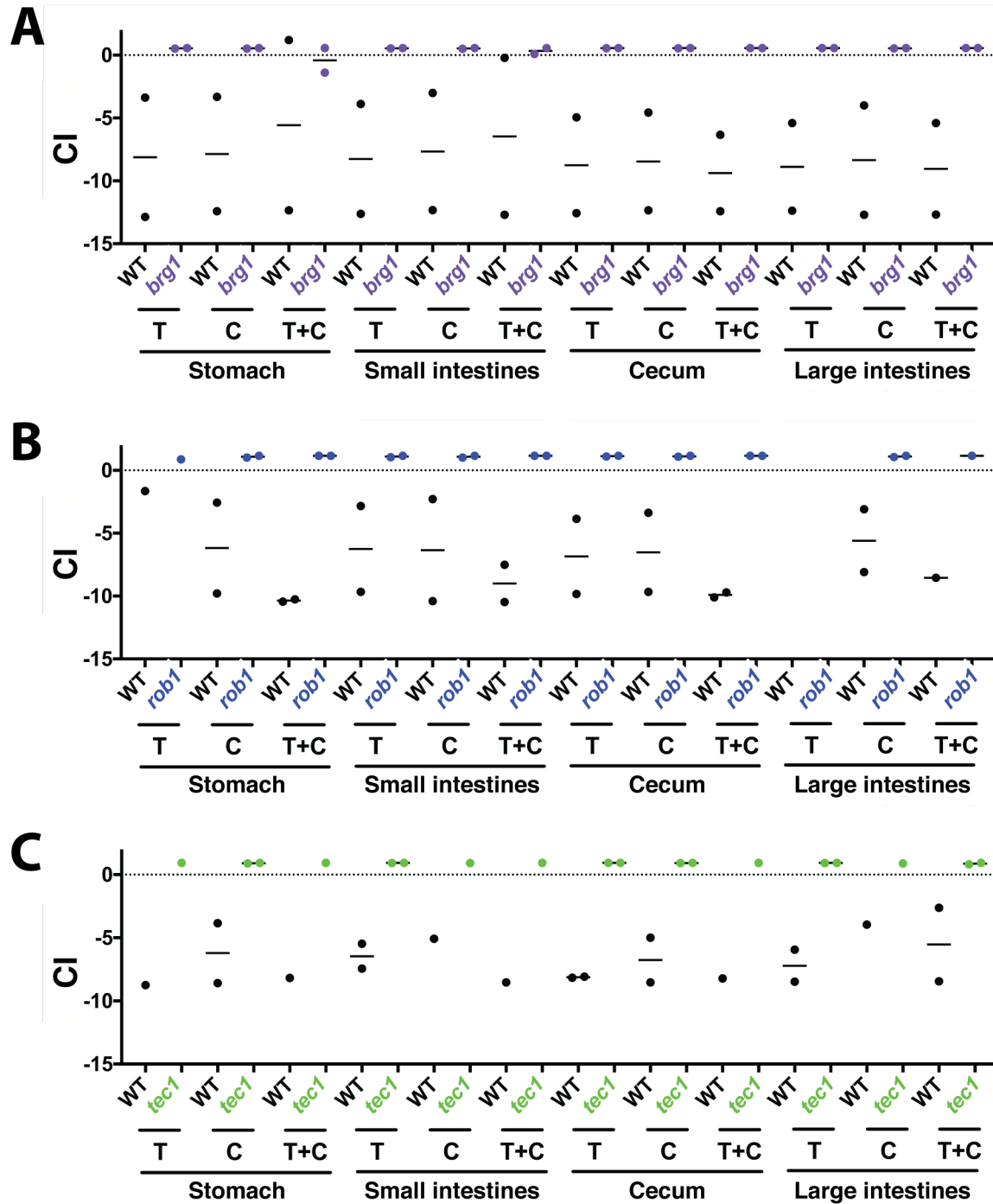


**Figure 2.S2. Assessment of competitive fitness of strains recovered directly from the host.** Animals used for the experiments presented in Figure 2C, D, and E were euthanized following collection of the Day 25 feces sample. The indicated segments of the digestive tract were recovered, and the relative abundance of *C. albicans* strains associated with tissues, luminal contents, or both was determined by qPCR of genomic DNA. The similarity of results obtained from feces vs. segments of the gut supports the use of feces samples for monitoring of commensal fitness.

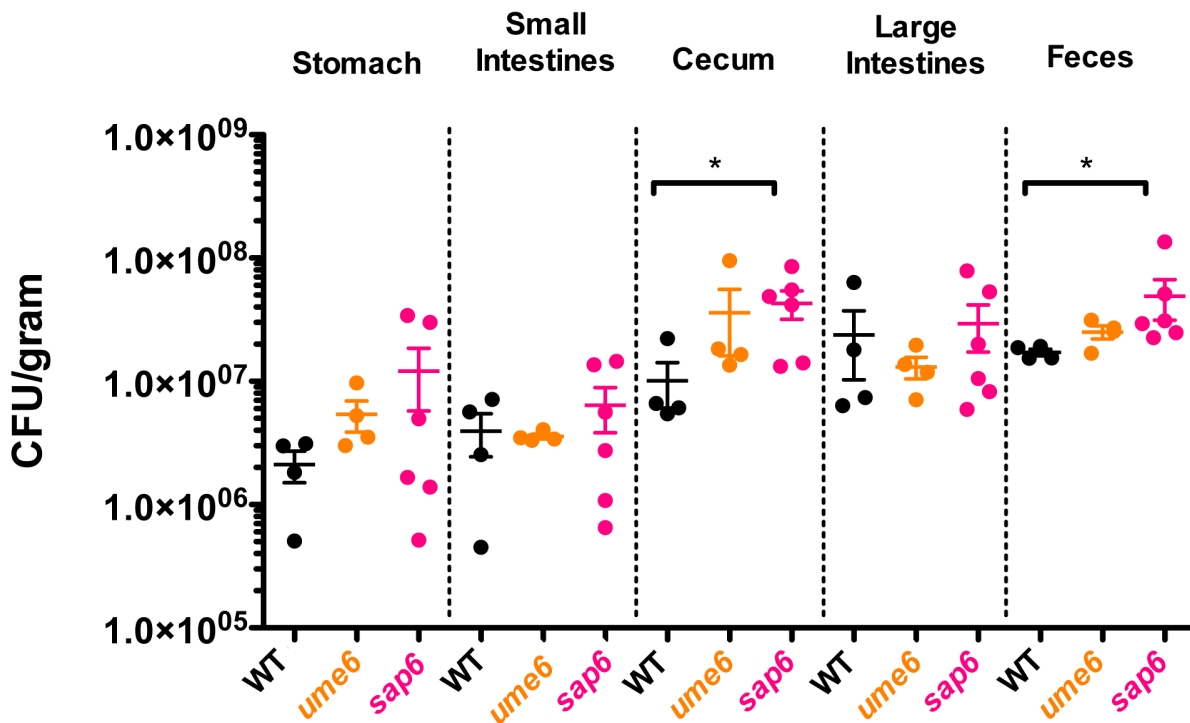


**Figure 2.S3. *ume6* and *sap6* mutants colonize the mammalian GI tract to similar levels as WT.**

Mice were gavaged with either WT (SN250), *ume6* (SN1479) or *sap6* (SN1664 or m886), as described in Star Methods. After 10 days, whole GI compartments were collected, weighed, homogenized, and plated onto Sabouraud agar plates containing antibiotics. CFUs were quantified one day after plating. \*  $p < 0.05$ , unpaired Student's t-test.



Hypha-inducing conditions

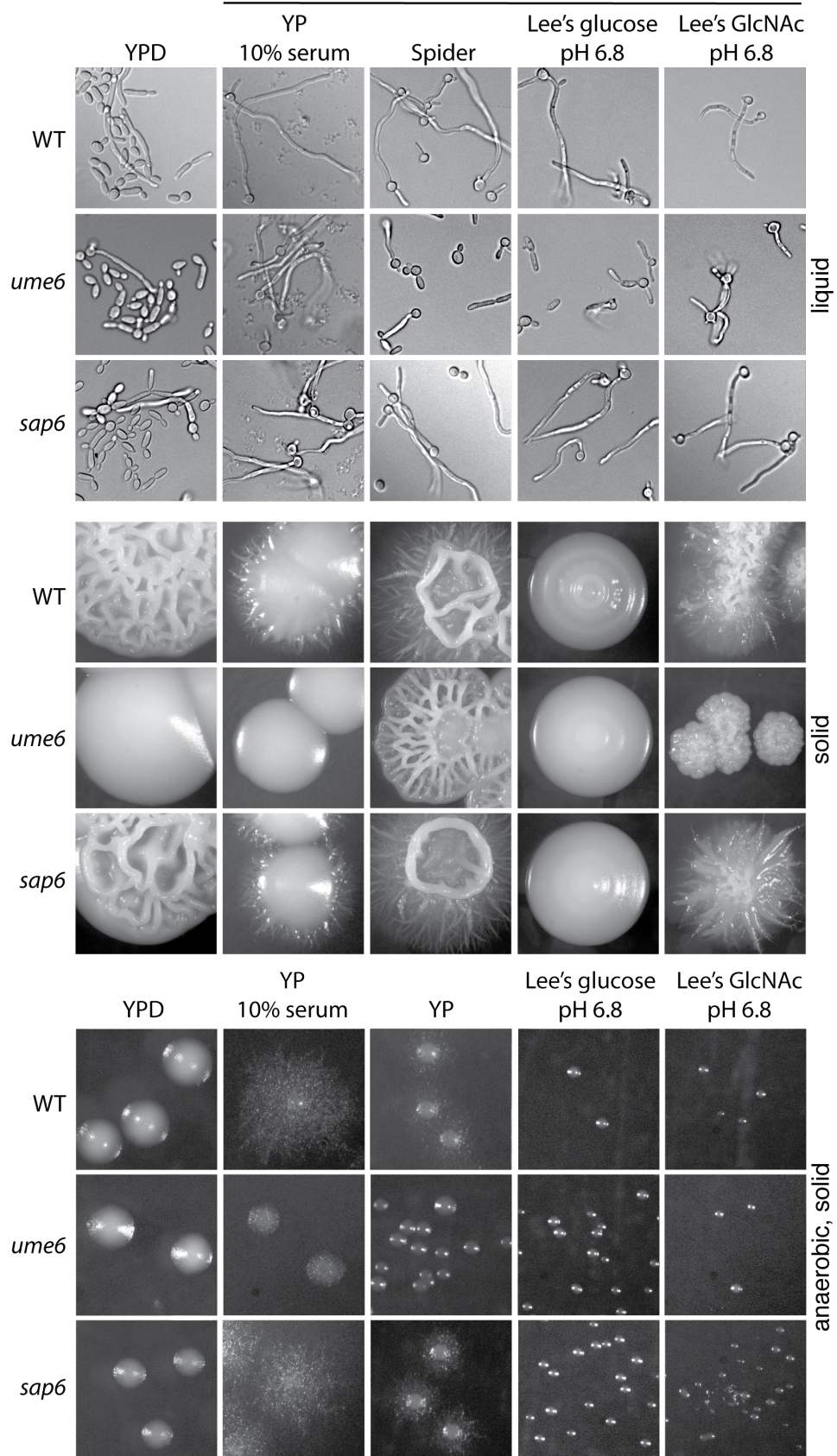


**Figure 2.S4. *ume6* is defective for filamentation *in vitro* but *sap6* displays normal filamentation.** Images depict representative cellular (upper) and colony (lower) morphology of wild-type *C. albicans* (SN250), *ume6* (SN1478), and *sap6* (m886). From saturated overnight cultures, cells for colony imaging were propagated on solid media (YPD/2% agar, YP+10% serum/2% agar, Spider/2% agar, Lee's glucose pH 6.8/2% agar, or Lee's GlcNAc pH 6.8/2% agar) for 5 days at 37°C, and those for imaging of cell morphology were diluted to  $A_{600}$  0.1 and propagated in liquid media (YPD, YP+10% serum, Spider, Lee's glucose pH 6.8, or Lee's GlcNAc pH 6.8) for 4 hours at 37°C. For assessment of colony morphology under anaerobic conditions, plated cells were propagated overnight in air at 37°C prior to being transferred to an airtight container containing a BD Anaerobe Gas Generator Pouch with Indicator for an additional 4 days at 37°C.

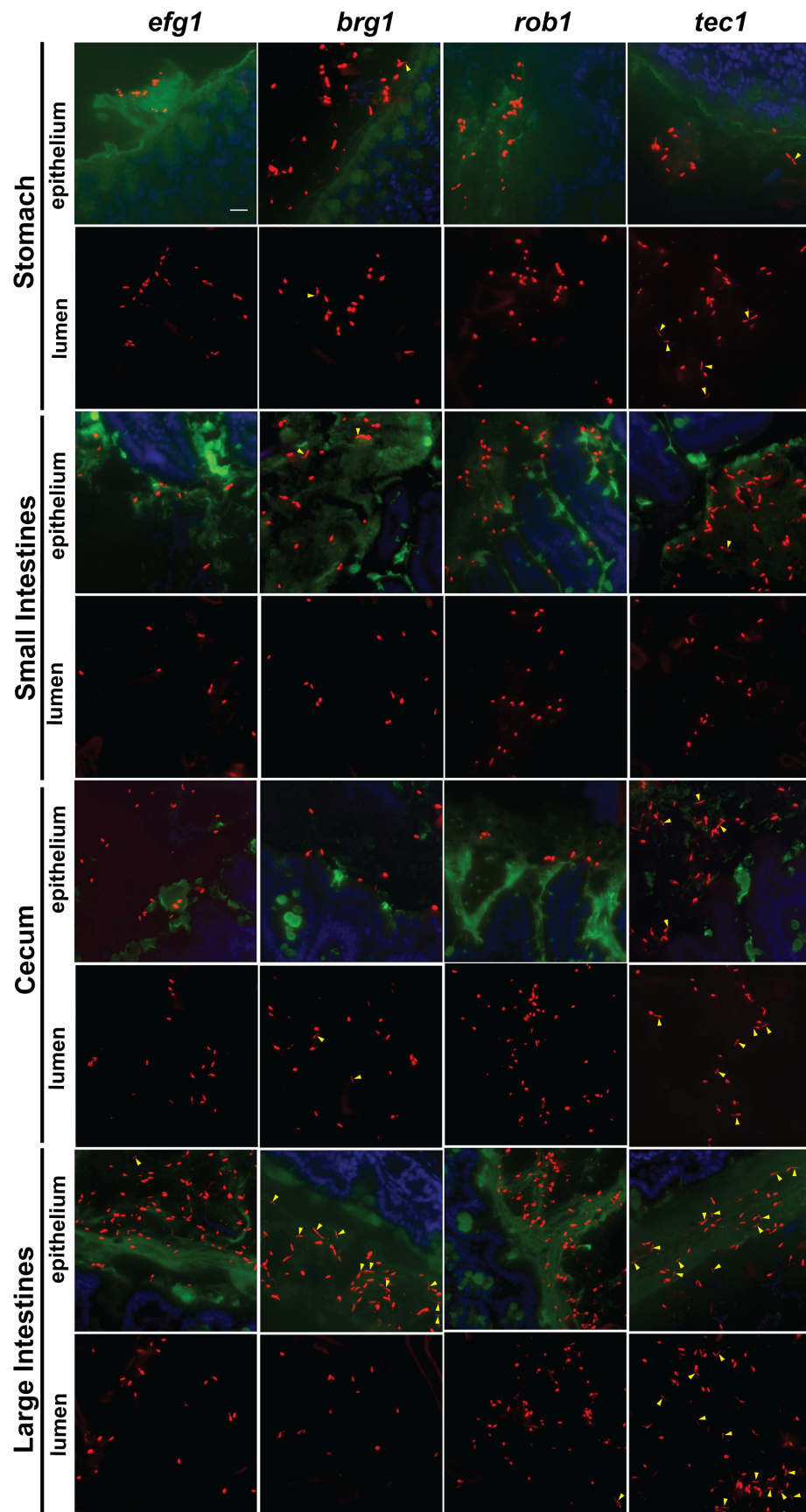


**Figure 2.S5. Propagation within the host GI tract suppresses the filamentation defect of *tec1* but not *efg1*, *brg1*, or *rob1*.** Groups of three mice were individually colonized with *efg1* (ySN1011), *rob1* (SN1439), *tec1* (SN1441), or *brg1* (SN1106) for 10 days prior to visualization of *C. albicans* morphology using FISH. Red: *C. albicans* (Cy3-coupled fungal-specific oligonucleotide), green: mucus (FITC-coupled lectin UEA-1 +/- WGA-1), blue: host epithelium (DAPI). Scale bar is 20  $\mu$ m. Images are representative 18 fields of view assessed for each strain.

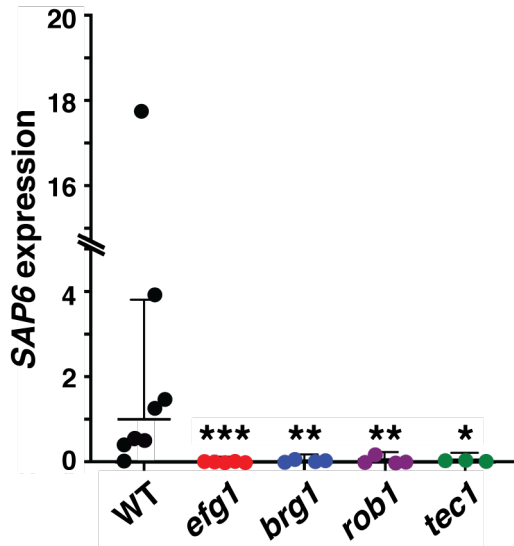


**Figure 2.S6. *SAP6* expression is downregulated in commensally propagated *efg1*, *brg1*, *rob1*, and *tec1* mutants.** Animals were individually colonized with WT (SN250, n=8 mice), *efg1* (SN1011, n=5 mice), *brg1* (SN1106, n=4 mice), *rob1* (SN1439, n=4 mice), or *tec1* (SN1441, n=3 mice). RNA was extracted from the contents of the large intestines (*efg1*, *brg1*, *rob1*, *tec1*) or feces (WT), and RT-qPCR was performed to quantify *SAP6* levels; levels of the housekeeping gene *PMA1* were quantified as an internal control. Three technical replicates were performed for each reaction, and each data point represents the mean result for *SAP6* expression (normalized to *PMA1*) in one animal. Also shown are the mean and standard deviation of the mean for each set of biological replicates. The significance of differences between WT and each mutant was determined using a one-tailed Mann-Whitney U test, \*p<0.05, \*\*p<0.01, \*\*\*p<0.001.

**Table 2.S1-Strains used in this chapter**

Strain	Common Name	Full Genotype	Reference
SN87	Wild type	<i>leu2Δ/leu2Δ, ura3Δ/URA3, his1Δ/his1Δ, iro1Δ/IRO1, MTLα/MTLα</i>	[53]
SN152	Wild type	<i>leu2Δ/leu2Δ, ura3Δ/URA3, his1Δ/his1Δ, arg4Δ/arg4Δ, iro1Δ/IRO1, MTLα/ MTLα</i>	[53]
SN226	Wild type	<i>leu2Δ::C.d.HIS1/leu2Δ::C.m.LEU2, ura3Δ/URA3, his1Δ/his1Δ, iro1Δ/IRO1, MTLα/ MTLα</i>	[53]
SN228	Wild type	<i>leu2Δ::C.m.LEU2/leu2Δ, ura3Δ/URA3, his1Δ/his1Δ, arg4Δ/arg4Δ, iro1Δ/IRO1, MTLα/ MTLα</i>	This study
SN235	Wild type	<i>leu2Δ::C.d.HIS1/leu2Δ, ura3Δ/URA3, his1Δ/his1Δ, arg4Δ/arg4Δ, iro1Δ/IRO1, MTLα/ MTLα</i>	[16]
SN250	Wild type	<i>leu2Δ::C.d.HIS1/leu2Δ::C.m.LEU2, ura3Δ/URA3, his1Δ/his1Δ, arg4Δ/arg4Δ, iro1Δ/IRO1, MTLα/ MTLα</i>	[53]
SN425	Wild type	<i>leu2Δ::C.d.HIS1/leu2Δ::C.m.LEU2, ura3Δ/URA3, his1Δ/his1Δ, arg4Δ::C.d.ARG4/arg4Δ, iro1Δ/IRO1, MTLα/ MTLα</i>	[53]
SN1555	Wild type	<i>leu2Δ::C.d.HIS1-bar1/leu2Δ::CatetR, ura3Δ/URA3, his1Δ/his1Δ, arg4Δ/arg4Δ, iro1Δ/IRO1, MTLα/ MTLα</i>	This study
SN1556	Wild type	<i>leu2Δ::C.d.HIS1-bar2/leu2Δ::CatetR, ura3Δ/URA3, his1Δ/his1Δ, arg4Δ/arg4Δ, iro1Δ/IRO1, MTLα/ MTLα</i>	This study
SN119	<i>efg1</i>	<i>efg1Δ::C.d.HIS1-ST1/efg1Δ::C.m.LEU2-ST49, leu2Δ/leu2Δ, ura3Δ/URA3, his1Δ/his1Δ, iro1Δ/IRO1, MTLα/ MTLα</i>	[53]
SN1011	<i>efg1</i>	<i>efg1Δ::C.d.HIS1/efg1Δ::C.m.LEU2, leu2Δ/leu2Δ, ura3Δ/URA3, his1Δ/his1Δ, arg4Δ/arg4Δ, iro1Δ/IRO1, MTLα/ MTLα</i>	[52]
SN1106	<i>brg1</i>	<i>brg1Δ::ST32-C.d.HIS1/brg1Δ::ST32-C.m.LEU2, leu2Δ/leu2Δ, ura3Δ/URA3, his1Δ/his1Δ, arg4Δ/arg4Δ, iro1Δ/IRO1, MTLα/ MTLα</i>	[52]
SN1107	<i>brg1</i>	<i>brg1Δ::ST32-C.d.HIS1/brg1Δ::ST32-C.m.LEU2, leu2Δ/leu2Δ, ura3Δ/URA3, his1Δ/his1Δ, arg4Δ/arg4Δ, iro1Δ/IRO1, MTLα/ MTLα</i>	[52]
SN1180	<i>brg1; ARG4 addback</i>	<i>brg1Δ::ST32-C.d.HIS1/brg1Δ::ST32-C.m.LEU2, leu2Δ/leu2Δ, ura3Δ/URA3, his1Δ/his1Δ, arg4Δ::C.d.ARG4/arg4Δ, iro1Δ/IRO1, MTLα/ MTLα</i>	This study
SN1439	<i>rob1</i>	<i>rob1Δ::ST13-C.d.HIS1/rob1Δ::ST13-C.m.LEU2, leu2Δ/leu2Δ, ura3Δ/URA3, his1Δ/his1Δ, arg4Δ/arg4Δ, iro1Δ/IRO1, MTLα/ MTLα</i>	[52]

Strain	Common Name	Full Genotype	Reference
SN1440	<i>rob1</i>	<i>rob1Δ::ST13-C.d.HIS1/rob1Δ::ST13-C.m.LEU2, leu2Δ/leu2Δ, ura3Δ/URA3, his1Δ/his1Δ, arg4Δ/arg4Δ, iro1Δ/IRO1, MTLα/ MTLα</i>	[52]
SN1441	<i>tec1</i>	<i>tec1Δ::ST23-C.d.HIS1/tec1Δ::ST23-C.m.LEU2, leu2Δ/leu2Δ, ura3Δ/URA3, his1Δ/his1Δ, arg4Δ/arg4Δ, iro1Δ/IRO1, MTLα/ MTLα</i>	[52]
SN1442	<i>tec1</i>	<i>tec1Δ::ST23-C.d.HIS1/tec1Δ::ST23-C.m.LEU2, leu2Δ/leu2Δ, ura3Δ/URA3, his1Δ/his1Δ, arg4Δ/arg4Δ, iro1Δ/IRO1, MTLα/ MTLα</i>	[52]
SN1478	<i>ume6</i>	<i>ume6Δ::ST21-C.d.HIS1/ume6Δ::ST69-C.m.LEU2, leu2Δ/leu2Δ, ura3Δ/URA3, his1Δ/his1Δ, arg4Δ/arg4Δ, iro1Δ/IRO1, MTLα/ MTLα</i>	This study
SN1479	<i>ume6</i>	<i>ume6Δ::ST21-C.d.HIS1/ume6Δ::ST69-C.m.LEU2, leu2Δ/leu2Δ, ura3Δ/URA3, his1Δ/his1Δ, arg4Δ/arg4Δ, iro1Δ/IRO1, MTLα/ MTLα</i>	This study
SN1557	<i>tetO-Ume6</i>	<i>FRT-MAL2p-FLP-SAT1-FRT-tetO-UME6/UME6 leu2Δ::C.d.HIS1-bar4/leu2Δ::CatetR, ura3Δ/URA3, his1Δ/his1Δ, arg4Δ/arg4Δ, iro1Δ/IRO1, MTLα/ MTLα</i>	This study
SN1558	<i>tetO-Ume6</i>	<i>FRT-tetO-UME6/UME6 leu2Δ::C.d.HIS1-bar8/leu2Δ::CatetR, ura3Δ/URA3, his1Δ/his1Δ, arg4Δ/arg4Δ, iro1Δ/IRO1, MTLα/ MTLα</i>	This study
m886	<i>sap6</i>	<i>sap6Δ::ST22-C.d.HIS1/sap6Δ::ST22-C.m.LEU2, leu2Δ/leu2Δ, ura3Δ/URA3, his1Δ/his1Δ, arg4Δ/arg4Δ, iro1Δ/IRO1, MTLα/ MTLα</i>	[53]
SN1663	<i>sap6 het</i>	<i>sap6Δ::ST22-C.m.LEU2/SAP6, leu2Δ/leu2Δ, ura3Δ/URA3, his1Δ/his1Δ, arg4Δ/arg4Δ, iro1Δ/IRO1, MTLα/ MTLα</i>	This study
SN1664	<i>sap6</i>	<i>sap6Δ::ST22-C.d.HIS1/sap6Δ::ST22-C.m.LEU2, leu2Δ/leu2Δ, ura3Δ/URA3, his1Δ/his1Δ, arg4Δ/arg4Δ, iro1Δ/IRO1, MTLα/ MTLα</i>	This study
SN510	<i>hyr1</i>	<i>hyr1Δ::ST7-C.d.HIS1/hyr1Δ::ST55-C.m.LEU2, leu2Δ/leu2Δ, ura3Δ/URA3, his1Δ/his1Δ, arg4Δ/arg4Δ, iro1Δ/IRO1, MTLα/ MTLα</i>	[53]
SN511	<i>hyr1</i>	<i>hyr1Δ::ST7-C.d.HIS1/hyr1Δ::ST55-C.m.LEU2, leu2Δ/leu2Δ, ura3Δ/URA3, his1Δ/his1Δ, arg4Δ/arg4Δ, iro1Δ/IRO1, MTLα/ MTLα</i>	[53]
SN1796	<i>sap6; SAP6 addback</i>	<i>sap6Δ::SAP6-FRT/sap6Δ::ST22-C.m.LEU2, leu2Δ/leu2Δ, ura3Δ/URA3, his1Δ/his1Δ, arg4Δ/arg4Δ, iro1Δ/IRO1, MTLα/ MTLα</i>	This study
SN1798	<i>SAP6-OE</i>	<i>sap6Δ::ST22-C.d.HIS1/sap6Δ::FRT-FLP-SAT1-FRT-TDH3prom-SAP6, leu2Δ/leu2Δ, ura3Δ/URA3, his1Δ/his1Δ, arg4Δ/arg4Δ, iro1Δ/IRO1, MTLα/ MTLα</i>	This study

## CHAPTER III: *LACTOBACILLUS PLANTARUM* COUNTERACTS GASTROINTESTINAL COMMENSAL ADVANTAGE OF *CANDIDA ALBICANS* GUT CELLS

### ABSTRACT

*Candida albicans*' role as the primary human fungal pathogen has been widely studied, but its predominant role as a commensal is less well understood. While *C. albicans* can exist as a commensal in many host niches, its primary reservoir is the GI tract. As a member of the GI commensal microbiota, *C. albicans*' interactions with bacterial members of the microbiome are critical for commensal colonization. We previously reported that WOR1 overexpressing (*WOR1<sup>OE</sup>*) *C. albicans* undergoes a unique morphological switch in the GI tract to GUT cells, which are specialized for survival in this niche. Here, we report that the GUT cell commensal advantage is lost in mice with high levels of *Lactobacillus spp.* Interestingly, *Lactobacilli* also promote robust filamentation of GUT cells via high levels of lactic acid production. These findings provide novel insights into how the bacterial and fungal components of the microbiome interact with each other and the effect that *Lactobacillus spp.* have on *C. albicans*' ability to maintain a commensal state.

### INTRODUCTION

Of the 20 species of *Candida* responsible for the millions of Candidiasis infections every year, *C. albicans* is the most common<sup>102</sup>. Disease manifestations include infections of the mouth, skin, and vagina, as well as disseminated disease.

Despite predominantly being known for its role as a pathogen, *C. albicans* primarily exists as a commensal, inhabiting approximately 70% of the healthy human population as a benign member of the microbiome<sup>103</sup>. Most individuals are colonized at a young age and the initial colonizers persist throughout an individual's lifetime causing no harm to the host<sup>39</sup>.

While *C. albicans* exists as a commensal in many different host niches, the gastrointestinal tract is its primary reservoir<sup>104</sup>. Like many commensal bacterial species, colonization with *C. albicans* may be beneficial, as this species has been implicated in development of the mucosal immune system in mice<sup>12</sup>. The fungal component of the gastrointestinal microbiome, however, is less well studied than the bacterial compartment, even though fungi make up a significant portion of the GI microbial biomass<sup>8</sup>. Many of the studies investigating the GI mycobiota have focused on species composition as it relates to other microorganisms, with very little investigation into how species-species interactions influence commensal colonization<sup>10,103,105</sup>.

A clear role for interspecies interactions in altering colonization is apparent in the standard models for *C. albicans* colonization in the mouse. While *C. albicans* is a naturally occurring member of the human mycobiota, most laboratory bred mouse strains are naturally resistant to this particular species<sup>106</sup>. Although a variety of factors, such as diet, can be manipulated to promote intestinal colonization in mice, antibiotics are the most common method to achieve robust and persistent colonization of the GI tract<sup>29</sup>. This indicates that interactions between bacterial species and *C. albicans* directly affects colonization establishment, and could potentially affect commensal fitness. Previous studies in mice reveal that commensal bacteria can inhibit *C. albicans*



colonization by promoting host expression of an antimicrobial peptide and an activator of the innate immune system<sup>30</sup>. In humans, it well known that antibiotic administration directly affects fungal growth or inhibition<sup>107</sup>. One of the most commonly cited examples is oral thrush, or *C. albicans* overgrowth on the tongue and mouth, that can accompany prolonged antibiotic administration. Within the human GI tract, the presence of *Lactobacillus spp.* has commonly been associated with reduced *C. albicans* numbers<sup>108,109</sup>.

*Lactobacillus spp.* belong to the bacterial phylum, Firmicutes, one of the most common bacterial phyla found in the human GI tract<sup>110</sup>. They have been isolated from all compartments of the human gut<sup>111</sup>. Studies in rodents naturally colonized with *Lactobacillus spp.* reveal that most are concentrated in the proximal gut<sup>112</sup> (primarily stomach and small intestine), but are still present in other compartments making up about 25% of the bacteria in the colon<sup>111</sup>.

The interaction between *Lactobacillus spp.* and *C. albicans* has been suggested to be antagonistic based on observations using both *in vitro* and *in vivo* models. *In vitro*, *Lactobacillus* inhibits *C. albicans* growth, hyphal morphogenesis, adhesion, and biofilm formation all of which are important characteristics that promote *C. albicans* pathogenesis<sup>113,114</sup>. An *in vitro* model that mimics the human gut demonstrated that addition of *Lactobacillus spp.* significantly decreased *C. albicans* numbers throughout the flow culture system<sup>115</sup>. Mouse models of GI commensal colonization reveal that the presence of *Lactobacillus spp.* may inhibit colonization with *C. albicans*<sup>116</sup> and addition of *Lactobacillus spp.* as a probiotic has been associated with decreased *C. albicans* cell numbers in the gut of a small cohort of human patients with Familial Mediterranean

Fever<sup>117</sup>. Interestingly, experimental colonization of mice with *C. albicans* post antibiotic treatment has been reported to prevent resurgence of *Lactobacillus spp.* that were present prior to antibiotic administration<sup>31</sup>, indicating that the antagonism between these two species may be bidirectional. Similar observations have been made in humans, whereby oral administration of *Lactobacillus* to adults and babies significantly decreased *Candida* colonization as assessed by fungal cultures from saliva or the GI tract respectively<sup>108,109</sup>

These studies suggesting possible antagonism between *Lactobacillus spp* and *C. albicans* growth and morphogenesis, were conducted with *C. albicans* white cells, the phenotypic form of *C. albicans* that is most commonly observed and isolated under *in vitro* conditions. Previous work in our lab, however, has revealed that *C. albicans* undergoes a phenotypic switch in the GI tract to GUT cells<sup>16</sup>, which are uniquely adapted for survival in the mammalian GI tract. GUT cells were first discovered because a *C. albicans* strain overexpressing the transcription factor *WOR1*, formed greyer, flatter colonies on plates approximately 10-15 days after colonization of the GI tract. These phenotypically distinct colonies were composed of elongated cells, as compared to the standard round-to-oval shaped white cells. Once formed GUT cells quickly dominate the fungal population and are maintained throughout the course of the experiment. When reintroduced into naïve animals, GUT cells are immediately hypercompetitive compared to white strains. To understand how bacterial-fungal interactions mediate commensal colonization in the mammalian gastrointestinal tract, it will be important to examine the interactions of bacteria with GUT cells.

In this study, we demonstrate that species-species interactions between *C. albicans* GUT cells and *Lactobacillus plantarum* counteract the ability of GUT cells to persist in the GI tract. While GUT cells consistently outcompete *C. albicans* white cells in gut colonization experiments of animals reared in a local mouse facility (Hollister, California), we observed that this is not the case in genetically identical animals obtained from a more distant facility (Kingston, NY). The major difference in bacterial microbiome composition is the abundance of *Lactobacillus spp.* in Kingston mice. We demonstrate that *Lactobacillus spp.* both antagonize recovery of GUT cells from the GI tract and promote filamentation in GUT cells under *in vitro* conditions, which are normally less responsive to classic filamentation cues. This study provides an example of how species-species interaction influences fungal commensal colonization of the mammalian GI tract.

## **RESULTS**

### **Reduced propensity of GUT cells to filament promotes their GI commensal advantage**

We previously showed that passage of a *C. albicans* strain that constitutively expresses *WOR1* (*WOR1*<sup>OE</sup>) through a murine gastrointestinal colonization model induces a cell type switch to the GUT phenotype, which is uniquely adapted for survival in the mammalian GI tract. The switch to GUT cells only occurs after passage through the GI tract and in the presence of high levels of *WOR1* expression, suggesting the importance of both of these signals in the formation and maintenance of the GUT phenotype. While we believe that wild-type *C. albicans* is also able to form GUT cells,

we have only detected this phenotype in strains where *WOR1* is constitutively expressed because *WOR1* is required to stabilize the phenotype, and *WOR1* is not typically expressed when cells are propagated under laboratory conditions.

One of the reasons we hypothesize that GUT cells possess a commensal fitness advantage is because of their decreased ability to respond to classic filamentation cues. As hyphae have primarily been characterized for their role in virulence and pathogenesis, the GUT cell's commensal fitness advantage may be partially explained by their lowered propensity to filament. In separate work, we demonstrated that the certain hypha-specific proteins, such as Sap6, substantially reduce the fitness of *C. albicans* in the GI tract (Witchley, Penumetcha, *et al.* submitted). Here, we used fluorescence *in situ* hybridization (FISH) to compare the morphology of commensal *C. albicans* white cells vs. GUT cells in the murine commensal model. Mice were orally gavaged with either, wild-type white, *WOR1<sup>OE</sup>* white, or *WOR1<sup>OE</sup>* GUT cells. After 3 days of colonization, mice were sacrificed and sections of the GI tract (stomach, small intestines, cecum and large intestines) were removed and preserved in methacarn, a fixative that preserves the mucus layer of the gut. Histological examination of *C. albicans* in each compartment with a pan-fungal FISH probe revealed that white and *WOR1<sup>OE</sup>* white cells predominate as yeasts proximally (stomach and small intestines), but form high levels of hyphae distally (cecum and large intestines; Figure 3.1; Figure 3.S1). This is consistent with the high levels of hyphal inducing signals in the distal GI tract (hypoxia, hypercarbia and the presence of N-acetylglucosamine), as well as previous observations made in Chapter II. *WOR1<sup>OE</sup>* GUT cells, on the other hand, primarily colonize as yeasts in all observed compartments, with significantly higher

levels of yeast than both white and *WOR1<sup>OE</sup>* white cells in distal compartments (Figure 3.1).

To determine whether GUT cell filamentation is also reduced under *in vitro* conditions, we tested the ability of GUT cells to form hyphae on Spider medium, a medium that promotes filamentous growth<sup>118</sup> at 37°C. As compared to YPD medium, both white and *WOR1<sup>OE</sup>* white cells grew as wrinkled colonies on the plate, which, upon microscopic examination, were confirmed to be filamentous hyphae (Figure 3.1). GUT cells, however, grew as smooth colonies on both YPD and Spider media, and remained as yeasts (Figure 3.1). Taken together, these results indicate that GUT cells are less responsive to the filamentation cues found in the distal GI tract, as well as upon exposure to filament-inducing conditions *in vitro*.

### **GUT cell commensal advantage is lost in mice co-colonized with *Lactobacillus spp.***

Our animal experiments are routinely performed with BALB/c mice purchased from a commercial vendor, Charles River, whose nearest facility is in Hollister, California. For a six-month period, the Hollister facility was unavailable and animals from other Charles River locations were used. To our surprise, we were no longer able to recover *C. albicans* GUT cells from the GI commensalism model during this period (J. Witchley, data not shown). We therefore asked whether differences among animals bred at different facilities might account for the observed differences in the recovery and persistence of GUT cells from the GI tract.

We obtained 4 animals each from Charles River facilities in Hollister, California, Kingston, New York, and Canada. Two mice from the Kingston facility were contaminated with pen/strep resistant bacteria and were not used in subsequent analysis. The mice were colonized with a one-to-one competition of white cells to *WOR1<sup>OE</sup>* white cells (the latter are capable of stable switching to the GUT phenotype in the GI tract), because GUT cells were first identified when *WOR1<sup>OE</sup>* white cells outcompeted white cells *in vivo*. Feces were plated onto Sabouraud plates containing penicillin (1500un/ml) and streptomycin (2mg/ml) to monitor for appearance of GUT cells and abundances of wild-type and *WOR1<sup>OE</sup>* white strains. *C. albicans* recovered from Hollister facility mice displayed the normal trajectory of GUT cell development, whereby GUT cells appeared around day 10 post colonization and then persisted for the remainder of the experiment (Figure 3.2). In mice from the Canada facility, however, GUT cells appeared starting at day 10, but did not dominate the population even after thirty days of colonization. Most interestingly, in the Kingston facility, GUT cells appeared and dominated the population at day 15, but were rapidly depleted by day 20 (Figure 3.2), concomitant with a decreased abundance of the *WOR1<sup>OE</sup>* white strain, as determined by qPCR (J. Witchley, data not shown). These data suggested that the microbiome plays a role in both appearance and persistence of GUT cells.

To determine whether the Kingston microbiota's effect on GUT colonization was dominant over the Hollister microbiota, we performed a co-housing experiment. After 30 days of colonization, one mouse from each Kingston cage was co-housed with one mouse from each Hollister cage (total of 4 animals) and GUT cell recovery was assessed as before by plating fecal CFUs. Indeed, we observed that, while co-housing

the Kingston and Hollister animals caused an initial reappearance of GUT cells in Kingston mice, this was followed by a rapid clearance of this cell type in both Kingston and Hollister mice. (Figure 3.2). This suggested that the Kingston microbiota exerted a dominant effect over the Hollister microbiota in antagonizing GUT cell commensal colonization.

As the mice from all of these facilities are genetically identical, we hypothesized that differences in the bacterial microbiota of animals reared at different facilities might impact GUT cell fitness. Specifically, we hypothesized that Kingston animals are colonized with bacterial species that adversely affect the fitness of *C. albicans* GUT cells. In collaboration with the Koh lab, we used qPCR primers that hybridize to most bacteria and ones with specific for *Enterobacteriaceae*, *Bacteroides spp.*, *Clostridial cluster IV* and *Lactobacillus spp.*, we assessed bacterial levels in mice prior to and 20 days post colonization with *C. albicans*. At day 20, when GUT cells start to decrease in Kingston mice, *Lactobacilli* are the only class of bacteria that was significantly enriched in Kingston animals compared to Hollister animals (Figure 3.2). From these results, we hypothesized that *Lactobacilli* may be responsible for counteracting the GUT cell fitness advantage in Kingston mice.

### ***Lactobacillus* counteracts GUT cell commensal advantage in Hollister mice**

To determine whether *Lactobacillus* alone is capable of promoting GUT cell loss, we asked whether introduction of *Lactobacillus* to the Hollister mice (which normally have low levels of *Lactobacilli* compared to Kingston mice) would be sufficient to prevent GUT cell recovery from the GI tract. To perform co-infections of these two

species, however, we had to modify our mouse model. Normally, animals receive drinking water that contains penicillin and streptomycin starting 7 days prior to gavage, continuing for the duration of the experiment. Most *Lactobacillus* species, however, are sensitive to penicillin, so we removed this antibiotic from the treatment regimen. Of the *Lactobacillus* species we tested (*L. casei*, *L. brevis*, *L. acidophilus*, *L. reuteri*, *L. rhamnosus*, and *L. plantarum*) *L. plantarum* displayed the highest levels of resistance to streptomycin (Figure 3.S2). This species is among the most abundant *Lactobacilli* species that are isolated from the human GI tract<sup>111</sup>, so all *in vivo* experiments were conducted with this species.

We wanted to determine whether introduction of high levels of *L. plantarum* into Hollister mice would impact GUT cell recovery from the GI tract. Seven mice total over two independent experiments were first orally gavaged with two successive doses of  $1 \times 10^9$  *L. plantarum*, followed by  $1 \times 10^8$  *WOR1<sup>OE</sup>* white *C. albicans* 6 days later. In mice that were only colonized with *C. albicans*, we saw normal levels of white-to-GUT switching (90%-100% of cells at day 10 post *C. albicans* gavage), as well as maintenance and predominance of the GUT phenotype, once formed (Figure 3.3). In the presence of *L. plantarum*, however, we were not able to recover GUT cells throughout the course of the experiment and also observed an overall decrease in CFUs (Figure 3.3). Given that GUT cells were able to form, but not maintain their commensal dominance in Kingston mice (Figure 3.2), these results suggest that *L. plantarum* promotes rapid loss of GUT cell CFUs from the GI tract, such that they cannot be recovered *ex vivo*.



### ***Lactobacilli* promote filamentation in GUT cells *in vitro*, but not *in vivo***

Given that GUT cells are lost in mice pre-colonized with *Lactobacillus spp.*, we were intrigued by a report that certain *Lactobacillus spp.* induce filamentation in *C. albicans* opaque cells<sup>119</sup>, the sexually competent cell type in this species. Opaque cells have an elongated shape that is similar to that of GUT cells, but the two cell types are genetically and functionally distinct. To determine whether *Lactobacillus spp.* affect the cell morphology of GUT cells, we tested a panel of bacteria against *C. albicans* and found robust filamentation in GUT cells exposed to *L. plantarum*, but not white or WOR1<sup>OE</sup> white cells (Figure 3.4). This phenotype was reproducible with different species of *Lactobacillus*, such as *L. casei*, *L. rhamnosus* and *L. brevis*, but not other bacterial species such as *E. coli*, *S. epidermidis* and *E. faecalis* (Figure 3.S3). We verified that *Lactobacillus spp.* induce the formation of true hyphae in GUT cells by staining septae (demarcations of cell walls between hyphal daughter cells) with calcofluor white (Figure 3.4). Taken together, these results indicate that *Lactobacillus spp.* promote true hyphal elongation in GUT cells, which are less responsive to classic *in vitro* filamentation cues.

As we have previously shown that filamentation is detrimental to GI commensalism (Chapter II), we hypothesized that *Lactobacillus*-mediated filamentation was the reason GUT cells are not recovered from mice colonized with *L. plantarum*. We pre-colonized mice with either white, WOR1<sup>OE</sup> white or WOR1<sup>OE</sup> GUT cells followed by a dose of *L. plantarum* one day later. Surprisingly, we saw that GUT cells were still less filamentous than white cells even in the presence of *L. plantarum* (Figure 3.5). It is possible that because many compartments of the GI tract are replete with hyphal

inducing conditions (hypoxia, CO<sub>2</sub>, high pH, temperature), these signals override the anti-filamentation effect of *L. plantarum* on white cells and, therefore, any differences between white and GUT cells are muted. Regardless, we also do not observe increased filamentation in GUT cells co-colonized with *L. plantarum* as compared to mice colonized with GUT cells alone, with the exception of a insignificant increase in hyphae in the cecum (Figure 3.5). Therefore, while *L. plantarum* is a strong inducer of GUT cell filamentation *in vitro*, GUT cells are not sensitive to the pro-filamentation effects of this bacterium in our mouse model.

In previous work (Chapter II), we found the expression of hypha-associated proteins, rather than hypha morphology per se, inhibits *C. albicans* fitness in the gut. To determine whether *in vivo* exposure to *L. plantarum* induces hypha-associated genes in GUT cells (without affected cell shape), we pre-colonized mice with white or GUT cells followed by gavage with *L. plantarum* on consecutive days, and performed mRNA-seq on large intestine content samples collected three days after the last *L. plantarum* gavage. A relatively low number of white cells recovered from animals co-infected with *L. plantarum* in this pilot experiment, and the results should be considered preliminary. Consistent with a decreased propensity for hypha formation, GUT cells expressed lower levels of transcripts for several hyphal-associated cell wall proteins compared to white cells, even in the presence of *L. plantarum* (Table 3.1). *In vivo* exposure of GUT cells to *L. plantarum* resulted in differential expression of only either genes compared to mice with GUT cells alone (Table 3.1). Interestingly, *UME6*, which encodes the ‘master regulator’ of hypha-associated genes<sup>64</sup>, is eight-fold upregulated in GUT cells in the presence of *L. plantarum*. Higher levels of Ume6 expression in GUT cells co-colonized

with *L. plantarum*, could indicate the transcriptional program of GUT cells starts to resemble hyphal cells early, but that full expression of hyphal associated proteins takes longer to establish. This idea is supported by the results in Table 3.1, which show that many of the hyphal associated proteins show a greater than 2-fold increase in mice co-colonized with GUT cells and *L. plantarum*, as compared to mice with just GUT cells, with the differential of Als3 expression approaching significance. Further studies investigating how *L. plantarum* changes GUT cell expression long term during GI colonization is required to fully understand how *L. plantarum* antagonizes GUT cell commensal fitness.

### **Lactate dehydrogenase genes are responsible for *L. plantarum* induced GUT cell filamentation**

To understand whether *L. plantarum* induced GUT cell filamentation was dependent on metabolic processes of the bacteria, we co-incubated *C. albicans* with heat-killed *L. plantarum*. GUT cells no longer filamented when propagated near the heat-killed bacteria (Figure 3.6), suggesting that active metabolism is required for the filament-inducing activity. Liang *et al.* reported that the pro-filamentation effect of *L. plantarum* on *C. albicans* opaque cells can be reproduced by exposure to lactic acid<sup>119</sup>, a major secreted metabolite of many *Lactobacillus* species. Using a strain of *L. plantarum* (TF103) that lacks both lactate dehydrogenase genes that are required for efficient lactic acid production, we saw a complete reversal of GUT cell filamentation that is normally observed in the presence of *L. plantarum* (Figure 3.6).

Interestingly, the TF103 is still able to make lactate at levels of 12-14mM, but this is far reduced compared to the 500mM that is produced in the matched wild-type strain (Liu et al., data not shown). The fact that GUT cell filamentation is dependent on the level of lactic acid produced by a particular *Lactobacillus* species is consistent with the observation that certain *Lactobacillus* species do not promote GUT cell filamentation (Figure 3.S3) and that WT *L. plantarum* induces a dose-dependent response of GUT cell filamentation, whereby 10-fold dilutions of *L. plantarum* causes a disappearance of GUT cell filamentation at a ratio of 1:100 (GUT cells:*L. plantarum*; Figure 3.S4). Additionally, the high levels of lactic acid production necessary to induce filamentation *in vitro* may be partially responsible for the lack of *Lactobacillus*-induced GUT cell filamentation *in vivo*, as seen in Figure 3.5. These findings suggest that *Lactobacillus*-mediated GUT cell filamentation is dependent not only on lactate dehydrogenase biochemical pathway, but also on the amount of lactate produced.

## DISCUSSION

Our gastrointestinal commensal microbiota is often thought of as an organ system itself because of its importance in maintaining intestinal health and homeostasis. A critical factor for determining how this compartment promotes health, is understanding how commensal populations are maintained in this niche. The great diversity of microbes within our guts implicates that microbial interactions are an integral factor in this process.

Microbial interactions in the mammalian gastrointestinal tract are not well understood, particularly, how the bacterial and fungal components interact with each

other to promote or inhibit GI commensal colonization. Previous work has firmly established *Lactobacillus spp.*, a common and prevalent colonizer of the mammalian gut, as antagonizers of *C. albicans* growth, hyphal formation and GI colonization. These studies, however, were all performed with white cells and not the commensally adapted GUT cell.

The observation that *Lactobacillus spp.* promoted GUT cell filamentation *in vitro* was surprising given that GUT cells are hypofilamentous in classic filament-inducing conditions. Even the presence of strong hypha-forming signals found in the distal GI tract (high levels of CO<sub>2</sub> and N-acetylglucosamine, and lower levels of oxygen) did not cause wild-type levels of filamentation in GUT cells. The loss of GUT cells from mice highly colonized with *Lactobacillus spp.* combined with the knowledge that filamentation is detrimental to commensal colonization suggested that filamentation may be responsible for GUT cell loss in the presence of *Lactobacilli*.

Surprisingly, however, we did not observe increased levels of GUT cell filamentation in mice co-colonized with *L. plantarum*, or compared to mice co-colonized with white cells and *L. plantarum*. Several explanations could account for this observation. First, the *in vitro* assay used to determine GUT cell-*L. plantarum* interaction, placed both species in direct contact with each other. It is possible that the fluidic, three-dimensional structures of the GI tract did not provide enough direct contact between the two species to induce filamentation.

The difficulty of reproducing *in vitro* bacterial-fungal interactions, *in vivo* has already been described with *C. albicans*-*P. aeruginosa* interactions. *In vitro*, *P. aeruginosa* quorum sensing molecules inhibit filamentation, but this effect is dampened

in hypoxic environments<sup>120</sup>. Similarly, the pH of the GI tract could complicate *L. plantarum*'s pro-filamentation effect on *C. albicans*, which we believe is in part mediated by lactate. Lactate can exist as lactic acid depending on the environmental pH. Lactic acid itself is membrane permeable, but lactate is not and requires a receptor to enter cells<sup>121</sup>. Lactic acid predominates in a low pH environment such as the stomach, but in high pH environments, such as the distal GI tract, it exists as lactate. Interestingly, GUT cells do not upregulate the *C. albicans*' lactate receptor, GPR1, in the mouse large intestines, as compared to GUT cells grown in standard media [30°C in YEPD; J. Witchley data not shown]. Therefore, it is possible that any lactate being produced by *L. plantarum* is not able to penetrate GUT cells and promote filamentation in the GI tract.

Finally, the level of lactate in the gut is likely a limiting factor in promoting GUT cell filamentation *in vivo*. First, lactate levels are variable along the GI tract and likely much lower than the high threshold required to see GUT cell filamentation *in vitro*. In fact, a study assessing lactate levels in patients with short bowel syndrome, found that lactate was observed at an upper threshold of 110mM<sup>122</sup>, far below the 500mM output that was observed in wild-type *L. plantarum* (bSN403).

While the mechanism of *L. plantarum* induced GUT cell loss *in vivo*, still remains to be determined, we provide strong evidence that a secreted bacterial metabolite promotes filamentation of a *C. albicans* morphotype *in vitro*. Secreted bacterial effectors are known to influence *Candida spp.* morphogenesis. *P. aeruginosa* has been shown to secrete both a secondary metabolite<sup>123</sup> and quorum sensing molecule<sup>124</sup> that inhibit hyphal formation. *E. faecalis*, another lactic acid producing bacterium, inhibits hyphal formation via a secreted bacteriocin<sup>125</sup>. Some bacterial cell wall components such as

muramyl dipeptides (components of the bacterial cell wall)<sup>126</sup> and peptidoglycan<sup>79</sup> have been shown to promote filamentation, but the majority of secreted bacterial effectors appear to inhibit hyphal morphogenesis. Therefore, our study provides a rare example of a secreted bacterial molecule promoting *C. albicans* filamentation. This phenomenon is particularly interesting because the hyphae inducing effect is specific to the commensally adapted GUT cells, which is normally less prone to filamentation. While it still remains to be determined how *L. plantarum*'s ability to promote GUT cell filamentation

We propose that *L. plantarum* induced GUT cell filamentation may be a mechanistic adaptation by *L. plantarum* to limit competition in the gastrointestinal tract. Because GUT cells are such robust colonizers of this niche, perhaps *L. plantarum* has evolved a mechanism to get rid of competitive species to reduce competition for resources. Further studies are required to determine the mechanisms behind this interaction. Overall, our study provides the first example of commensally relevant *C. albicans* interacts with the microbiome.

## **METHODS**

### **Strain Construction**

*C. albicans* strains construction has been previously described<sup>53</sup>. All *C. albicans* strains used in this study are detailed in Table 3.1. Bacterial strains were obtained from the ATCC or other labs (Table 3.2).

## Mouse Infections

All procedures involving animals were approved by the University of California at San Francisco Institutional Animal Care and Use Committee, which enforces the ethical and humane use of animals. *Monotypic Infections*: 6- to 8-week-old female BALB/c mice obtained from Charles River Laboratories, Hollister, Kingston or Canada facilities, were infected by oral gavage with *C. albicans* as previously described<sup>16</sup>. *Co-Infections with L. plantarum*: Mice were pre-treated with penicillin (Sigma #: PENNA-100MU) and streptomycin (Sigma #: S9137-100G) in their drinking water for 6 days, followed by streptomycin alone for three days prior to *L. plantarum* gavage. When mice were infected with *C. albicans* first, mice were pre-treated with pen/strep for 1 week and then water was changed to streptomycin alone at the time of gavage. All mice co-infected with *C. albicans* and *L. plantarum* were maintained on streptomycin water for the duration of the experiment. To prepare the *L. plantarum* inoculum, overnight cultures of *Lactobacillus* species (grown in MRS at 37°C) were re-inoculated onto 100mL of fresh MRS at an OD<sub>600</sub> of 0.1. Cultures were grown to an OD<sub>600</sub> of 0.8-1.0, washed 3X in saline and resuspended in saline to colonize mice with 1e9 CFUs. Mice were gavaged with *L. plantarum* on two consecutive days and all animals were co-housed. Following gavage, *L. plantarum* CFUs were confirmed by plating feces onto MRS + miconazole (Sigma #: M3512-5G), prior to *C. albicans* gavage one week later. *C. albicans* inocula were prepared as described above.



### ***C. albicans* and *L. plantarum* in vitro assays:**

*Combined growth for quantification:* *C. albicans* strains were streaked onto YPD media and incubated at 30°C. Bacterial strains were streaked onto MRS (Millipore Sigma #: 110660) or BHI (Becton Dickinson #: 211059) and incubated at 37°C. Cells were scrapped from plates and resuspended in dH<sub>2</sub>O to measure OD<sub>600</sub>. *C. albicans* cells were resuspended at an OD of 3.0 and bacterial cells were resuspended at an OD of 1.0. Yeast and bacterial cells were mixed together at a 1:1 ratio and 3uL was plated onto MRS plates. Single spots of yeast and bacteria were included for every experiment. Plates were incubated at 30°C for 6 days prior to analysis. For heat-killed *L. plantarum*, incubated cells (OD<sub>600</sub>=1.0) at 85°C for 10 minutes prior to mixing with *C. albicans*. To quantify percent filamentation, a small patch of cells was transferred onto a glass slide and stained with Calcofluor White (Sigma #: 18939-100ML-F) per manufacturer's instructions. Cells were imaged using Keyence microscope (BZ-X710) with a 40X objective and quantified 3-4 fields of view using Fiji. *Plating for single colonies:* *C. albicans* cells were streaked on selective SC media and then resuspended in dH<sub>2</sub>O, counted and resuspended in appropriate volume to plate 100 CFUs in 100uL onto YPD or Spider media. Plates were incubated at 37°C for 3 days prior to analysis.

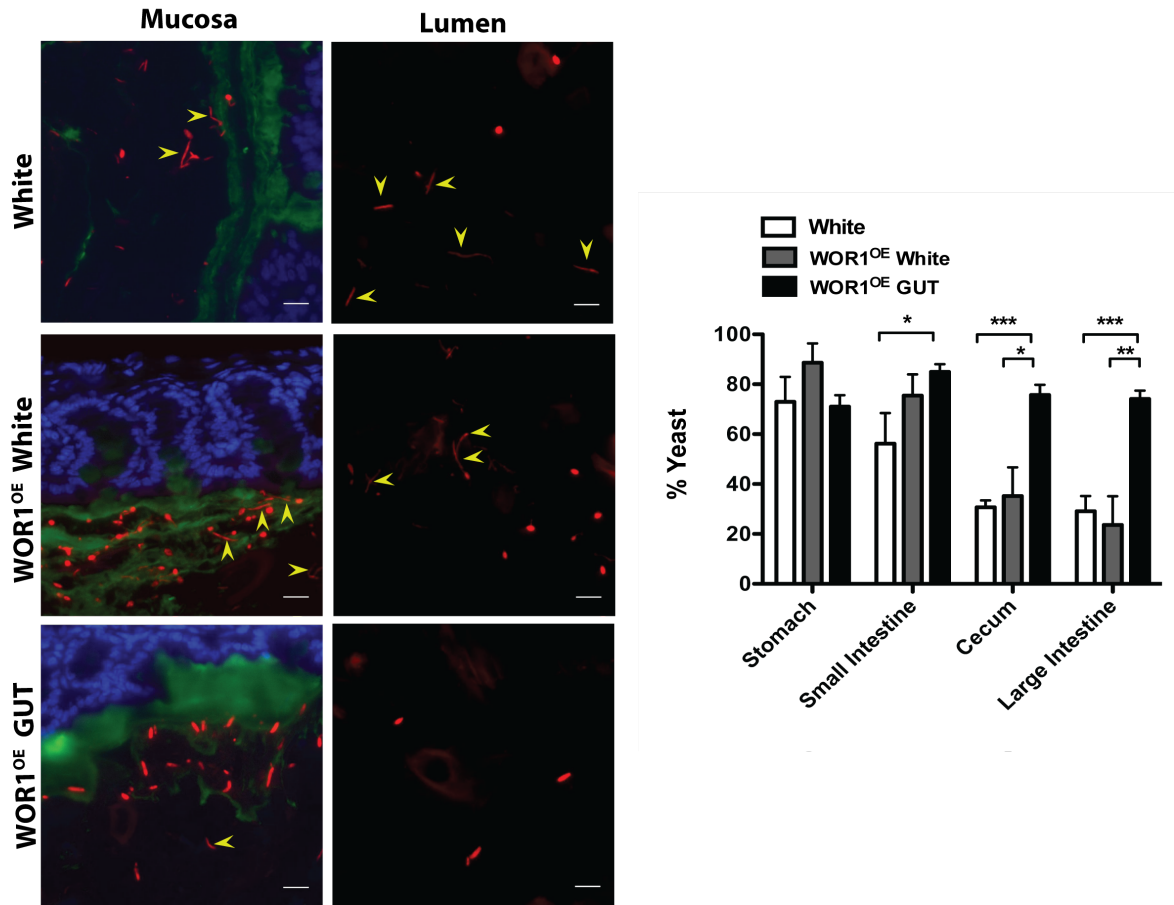
### **Fluorescence in situ hybridization (FISH):**

Gastrointestinal tissue (stomach, small intestine, cecum and large intestine) sections were dissected and preserved in methacarn (60% methanol, 30% chloroform and 10% glacial acetic acid) for at least 2 days (up to 2 weeks) at room temperature. Tissue sections were processed in the following washes: 2 x 35 minutes in methanol, 2 x 25

minutes in ethanol, 2 x 20 minutes in xylene and then places in melted paraffin wax (Sigma #: P3558-1KG) for two hours at 70°C. Paraffin embedded blocks and sectioned slides (4µm) were prepared by Nationwide Histology (Veradale, WA). Fluorescence *in situ* hybridization (FISH) was performed as previously described<sup>66</sup> with the following modifications: Fungal 28S rRNA was stained with a DNA oligonucleotide that is coupled to Cy3 (5'-Cy3-CTCTGGCTTCACCCTATTC-3'; Integrated DNA Technologies). Hybridization was performed for three hours at 50°C. Next, epithelial cell nuclei and mucin were counterstained with DAPI and FITC-conjugated UEA-1 (Sigma#: L9006-1MG), respectively, for 45 minutes at 4°C. Because staining of mucin in the small intestine and cecum specimens was less efficient, FITC-conjugated WGA-1 (Sigma#: L4895-2MG) was added for counterstaining of these sections. Sections were mounted with Vectashield (Vector Laboratories #: 101098-042) and imaged using Keyence microscope model BZ-X700. Yeasts and hyphae in 20 fields of view were quantified for each sample. Counts were analyzed using the cell counter plug-in for Fiji (ImageJ).

# FIGURES

A.



B.

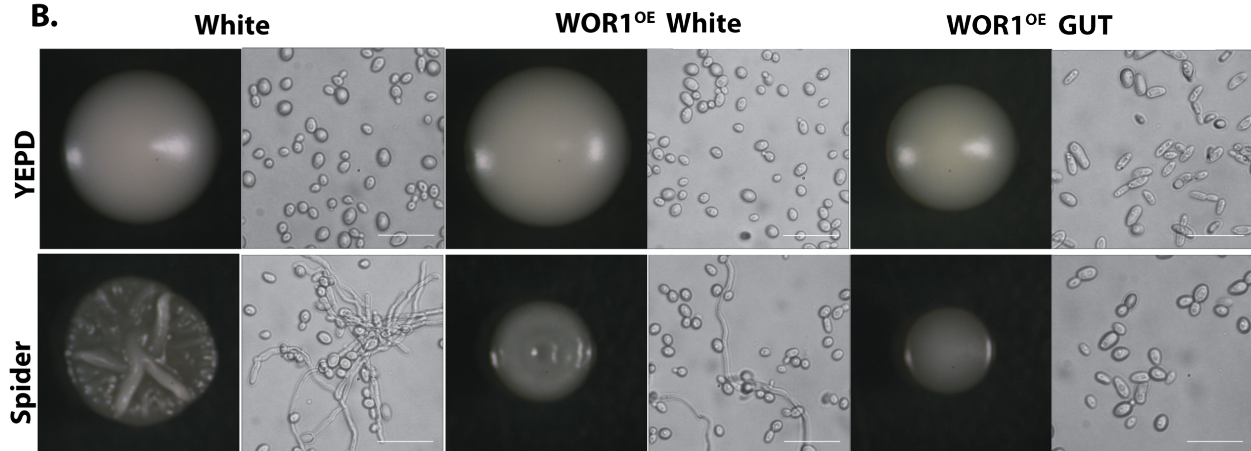


**Figure 3.1: GUT cells have a reduced response to classic filamentation cues *in vitro* and *in vivo***

(A): Mice monotypically infected with WT (ySN425), WOR1<sup>OE</sup> White (ySN928), or WOR1<sup>OE</sup> GUT (ySN1045), were sacrificed at day 3 post colonization. All compartments of the GI tract (stomach, small intestines, cecum and large intestines) were preserved in methacarn prior to fluorescence in situ hybridization (FISH). Images are from the large intestines. Images from other compartments are in Figure S1. Red=Cy3 labeled pan-fungal probe: *C. albicans*; Blue=DAPI: epithelial cells; Green=FITC labeled-UEA1: mucus layer. Yellow arrowheads indicate hyphae. Scale bar is 15 $\mu$ M. Error bars represent S.E.M. Unpaired student's t-test: n.s. indicates not significant, \* p<0.05, \*\* p<0.01, \*\*\* p<0.001, and \*\*\*\* p<0.0001.

(B): WT (ySN425), WOR1<sup>OE</sup> White (ySN928), or WOR1<sup>OE</sup> GUT (ySN1045) were scrapped from plates, re-suspended in dH<sub>2</sub>O and plated for single colonies onto YPD or Spider media. Plates were incubated at 37°C for 3 days. Scale bar is 15 $\mu$ M.

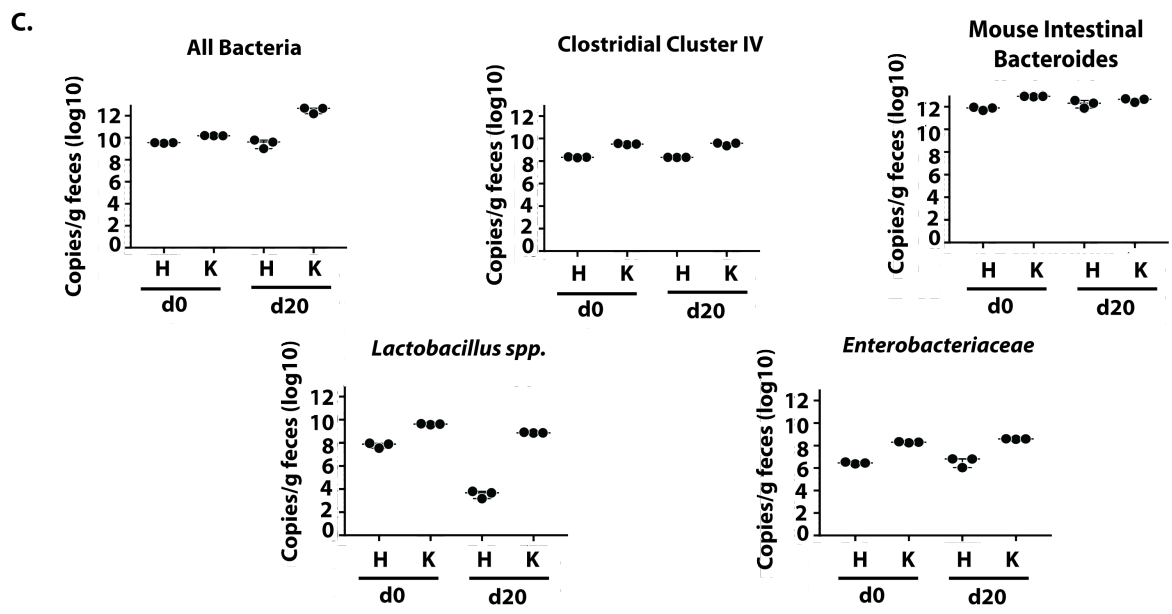
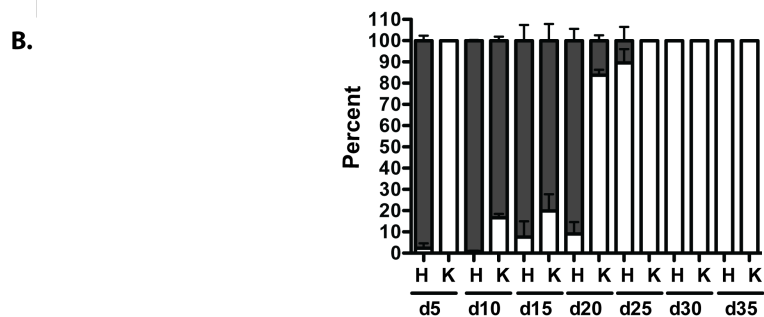
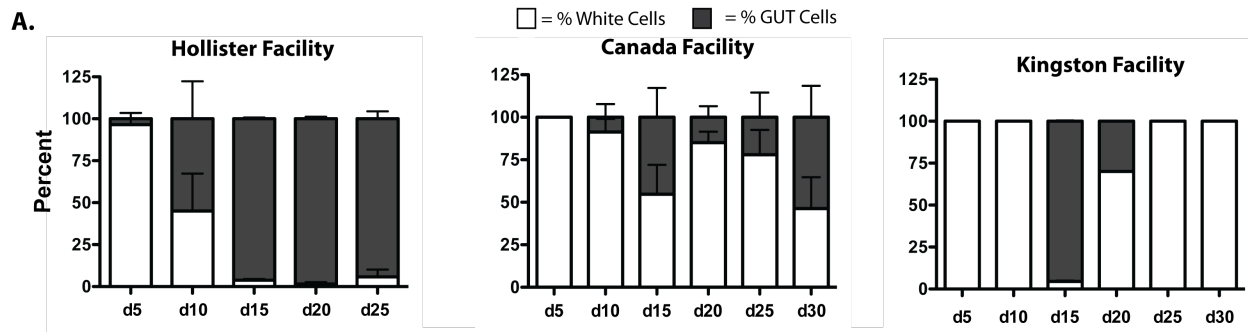


**Figure 3.2: Commensal fitness advantage of GUT cells is lost in mice with high abundance of *Lactobacillus spp.***

(A): BALB/c mice from our standard (Hollister, n=4) or non-conventional (Kingston [n=2] and Canada [n=4]) facilities were infected with a 1:1 mixture of WT (SN250) and WOR1<sup>OE</sup> white (SN928) cells. Feces from Canada and Kingston mice were plated past day 25 to confirm that the identified phenotypes persisted. GUT cell identity was confirmed by colony morphology and inspection of cells under the light microscope.

Error bars represent S.E.M

(B): After 30 days of colonization, Hollister mice were co-housed with Kingston animals such that there was one mouse from each facility in a cage (n=2). H=Hollister, K=Kingston. Error bars represent S.E.M.

(C): qPCR using primers against all bacteria (EUBAC), Clostridial cluster IV (CLEPT), Bacteroides (MIB), *Enterobacteriaceae* (ENTERO) and *Lactobacillus spp.* (LACT), of fecal samples collected from Hollister and Kingston mice on day 0 (day of gavage) and 20 days post *C. albicans* gavage. One mouse from each facility was evaluated over time and each dot represents a technical replicate.

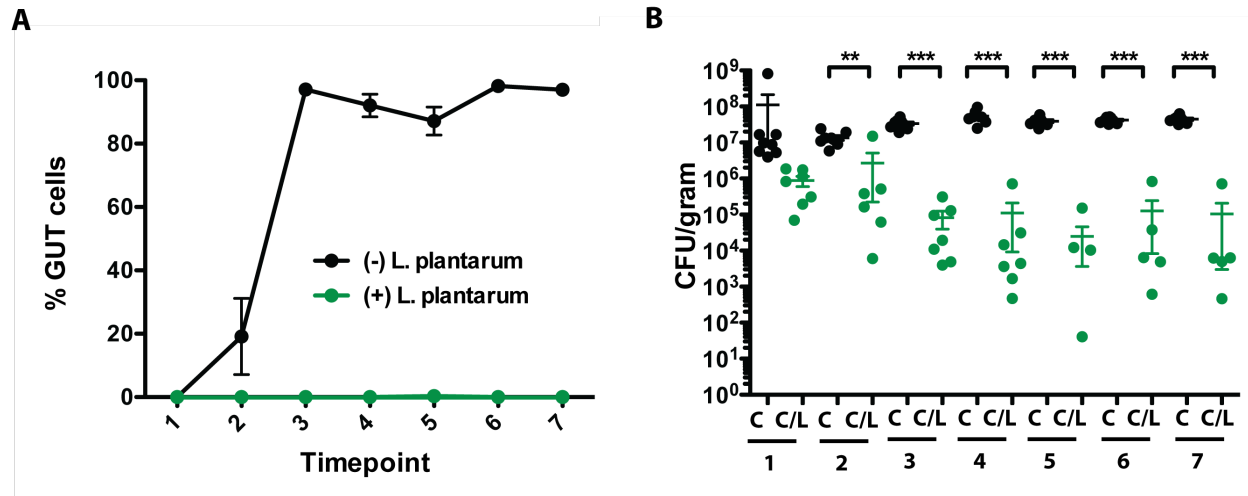


**Figure 3.3: GUT cells are not recovered from Hollister mice colonized with *L. plantarum***

(A) Hollister BALB/c mice were first colonized with two successive doses of  $1e9$  *L. plantarum* (bSN373) followed by  $1e8$  WOR1<sup>OE</sup> white *C. albicans* (SN928). Colony morphology of *C. albicans* was determined by plating fecal samples onto Sabouraud plates containing antibiotics. GUT cell morphology was confirmed by examination of cells under a light microscope. Results are a combination of two experiments and time points refer to the following days for each: 1=d2/3, 2=d5, 3=d10/8, 4=d14/12, 5=d17/16, 6=d21/20, 7=d25/24.

(B) Colony forming units (CFUs) were evaluated over the course of the experiment by plating fecal samples onto Sabouraud plates containing antibiotics. C=*C. albicans* alone; C/L=*C. albicans* + *L. plantarum*. Error bars represent S.E.M. Unpaired student's t-test: n.s. indicates not significant, \*  $p < 0.05$ , \*\*  $p < 0.01$ , \*\*\*  $p < 0.001$ , and \*\*\*\*  $p < 0.0001$ .

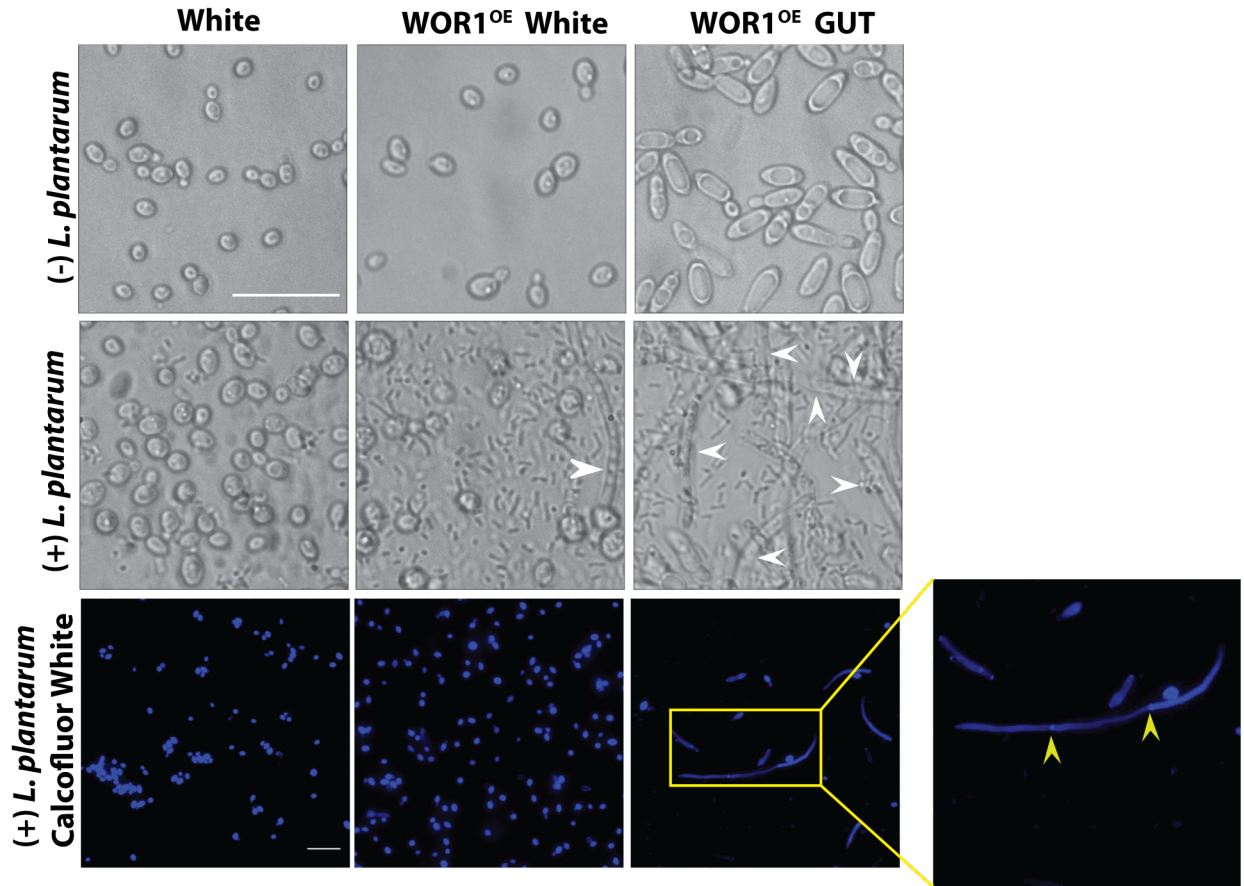


**Figure 3.4: GUT cells are filamentous when co-cultured with *L. plantarum***

(A) *C. albicans* cells (WT=ySN425, WOR1<sup>OE</sup> White=ySN928, and WOR1<sup>OE</sup> GUT=ySN1045; OD<sub>600</sub>=3.0) were combined in a 1:1 ratio w/ *L. plantarum* (bSN373; OD<sub>600</sub>=1.0) and 3μL was spotted onto MRS plates. Plates were incubated at 30°C for 6 days prior to analysis. A small patch of cells were transferred to a glass slide and stained with Calcofluor White according to manufacturer's instructions. Cells were imaged on the Keyence microscope. White arrowheads indicate hyphae and yellow arrowheads indicate septae. Scale bars are 15μM.



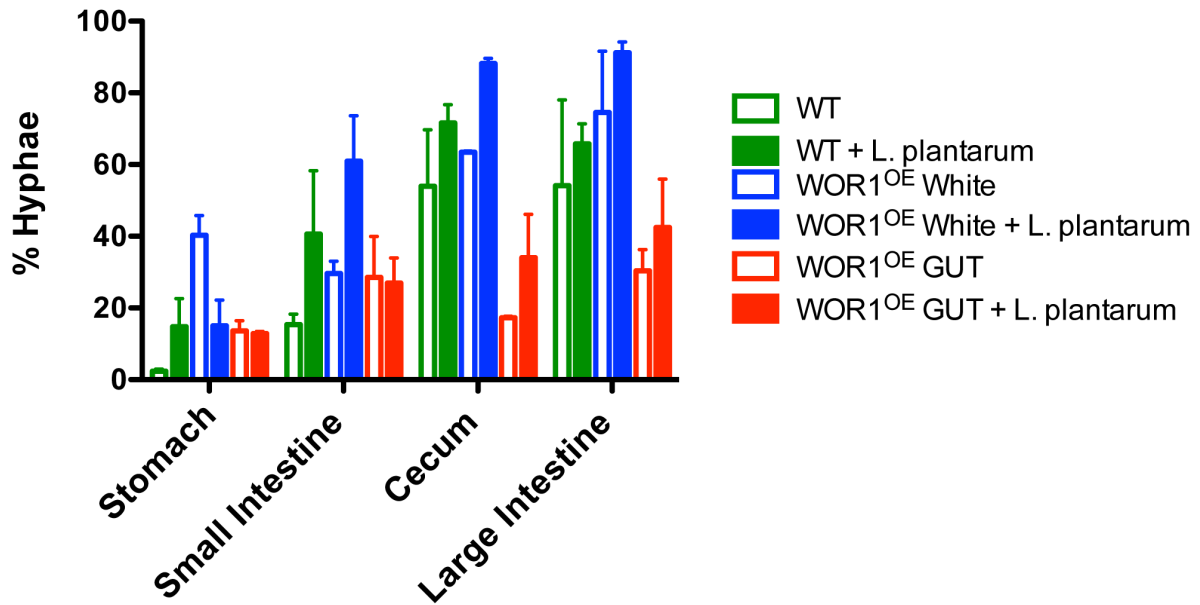


**Figure 3.5: GUT cells do not filament when co-colonized with *L. plantarum***  
 1e8 *C. albicans* (WT=ySN425, WOR1<sup>OE</sup> White=ySN928, and WOR1<sup>OE</sup> GUT=ySN1045) cells were gavaged into mice 7 days post-antibiotic (pen/strep) treatment. *L. plantarum* (bSN373) was gavaged 1 day post *C. albicans* at 1e9. GI compartments were fixed in methacarn 3 days post *L. plantarum* colonization, processed and stained with the Cy3-conjugated pan-fungal probe. Yeast and hyphal structures were quantified as described in the methods.

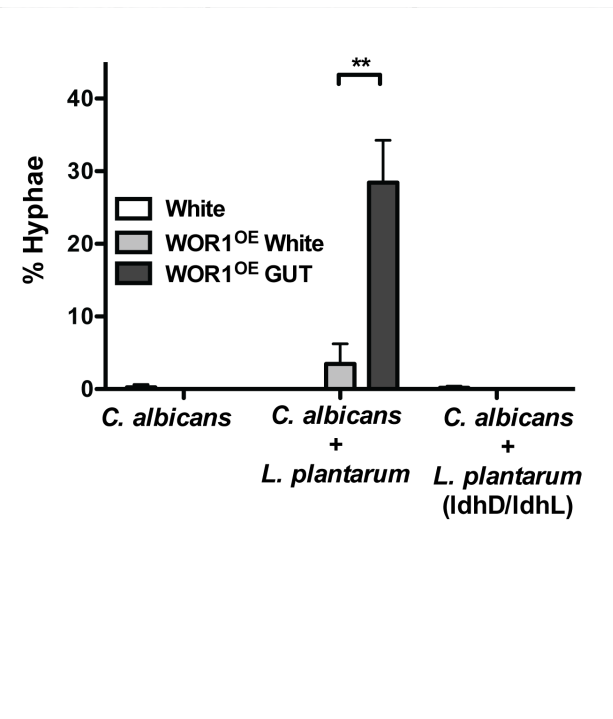
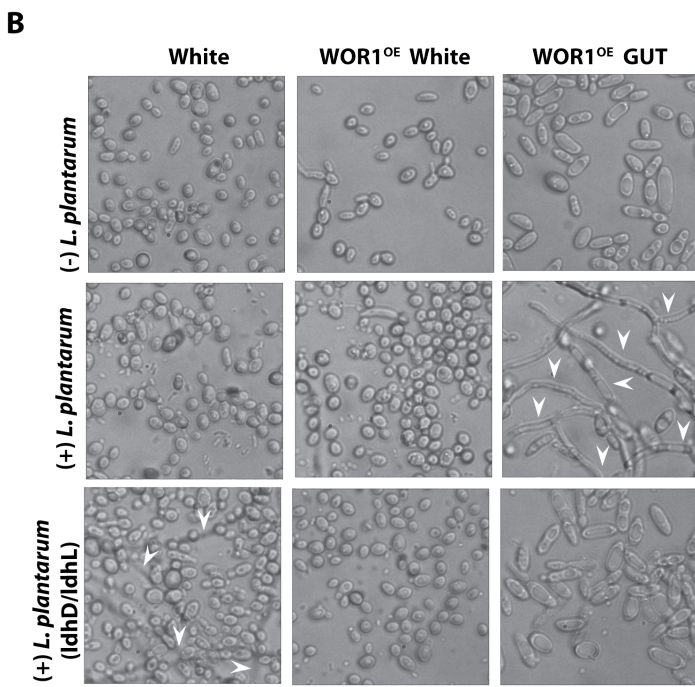
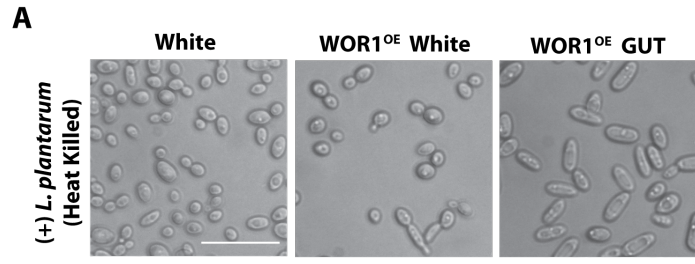


**Figure 3.6: GUT cell filamentation is dependent on *L. plantarum* lactate dehydrogenase genes**

(A) *C. albicans* cells (WT=ySN425, WOR1<sup>OE</sup> White=ySN928, and WOR1<sup>OE</sup> GUT=ySN1045; OD<sub>600</sub>=3.0) were combined with heat killed (85°C for 10 minutes) *L. plantarum* (bSN373; OD<sub>600</sub>=1.0) at a 1:1 ratio and spotted on MRS plates. Plates were incubated at 30°C for 3 days. Scale bar is 15µM.

(B) *C. albicans* cells (WT=ySN425, WOR1<sup>OE</sup> White=ySN928, and WOR1<sup>OE</sup> GUT=ySN1045; OD<sub>600</sub>=3.0) were combined with either WT *L. plantarum* (bSN403) or *ldhD/ldhL* *L. plantarum* (bSN404) at an OD<sub>600</sub>=1.0) in a 1:1 ratio and spotted onto MRS plates. Plates were incubated at 30°C for 6 days prior to analysis. Arrowheads indicate hyphae. Error bars represent S.E.M. Unpaired student's t-test: n.s. indicates not significant, \* p<0.05, \*\* p<0.01, \*\*\* p<0.001, and \*\*\*\* p<0.0001.

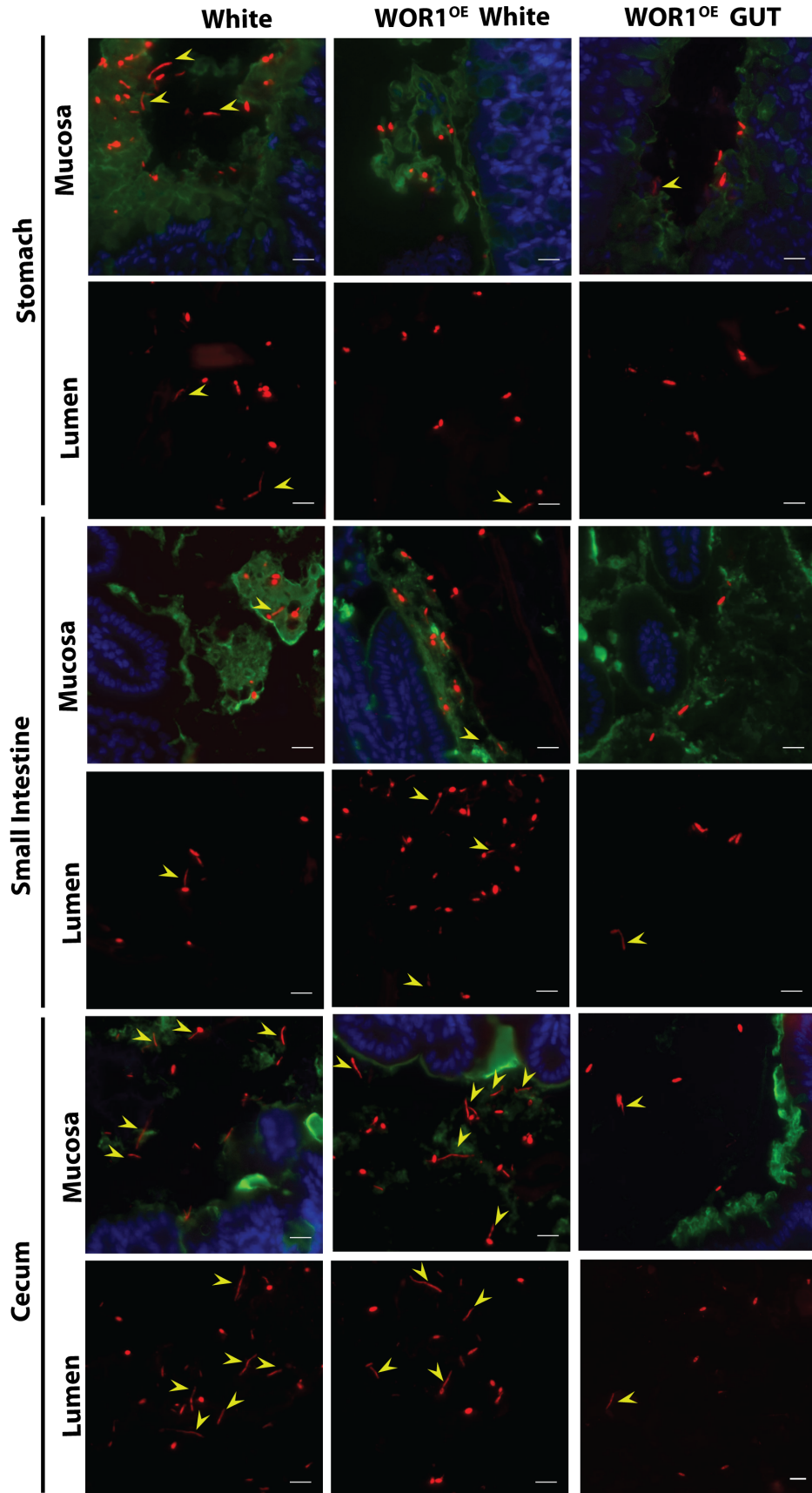


**Figure 3.S1: GUT cells display low levels of filamentation in all compartments of the GI tract**

FISH images of *C. albicans* (WT=ySN425, WOR1<sup>OE</sup> White=ySN928, and WOR1<sup>OE</sup> GUT=ySN1045) in the stomach, small intestine and cecum of mice harvested 3 days post colonization. Red=Cy3 labeled pan-fungal probe: *C. albicans*; Blue=DAPI: epithelial cells; Green=FITC labeled-UEA1: mucus layer. Yellow arrowheads indicate examples of hyphae. Scale bar is 15 $\mu$ M.

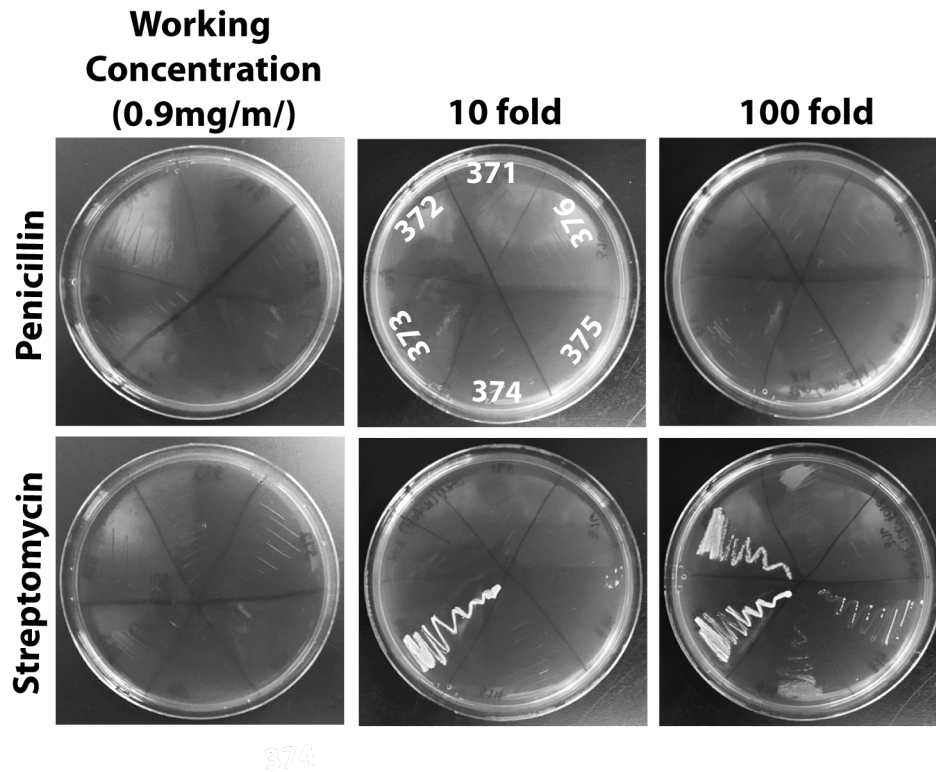


**Figure 3.S2: *L. plantarum* is the most resistant *Lactobacillus* spp. to streptomycin** *Lactobacillus* spp. were streaked from freezer stocks onto MRS plates containing the indicated concentrations of antibiotics at 37°C for one day. Working concentration refers to dosage used in our animal model. Subsequent plates are 10 and 100 fold dilutions of each antibiotic. 371: *L. casei*, 372: *L. rhamnosus*, 373: *L. plantarum*, 374: *L. brevis*, 375: *L. reuteri*, 376: *L. acidophilus*.

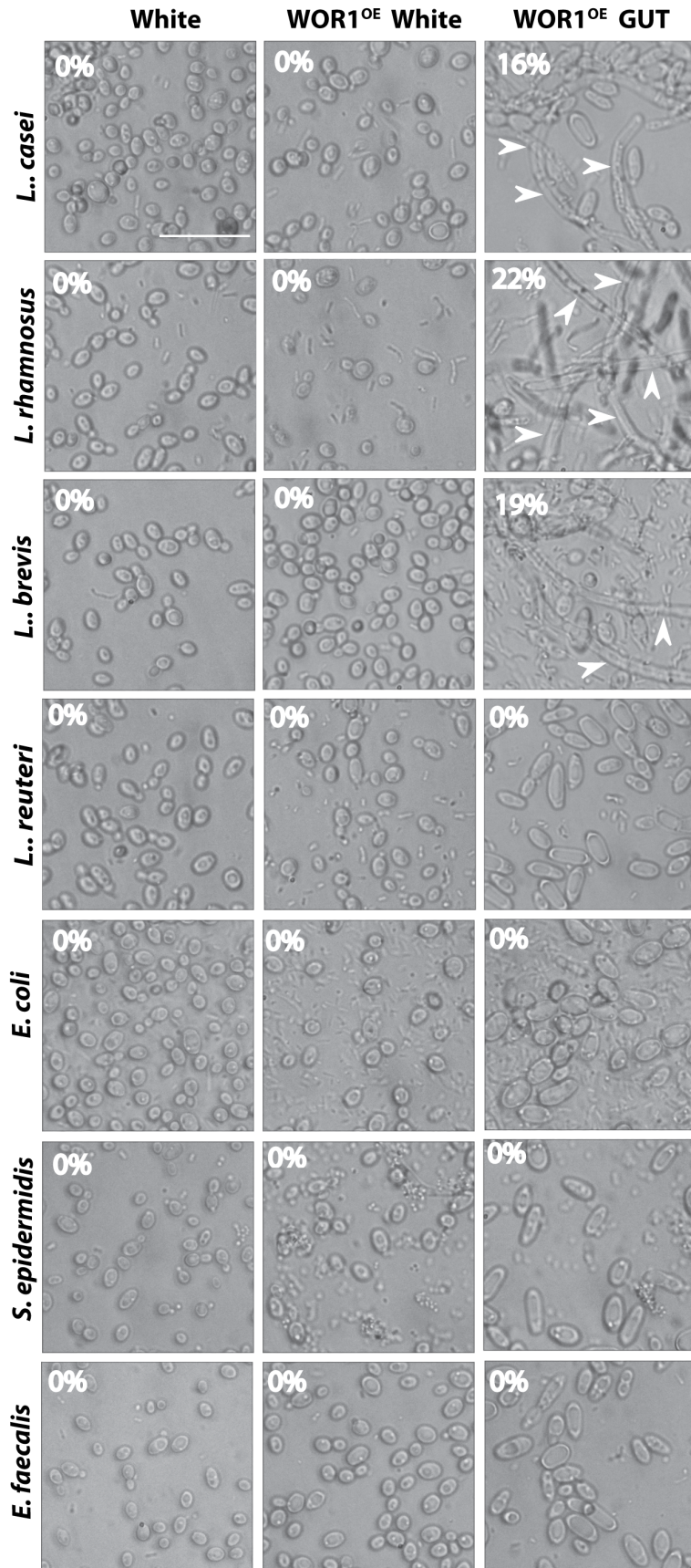


**Figure 3.S3: *Lactobacillus*-induced *C. albicans* GUT cell filamentation is specific to certain species of *Lactobacilli***

*C. albicans* cells (WT=ySN425, WOR1<sup>OE</sup> White=ySN928, and WOR1<sup>OE</sup> GUT=ySN1045; OD<sub>600</sub>=3.0) were combined in a 1:1 ratio w/ bacterial cells (*L. casei*=bSN371, *L. rhamnosus*=bSN372, *L. brevis*=bSN374, *L. reuteri*=bSN375, *E. coli*=bSN95, *S. epidermidis*=SN174, and *E. faecalis*=SN182; OD<sub>600</sub>=1.0) and spotted onto MRS plates. Plates were incubated at 30°C for 6 days prior to analysis. Calcofluor white was used to quantify cells as described in the Methods. Numbers represent percentage of filamentous cells. White arrowheads indicate examples of yeast.

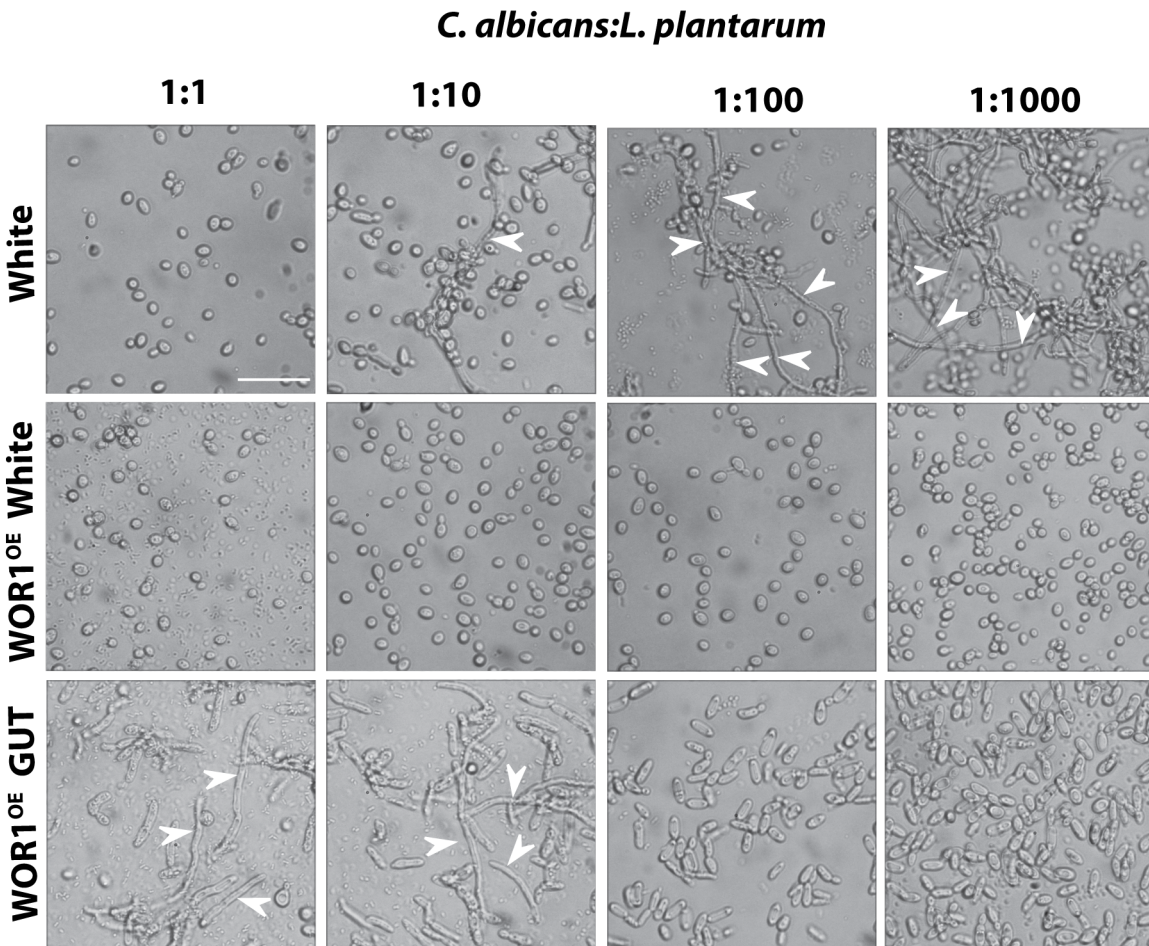


**Figure 3.S4: *Lactobacillus* induced *C. albicans* GUT cell filamentation is dose dependent on the amount of *L. plantarum* present**

*C. albicans* cells (WT=ySN425, WOR1<sup>OE</sup> White=ySN928, and WOR1<sup>OE</sup> GUT=ySN1045; OD<sub>600</sub>=3.0) were combined with *L. plantarum* (OD<sub>600</sub>=1.0) in 10-fold dilutions. Combined cells were spotted onto MRS plates and incubated at 30°C for 3 days prior to analysis. Scale bar is 15µM. White arrowheads indicate examples of hyphae.



**Table 3.1-Summary of mRNA-seq in mice co-colonized with *C. albicans* and *L. plantarum***

Gene Name	Function	GUT + <i>L.p</i> vs. White + <i>L.p</i> (p value)	GUT + <i>L.p</i> vs. GUT (p value)
<b>HYPHAL ASSOCIATED PROTEINS</b>			
Als3	Cell wall adhesin	-2.74 (0.00041)	2.92 (0.051)
Ece1	Secreted toxin	-2.45 (0.00092)	3.10 (0.20)
Hwp1	Hyphal cell wall protein	0.12 (0.90)	2.72 (0.23)
Hyr1	Hyphal cell wall protein	0.20 (0.86)	2.80 (0.32)
Sap6	Secreted aspartyl protease	-3.87 (0.021)	2.33 (0.31)
<b>PROTEINS SIGNIFICANTLY UPREGULATED IN GUT + <i>L.p</i></b>			
Cfl11	NADPH oxidase	-1.99 (0.15)	2.65 (0.017)
Mrv4	Unknown	-4.20 (0.0027)	2.60 (0.049)
Ume6	Transcription Factor	-1.70 (0.18)	3.07 (0.040)
Trx2	Putative thioredoxin	-2.33 (0.0015)	-1.25 (0.021)

**Table 3.S1-C. *albicans* Strains Used in this Chapter**

Strain	Common Name	Notes	Full Genotype	Reference
SN425	Wild type white	Derivative of SC5314	<i>leu2Δ::C.d.HIS1/leu2Δ::C.m.LEU2, ura3Δ/URA3, his1Δ/his1Δ, arg4Δ/arg4Δ::C.d.ARG4, iro1Δ/IRO1, MTLα/MTLα</i>	[16]
SN928	WOR1 <sup>OE</sup> White	Cells prior to passage through GI tract	<i>SAT1-TDH3promWOR1/wor1::C.d.ARG4, leu2::C.m.LEU2/leu2::C.d.HIS1, ura3/URA3, his1/his1, arg4/arg4, iro1/IRO1, MTLα/MTLα</i>	[16]
SN1045	WOR1 <sup>OE</sup> GUT	SN928 recovered from mouse GI commensalism model	<i>SAT1-TDH3promWOR1/wor1::C.d.ARG4, leu2::C.m.LEU2/leu2::C.d.HIS1, ura3/URA3, his1/his1, arg4/arg4, iro1/IRO1, MTLα/MTLα</i>	[16]
SN1495	WO-1	White-opaque switching capable; Isolate #1		[17]

**Table 3.S2-Bacterial Species Used in this Chapter**

Strain	Common Name	Notes
bSN371	<i>L. casei</i>	WT
bSN372	<i>L. rhamnosus</i>	WT
bSN373	<i>L. plantarum</i>	WT
bSN374	<i>L. brevis</i>	WT
bSN375	<i>L. reuteri</i>	WT
bSN403	<i>L. plantarum</i>	WT
bSN404	<i>L. plantarum</i>	Strain TF103 <i>ldhL/ldhD</i>
bSN95	<i>E. coli</i>	DH5α WT
bSN174	<i>S. epidermidis</i>	WT
bSN182	<i>E. faecalis</i>	WT

## CHAPTER IV: HYPHAL SPECIFIC CELL SURFACE PROTEINS AND THEIR ROLE IN GI COMMENSALISM

While there is a well-established positive correlation between hyphal induction and virulence, the relationship between hyphal formation and gene expression in the context of GI commensalism is less well understood. As discussed in Chapter II, the *C. albicans* filamentation program is strongly detrimental to commensal fitness, but as opposed to hyphal formation, this antagonistic effect is due to hyphal specific gene expression. We wanted to understand whether other hyphal specific cell surface proteins, besides *SAP6*, also played a role in commensalism and, if so, in what direction they mediate this effect.

To test this, we passaged a small pool of hyphal cell surface proteins (*ECE1*, *HYR1*, *HWP1*, and *ALS3*) along with *BCR1* (a transcriptional regulator) and a matched wild-type control through our mouse model of commensalism. *ECE1* is a recently described toxin that elicits epithelial cell damage in the oral cavity<sup>23</sup>. Both *HWP1* and *HYR1* are commonly used markers of the hyphal cell surface<sup>73,127</sup>. *ALS3* is also a commonly used marker of the hyphal cell surface, but is also known to bind to cadherins on epithelial cells and allow for *C. albicans* entry<sup>20</sup>. *BCR1* is a transcription factor that positively regulates expression of all the mentioned hyphal cell surface markers<sup>128</sup>. We use two independent isolates of each strain in two distinct pools. Each strain was grown separately to log phase ( $OD_{600}=1.0$ ) and then combined in an equal ratio prior to oral gavage. Fecal pellets were plated every 5 days on sabouraud plates containing antibiotics and competitive fitness was determined by barcode-based qPCR, as previously described<sup>53</sup>.

Interestingly, we find that all mutants are outcompeted by either the *ece1* mutant (in pool M1) or the *als3* mutant (in pool M2; Figure 4.1). Because phenotypes in a pooled assay can be masked or amplified based on the presence of other mutants, we verified the phenotypes of the two hypercompetitive mutants (*als3* and *ece1*) in 1:1 competitions with wild type. We find that while both isolates of the *als3* mutant recapitulate the hypercompetitive phenotype seen in pool #2, one strain of the *ece1* mutant is hypocompetitive and the other exhibits a cage-specific phenotype (Figure 4.2). As, parsing out the *ece1* phenotype likely requires making more independent isolates of this mutant, we decided to follow up on the *als3* mutant.

*ALS3* has been previously described as mediator of epithelial invasion in in both epithelial and endothelial cells. Our RNA profiling of the mammalian GI tract shows us that *ALS3* is highly expressed along the length of the gut (Chapter II), which makes the hypercompetitive phenotype of the *als3* mutant, somewhat curious. As we see in chapter II, however, hyphal cell surface proteins, such as *SAP6*, appear to be responsible for alerting the host of detrimental hyphae, which we believe the host actively clears. *ALS3* expression levels are likely high throughout the GI tract despite this protein being a negative regulatory signal, because there are many strongly hypha-inducing conditions in the GI tract that promote continual hyphal formation. The hyphae are likely cleared by the host on a micro-scale, which explains why the overall level of gene expression remains high.

Interestingly, similar to both *sap6* and *ume6*, *als3* is able to form hyphae along the length of the GI tract at levels similar to wild-type (Figure 4.2). Therefore, we once again observe that expression of particular hyphal markers, and not cell shape,

determines commensal fitness, as is the case with *sap6*. Therefore, *ALS3* appears to be another hyphal associated negative mediator of GI commensal fitness.

In summary, this study demonstrates that 1) it is likely that hyphal cell surface proteins in general are detrimental to GI commensalism. This is contrary to the existing literature, which has also demonstrated that hyphal cell surface proteins are highly expressed in the GI tract, but has generally explained this intriguing result by rationalizing that hyphal cell surface proteins on yeasts somehow promote commensal colonization. However, we and others have shown that *C. albicans* is able to colonize the gut as both yeasts and hyphae and, thus, it is more likely that multiple hyphal specific cell surface proteins, like *ALS3*, are acting as hyphal clearing signals in the GI tract. Further studies need to be done understand the mechanism that underlies host hyphal clearance mediated by hyphal cell surface proteins, as well as understanding the role that other hyphal specific cell surface proteins such as, *HWP1*, *HYR1* and *ECE1*, play in regulating the *C. albicans* GI commensal population.

## **METHODS**

### **Mouse Infections**

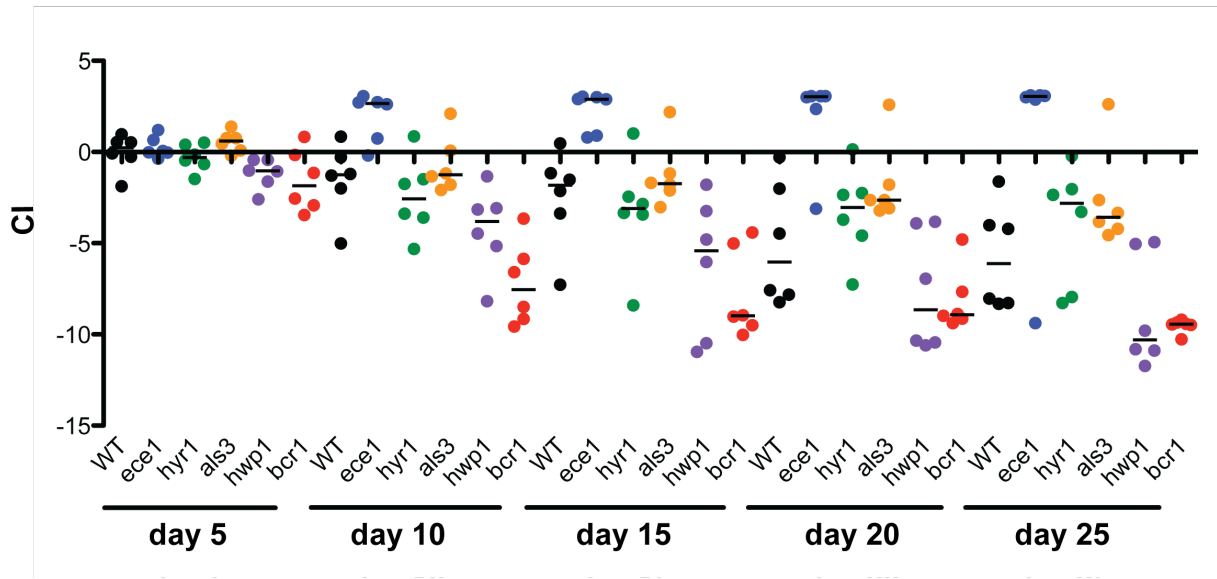
All procedures involving animals were approved by the University of California at San Francisco Institutional Animal Care and Use Committee, which enforces the ethical and humane use of animals. 6- to 8-week-old female BALB/c mice were infected with equal portions of WT and mutant strains as described previously<sup>16</sup> infected by oral gavage with either wild-type *C. albicans*, or the mutants of interest. Relative abundance of each

strain in the infecting inoculum and recovered fecal pellets was determined by qPCR using strain specific primers.

### **Fluorescence *In Situ* Hybridization (FISH)**

GI sections (stomach, proximal and distal small intestine, cecum and large intestine), were dissected with contents in tact and fixed in methacarn (60% methanol, 30% chloroform, 10% glacial acetic acid) for at least 3 hours and up to two weeks at room temperature. Tissue sections were processed in the following washes: 2 x 35 minutes in methanol, 2 x 25 minutes in ethanol, 2 x 20 minutes in xylene and then places in melted paraffin wax for two hours at 70°C. Following processing, sections were embedded and cut at 4µm. FISH was performed using a pan-fungal probe conjugated to Cy3 (IDT: /5Cy3/-CTCTGGCTTCACCCTATTC), as previously described<sup>66</sup> with the following modifications: performed hybridization for three hours at 50°C, and mucus layer was visualized using FITC conjugated UEA-1 (Sigma#: L9006-1MG) for stomach and large intestine sections, or FITC conjugated UEA-1 and FITC-conjugated WGA-1 (Sigma#: L4895-2MG) for small intestine and cecum sections, at 4°C for 45min. All sections were stained with DAPI (EMD Millipore #: 5087410001) at the same time as mucus layer staining. Sections were mounted with Vectashield (Vector Laboratories #: 101098-042) and imaged on Keyence microscope (BZ-X700). 30 fields of view were quantified per sample using Fiji.

### M1



### M2

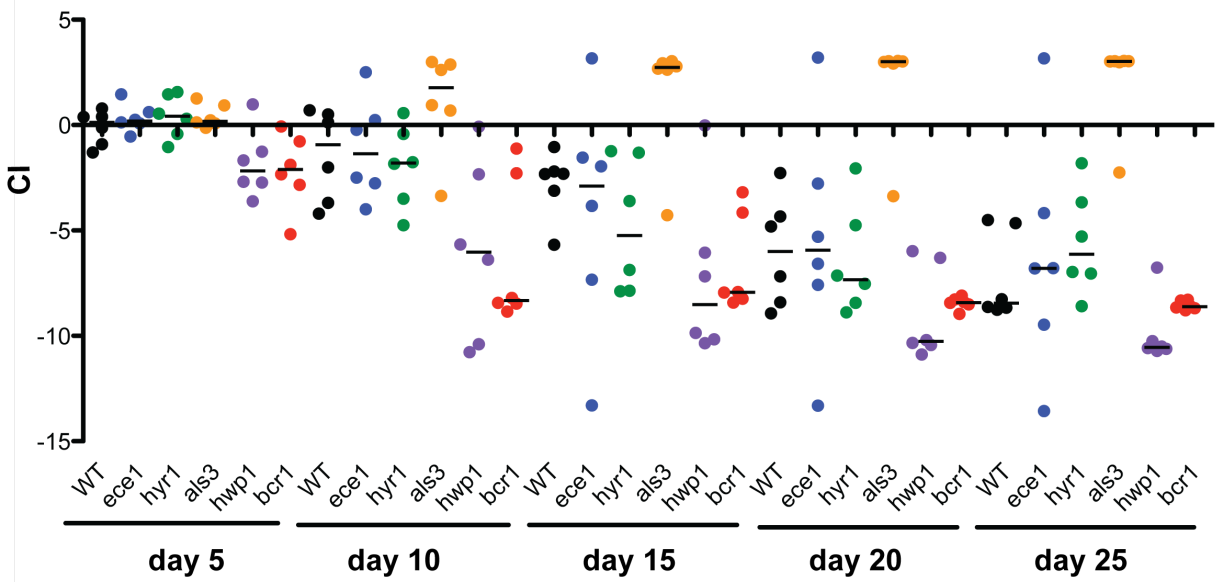


**Figure 4.1-Hyphal cell surface proteins predominate as negative regulators of commensalism.** Wild-type (SN250; black; primers: SNO183/SNO322), *ece1* (SN279 and SN1513; blue; primers: ST24/SNO322), *hyr1* (SN510 and SN511; green; primers: ST07/SNO322), *als3* (SN1516 and SN1517; orange; primers: ST18/SNO322), *hwp1* (SN1518 and SN1519; purple; primers: ST19/SNO322) and *bcr1* (SN1514 and SN1515; red; primers: ST35/SNO322) were combined at equal ratios into two distinct pools (M1: SN250, SN279, SN510, SN1514, SN1516, and SN1518; M2: SN250, SN1513, SN511, SN1515, SN1517, and SN1519) and passaged through our standard mouse model. Relative abundance was determined by qPCR using strain specific primers.  $CI = \log_2(R/I)$  represents the log ratio of the abundance of each strain after recovery from the feces of a given animal (R) compared to the level in the infecting inoculum (I).



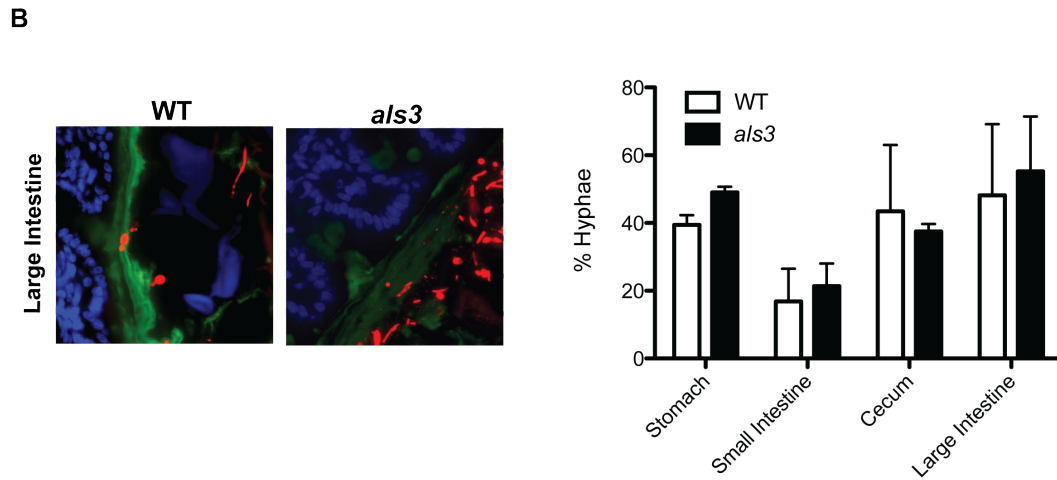
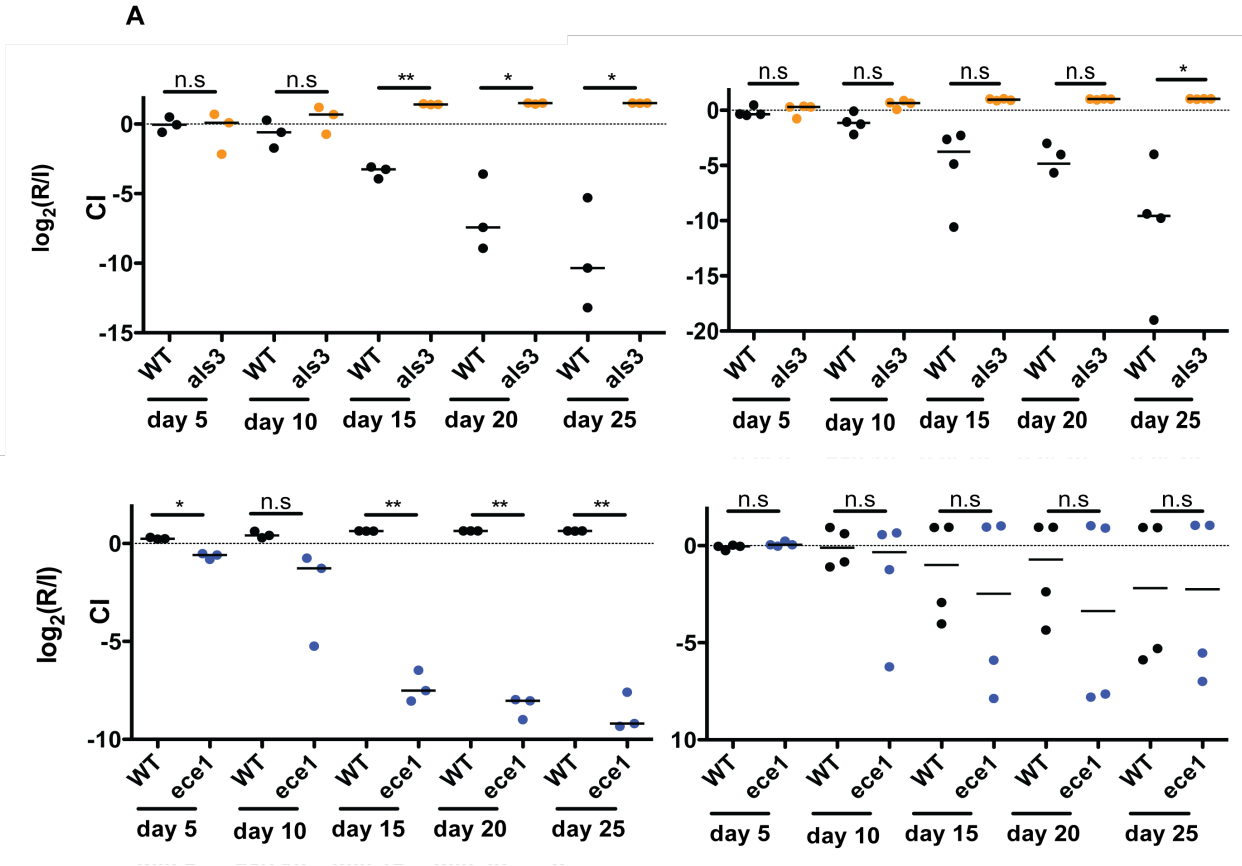


**Figure 4.2-ALS3 is a negative regulator of GI commensalism, but *ECE1*'s role in remains unclear.** Competition experiments between WT (SN250; black; primers: SNO183/SNO322) and mutant strains in our conventional mouse model. Relative abundance was determined by qPCR using strain specific primers.  $\text{Log}_2(R/I)$  represents the log ratio of the abundance of each strain after recovery from the feces of a given animal (R) compared to the level in the infecting inoculum (I). Significance was determined using a paired two-sided t test, with \* signifying  $p < 0.05$ , \*\*  $p < 0.01$ , \*\*\*  $p < 0.001$ . (a) *als3* (SN1516 or SN1517; orange; primers: ST18/SNO322) vs. WT (SN250) and *ece1* (SN279 or SN1513; blue; primers: ST24/SNO322) vs. WT (SN250). Both isolates of *als3* significantly outcompete wild-type, whereas one isolate of *ece1* is hypocompetitive and the other has cage-specific effects. (b) Fluorescence *in situ* hybridization (FISH) using a pan-fungal probe (red) shows that *als3* is able to form hyphae similar to wild-type. Epithelial cells are visualized by DAPI (blue) and the mucus layer is visualized by FITC labeled UEA-1 (green). Error bars represent S.E.M.

**Table 4.S1-Strains used in this chapter**

<b>Strain</b>	<b>Common Name</b>	<b>Notes</b>	<b>Full Genotype</b>	<b>Reference</b>
SN250	WT		<i>leu2Δ::C.d.LEU2/leu2Δ::C.m.HIS1, his1Δ/his1Δ, arg4Δ/arg4Δ, ura3Δ/URA3, iro1/IRO1</i>	[53]
SN279	<i>ece1</i>	<i>ece1</i> null mutant; M1	<i>ece1Δ::C.d.LEU2/ece1Δ::C.m.HIS1 his1Δ/his1Δ, arg4Δ/arg4Δ, ura3Δ/URA3, iro1/IRO1</i>	[53]
SN1513	<i>ece1</i>	<i>ece1</i> null mutant; M2	<i>ece1Δ::C.d.LEU2/ece1Δ::C.m.HIS1 his1Δ/his1Δ, arg4Δ/arg4Δ, ura3Δ/URA3, iro1/IRO1</i>	This study
SN510	<i>hyr1</i>	<i>hyr1</i> null mutant; M1	<i>hyr1Δ::C.d.LEU2/hyr1Δ::C.m.HIS1 his1Δ/his1Δ, arg4Δ/arg4Δ, ura3Δ/URA3, iro1/IRO1</i>	[53]
SN511	<i>hyr1</i>	<i>hyr1</i> null mutant; M2	<i>hyr1Δ::C.d.LEU2/hyr1Δ::C.m.HIS1 his1Δ/his1Δ, arg4Δ/arg4Δ, ura3Δ/URA3, iro1/IRO1</i>	[53]
SN1516	<i>als3</i>	<i>als3</i> null mutant; M1	<i>als3Δ::C.d.LEU2/als3Δ::C.m.HIS1 his1Δ/his1Δ, arg4Δ/arg4Δ, ura3Δ/URA3, iro1/IRO1</i>	This study
SN1517	<i>als3</i>	<i>als3</i> null mutant; M2	<i>als3Δ::C.d.LEU2/als3Δ::C.m.HIS1 his1Δ/his1Δ, arg4Δ/arg4Δ, ura3Δ/URA3, iro1/IRO1</i>	This study
SN1518	<i>hwp1</i>	<i>hwp1</i> null mutant; M1	<i>hwp1Δ::C.d.LEU2/hwp1Δ::C.m.HIS1 his1Δ/his1Δ, arg4Δ/arg4Δ, ura3Δ/URA3, iro1/IRO1</i>	This study
SN1519	<i>hwp1</i>	<i>hwp1</i> null mutant; M2	<i>hwp1Δ::C.d.LEU2/hwp1Δ::C.m.HIS1 his1Δ/his1Δ, arg4Δ/arg4Δ, ura3Δ/URA3, iro1/IRO1</i>	This study
SN1514	<i>bcr1</i>	<i>bcr1</i> null mutant; M1	<i>bcr1Δ::C.d.LEU2/bcr1Δ::C.m.HIS1 his1Δ/his1Δ, arg4Δ/arg4Δ, ura3Δ/URA3, iro1/IRO1</i>	This study
SN1515	<i>bcr1</i>	<i>bcr1</i> null mutant; M2	<i>bcr1Δ::C.d.LEU2/bcr1Δ::C.m.HIS1 his1Δ/his1Δ, arg4Δ/arg4Δ, ura3Δ/URA3, iro1/IRO1</i>	This study

## CHAPTER V: DETERMINING THE GI COMMENSAL NICHE OF *C. ALBICANS* GUT CELLS

While we know that *C. albicans* GUT cells are specialized for survival in the GI tract due to their ability to outcompete wild-type cells, we still do not understand whether these GUT cells establish and maintain a renewable niche within the gut. The idea that members of the microbiota establish a niche in the GI tract has been observed with multiple bacterial species. *B. fragilis*, for example, resides deep within the crypts of the colonic epithelium<sup>129</sup>, whereas *H. pylori* can be found in the folds of the stomach epithelium<sup>130</sup>. We hypothesize that *C. albicans* establishes a similar niche protected in the folds of the gut epithelium to shield itself from the constantly changing environmental conditions within the GI tract.

To determine where GUT cells localize in the GI tract, we used a two-pronged approach to look at 1) where *Wor1* signal is highest throughout the GUT, and 2) which compartment GUT cells accumulate in at early time points after infection. To determine where *Wor1* signal was highest, we performed timed infections of our mouse commensal model with a *WOR1 promoter-FLP* strain. This strain contains one intact copy of the *WOR1* gene, as well as one copy of a wild-type *WOR1* promoter fused to the *FLP* gene, which encodes a site-specific DNA recombinase. In addition, the strain contains a copy of *URA3* (conferring sensitivity to 5-Fluoroorotic acid, 5-FOA) flanked by FRT recombination sites. When the *WOR1* promoter is turned on, *URA3* is excised (conferring resistance to 5-FOA), which is measured by plating recovered yeasts onto 5-FOA plates. Frequency of *bona fide URA3* excision events is validated by PCR. I performed a 3-day time course of mice infected with the *WOR1—FLP* strain. Every 24

hours, two mice were sacrificed, their GI tracts sectioned into four compartments (stomach, small intestine, cecum and large intestine), and *C. albicans* recovered separately from tissue and luminal contents were plated onto nonselective medium and 5-FOA-containing medium. As shown in Figure 5.1, *WOR1p* activity was highest in the small intestine tissue-associated segment after three days of colonization.

To determine when and where GUT cells first appear, I performed a 16-day time course of mice gavaged with a 1:1 mixture of wild-type (WT) and *WOR1*<sup>OE</sup> (which stabilizes the GUT phenotype, once it occurs) white strains. Appearance of GUT colonies was detected by colony appearance and validated by cell morphology via microscopic examination. As shown in Figure 5.1, there is an accumulation of GUT cells in the distal GI tract at day 4 post colonization, with a slight enrichment of GUT cells in tissue-associated samples as compared to luminal contents. Over the course of the experiment, once GUT cells form, they predominate the population of all compartments of the GI tract, except for the stomach, which saw a decrease in GUT cells for both tissue and lumen-associated populations (Figure 5.1). It is possible that the stomach environment, mainly characterized by an acidic pH), is inhospitable to GUT cells and favors white cell colonization. Of note, however, this experiment was done with a competition of white and GUT cells, so to understand the true kinetics of GUT cell maintenance in different GI compartments, it would be necessary to repeat this experiment with monotypic infections of either *WOR1*<sup>OE</sup> white or GUT cells.

Localizing *WOR1*<sup>OE</sup> GUT cells does not necessarily indicate where wild-type GUT cells first occur, because we believe that the GUT switch is reversible in wild-type cells. Presumably this is because the GUT phenotype requires both *Wor1* expression as

well as host signals to form, and is stabilized *ex vivo*, because of *Wor1* overexpression. We, however, wanted to observe the formation of GUT cells in wild-type strains *in situ* to try and visualize the GUT cell niche *in vivo*. To develop a GUT-specific reporter system, we used BirA\*, a biotin ligase that nonspecifically biotinylates all proteins within a small radius<sup>131</sup>. This technique has been used successfully in identifying novel proteins of the inner membrane complex in *Toxoplasma gondii*<sup>132</sup>. We hypothesized that tagging GUT specific cell surface proteins with this enzyme would allow for spontaneous biotinylation of the GUT cell surface in the GI tract, which could be visualized using standard enzyme-linked streptavidin staining protocols.

To validate that the *C. albicans* codon-optimized BirA\* protein we designed was functional, we constructed a strain that endogenously overexpressed the protein behind the TDH3 promoter. We validated that BirA\* promiscuously biotinylated proteins in *C. albicans* by performing a streptavidin western blot (Figure 5.2). To determine whether the BirA\* protein was still functional when fused to a cell surface protein, we constructed a strain where the BirA\* protein was inserted downstream of the ALS4 and PGA26 genes (before the GPI anchor sequence). We chose these genes both because they are cell surface proteins and, according to microarray data from our lab<sup>16</sup>, ALS4 is highly expressed in white cells and PGA26 is highly expressed in GUT cells and both are lowly expressed in the opposite cell type. Using these strains, we were also able to see ubiquitous biotinylation in the ALS4-BirA\* strain expressed in GUT cells, albeit at much lower levels than the TDH3 regulated BirA\* (Figure 5.2). The lower levels of expression could be due to non-optimal expression conditions for the ALS4 promoter, or BirA\* biotinylation may not be as robust because it is functioning as part of a fusion

protein. With PGA26-BirA\*, we observed higher levels of ubiquitous biotinylation in white cells as opposed to GUT cells, but in this case we saw low levels of biotinylation in GUT cells with PGA26-BirA\* as well (Figure 5.2). The fact that we are only able to see ubiquitous biotinylation of ALS4-BirA\* in GUT cells as opposed to white cells and saw higher levels of biotinylation in PGA26-BirA\* white cells as compared to GUT cells, implicates the need for improved cell type marker selection. Taken together, however, these results indicate that the modified BirA\* protein we constructed is functional both under the control of a robust promoter (TDH3), as well as in the form of a fusion protein.

While BirA\* produced low levels of biotinylation as a fusion protein, it is clear that further optimization is required to achieve high levels of biotinylation that would be required for this assay to function as a reliable marker system. As attaching a protein sequence to the end of an existing gene has the potential to cause complications in terms of protein folding and expression, two alternative approaches are possible. The first option is to knockout one copy of the selected cell type specific marker with BirA\* such that all the regulatory elements of the gene of interest will control BirA\* expression. We designed constructs for this purpose with both ALS4 and PGA26 and successfully assembled the construct necessary for transformation into *C. albicans* in *S. cerevisiae*. The second option is to design fusions proteins tagged on the N-terminus, as opposed to the C-terminus. Particularly for cell surface proteins GPI anchor proteins (which both ALS4 and PGA26 are), the C-terminus is post-translationally modified with the GPI anchor to enable the protein to sit on the cell surface. Therefore tagging the N-terminus would eliminate the possibility of interfering with post-translational modifications.

Taken together, these data provide initial insight as to where GUT cells are

concentrated in the GI tract. It appears the *WOR1p* activity is highest in proximal GI compartments at early time points after infection and that GUT cells themselves form earlier in distal GI compartments. This implies a sequential process of GUT cell formation *in vivo* whereby *Wor1* is expressed first followed by GUT cell formation. Further studies are required to assess true GUT cell formation *in vivo*. The BirA\* approach, with further optimization, could be a useful tool for locating native GUT cells *in vivo*. The BirA\* method also has the potential for other applications, such as FACS sorting cells of interest either in a mixed population of pure *C. albicans* or extracting *C. albicans* cell types from host tissues.

## **METHODS**

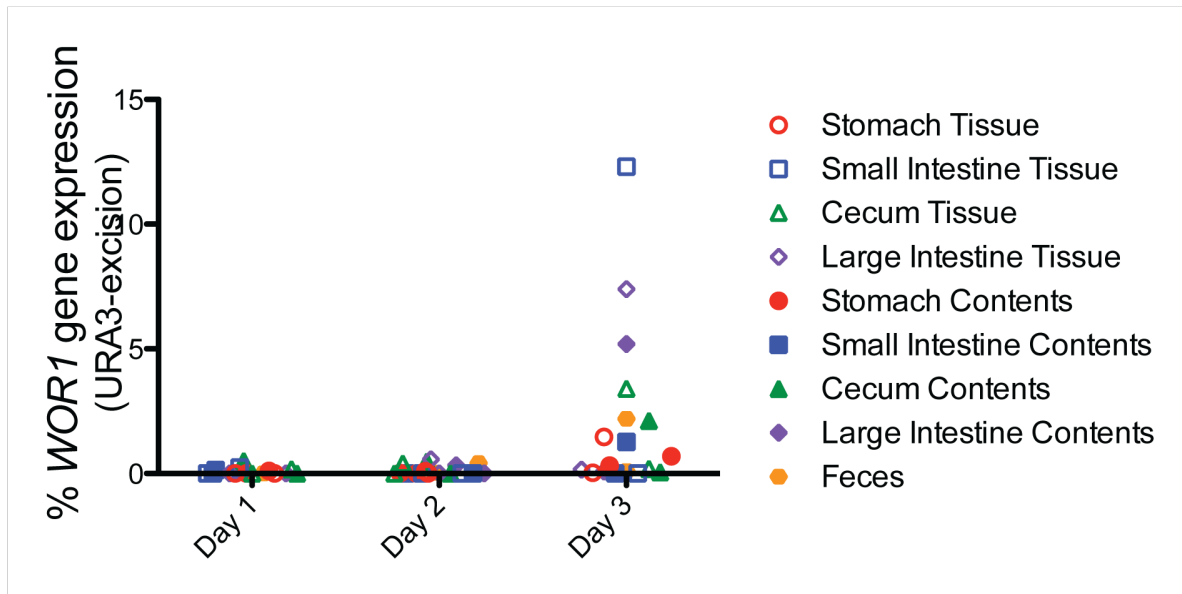
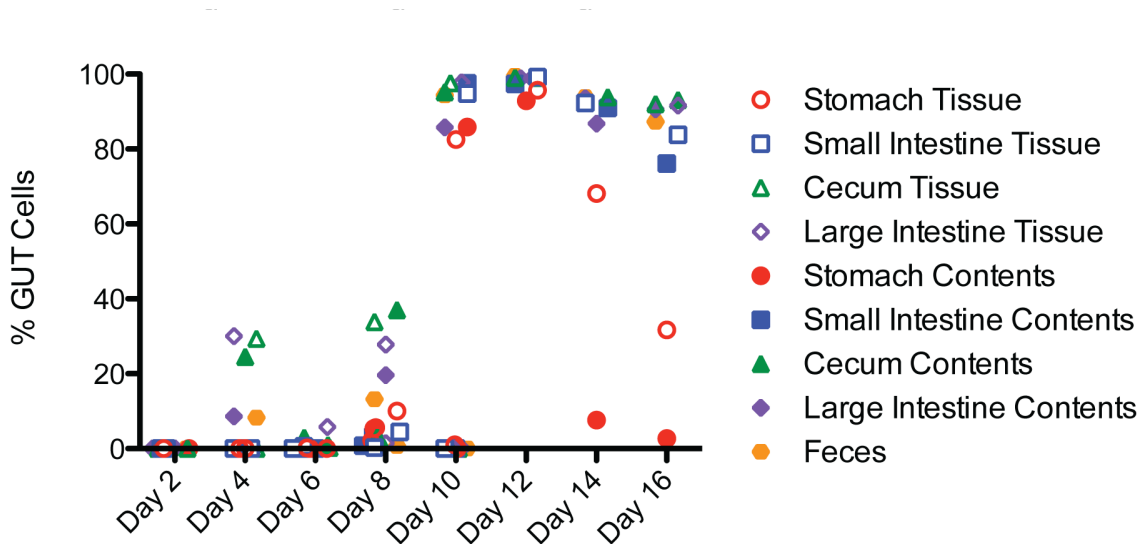
### **Mouse Infections:**

All procedures involving animals were approved by the University of California at San Francisco Institutional Animal Care and Use Committee, which enforces the ethical and humane use of animals. 6- to 8-week-old female BALB/c mice were colonized with *C. albicans* as previously described<sup>16</sup>. At the time of dissection, GI tract compartments (stomach, small intestine, cecum and large intestine) were dissected and tissues were separated from contents prior to homogenization and plating. Cells were plated onto 5-FOA media (with 25 µg/mL uridine) plates and/or Sabouraud plates containing ampicillin (50 µg/mL) and gentamicin (10 µg/mL). 5-FOA resistant colonies were verified for *Flp*-mediated recombination of the URA3 gene by PCR using primers SNO509 and SNO840. GUT cell colony morphology on Sabouraud plates was verified by microscopic examination of the cells.



**Western Blotting:**

Protein prepped the cells as previously described<sup>89</sup> and ran samples on an SDS-PAGE gel. Transferred samples to a nitrocellulose membrane according to the manufacturer's protocols (BioRad). Performed Ponceau S staining to ensure proper protein transfer. Blocked membrane with 3% milk in TBS + 0.1% Tween20 (TBST). Probed protein membrane with streptavidin-HRP (1:2000; BioLegend) overnight at 4°C and then washed in TBST 3X prior to developing with the ECL system (EMD Millipore).

**A****B**

**Figure 5.1-*Wor1p* expression and GUT cell formation appears to be sequential along the GI tract.** (a) Mice were monotypically colonized with the *WOR1*—*FLP* strain (SN1020). Two mice were sacrificed every 24 hours for 4 days. % *WOR1* gene expression refers to the ratio of 5-FOA resistant colonies to the total number of colonies from each compartment. (b) Mice were colonized with a 1:1 competition of WT (SN425) and *WOR1*<sup>OE</sup> GUT (SN1045) cells. 2 mice were sacrificed per time point up to day 10 and one mouse per time point was sacrificed thereafter. Percent GUT cells was determined by examination of colony morphology on Sabouraud plates.

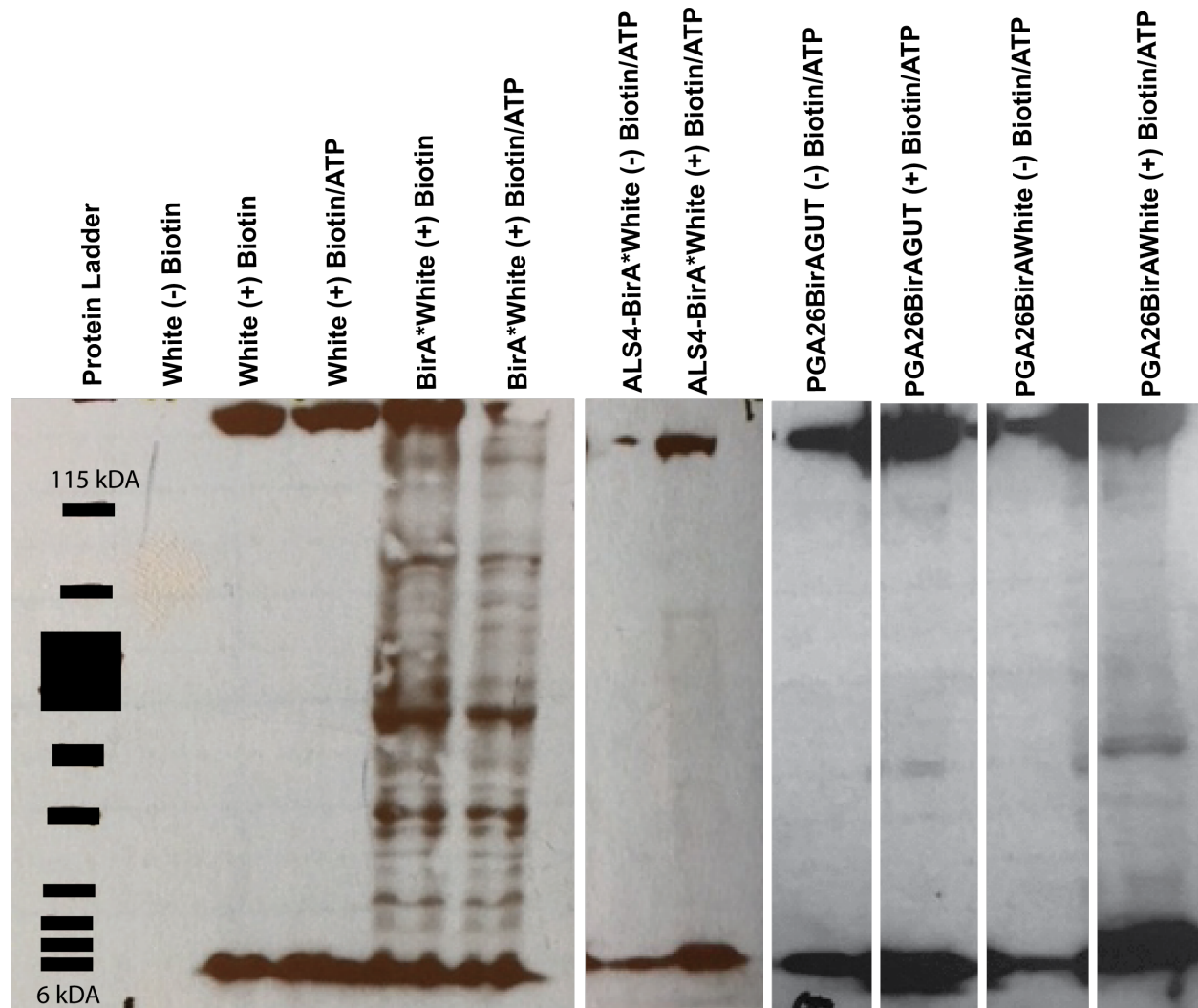


**Figure 5.2-BirA\* promiscuously biotinylates proteins in *C. albicans*** (a) Cells (SN235, SN2085-SN2089) were grown in YNB media without biotin (Sunrise Science Products) in the presence or absence of biotin (50 $\mu$ M) and ATP (a necessary co-factor for the reaction; 25 $\mu$ M) at 30°C for 24 hours. Protein samples were run on a 4-12% Tris-glycine gel. Nitrocellulose membranes were probed with 1:2000 streptavidin-HRP and developed using the ECL system. Multiple bands in the (+) biotin samples represent promiscuous biotinylation.

**Table 5.S1-Strains used in this chapter**

Strain	Common Name	Notes	Full Genotype	Reference
SN235	WT	His addback to SN152	<i>leu2Δ::C.d.HIS1Δ/leu2, his1Δ/his1Δ, arg4Δ/arg4Δ, ura3Δ/URA3, iro1/IRO1</i>	[16]
SN425	WT	Prototroph	<i>arg4Δ/arg4Δ::ST50-C.d.ARG4, leu2Δ::C.d.HIS1/leu2Δ::C.m.LEU2, his1Δ/his1Δ, ura3Δ/URA3, iro1Δ/IRO1</i>	[53]
SN1020	<i>WOR1p</i> reporter		<i>leu2Δ/leu2Δ::FRT-URA3-FRT, ura3Δ/ura3Δ, his1Δ/his1Δ, WOR1/wor1Δ::FLP-NAT</i>	[16]
SN1045	<i>WOR1<sup>OE</sup></i> GUT	Recovered from mouse GI commensal model	<i>SAT1-TDH3promWOR1/wor1::C.d.ARG4, leu2::C.m.LEU2/leu2::C.d.HIS1, ura3/URA3, his1/his1, arg4/arg4, iro1/IRO1, MTLα/MTLα</i>	[16]
SN2085	BirA Overexpression WT		<i>leu2Δ::C.d.HIS1Δ/leu2, his1Δ/his1Δ, arg4Δ/arg4Δ, ura3Δ/URA3, iro1/IRO1, TDH3promBirA*/TDH3</i>	This Work
SN2086	ALS4 dependent BirA* expression in GUT cells		<i>his1Δ/his1Δ, arg4Δ/arg4Δ, leu2Δ/ leu2Δ, URA3/ura3Δ, iro1/IRO1, wor1Δ::C.d.HIS1/SAT1- TDH3promWOR1, ALS4BirA* C.d.LEU2/ALS4</i>	This Work
SN2087	ALS4 dependent BirA* expression in white cells		<i>leu2Δ::C.d.HIS1Δ/leu2, his1Δ/his1Δ, arg4Δ/arg4Δ, ura3Δ/URA3, iro1/IRO1, ALS4BirA*C.d.LEU2/ALS4</i>	This Work
SN2088	PGA26 dependent BirA* expression in GUT cells		<i>his1Δ/his1Δ, arg4Δ/arg4Δ, leu2Δ/ leu2Δ, URA3/ura3Δ, iro1/IRO1, wor1Δ::C.d.HIS1/SAT1- TDH3promWOR1, PGA26BirA*C.d.LEU2/PGA26</i>	This Work
SN2089	PGA26 dependent BirA* expression in white cells		<i>leu2Δ::C.d.HIS1Δ/leu2, his1Δ/his1Δ, arg4Δ/arg4Δ, ura3Δ/URA3, iro1/IRO1, PGA26BirA*C.d.LEU2/PGA26</i>	This Work

## CHAPTER VI: CONCLUSIONS

*C. albicans*' status as a prominent commensal of the gastrointestinal tract in the majority of healthy humans implicates its importance in promoting human health. The studies presented here help us understand how phenotypic plasticity affects the *C. albicans* commensal lifestyle.

Principal among our findings is strong evidence that the filamentation program is detrimental to commensal colonization. While others have shown that hyphae are strongly associated with pathogenesis, what role, if any, hyphae play in commensal colonization had not been investigated. A commensal screen of ~600 *C. albicans* mutants in the GI tract revealed that mutants of filamentation specific transcription factors are hypercompetitive, suggesting that the presence of filaments is detrimental to commensal colonization. Interestingly, using a comprehensive FISH assay to visualize all compartments of the GI tract, we find that hyphae actually make up a significant portion of the colonizing population, particularly in the cecum and large intestines. To reconcile these two disparate observations, we propose a model whereby expression of hyphal specific cell surface and secreted proteins promotes active clearance of filaments from this niche, and filaments that do not expression these hyphal signals are better colonizers of the gut. The status of hyphal cell surface proteins as negative mediators of gut commensalism is further supported by observation that *ALS3* is both a strong negative regulator of GI commensalism, but also colonizes the GI tract as both yeasts and hyphae. The mechanism behind the fungal-host interactions that mediates hyphal protein directed filament clearance still remains to be determined.

In further support of the hypothesis that filaments are detrimental to

commensalism, we observe that GUT cells, which are normally hyperfit in the GI tract, seemingly lose their commensal advantage when exposed to *L. plantarum*, which elicits a pro-filamentation effect specific to GUT cells. While the mechanism behind this interaction *in vivo* is still not clear, it does appear that the effect of *L. plantarum* on GUT cells is partially dependent on lactic acid production levels. Interestingly, however, we were not able to visually observe increased filamentation of GUT cells in mice co-colonized with *C. albicans* and *L. plantarum*. To reconcile these differences *in vivo* and *in vitro*, we hypothesize that perhaps increased expression of hyphal specific proteins, as opposed to hyphal morphogenesis, may be responsible for clearing GUT cells, similar to our conclusions in Chapter II. This study provides the first example of how interactions with the *C. albicans*' GI specific commensal GUT cell and a prevalent member of the bacterial microbiome influence commensal colonization. Further studies are required to understand the mechanism behind *L. plantarum* induced GUT cell loss in the GI tract.

Finally, we began development of a unique and novel tool to visualize different phenotypic forms of *C. albicans* in *in situ*. We were able to show that a *C. albicans* optimized BirA\* protein functions robustly under the control of a constitutive promoter and has low levels of activity as a fusion protein. This method requires further optimization before it can be utilized in functional studies, but has the potential to inform how both phenotype and gene expression influence commensal niche maintenance.

Overall, the studies presented here provide novel insights into how the gastrointestinal environment influences both *C. albicans* gene expression and interactions with other microbiota to mediate commensal colonization. Understand how

this yeast maintains a commensal state could have important implications in human health by allowing scientists to promote maintenance of a commensal state to protect against pathogenic manifestations of *C. albicans*.

## REFERENCES:

1. Noble, S.M., Gianetti, B.A. & Witchley, J.N. *Candida albicans* cell-type switching and functional plasticity in the mammalian host. *Nat Rev Microbiol* **15**, 96-108 (2017).
2. Hoffmann, C. *et al.* Archaea and fungi of the human gut microbiome: correlations with diet and bacterial residents. *PLoS One* **8**, e66019 (2013).
3. Ghannoum, M.A. *et al.* Characterization of the oral fungal microbiome (mycobiome) in healthy individuals. *PLoS Pathog* **6**, e1000713 (2010).
4. Findley, K. *et al.* Topographic diversity of fungal and bacterial communities in human skin. *Nature* **498**, 367-70 (2013).
5. Merenstein, D. *et al.* Colonization by *Candida* species of the oral and vaginal mucosa in HIV-infected and noninfected women. *AIDS Res Hum Retroviruses* **29**, 30-4 (2013).
6. Pfaller, M.A. & Diekema, D.J. Epidemiology of invasive candidiasis: a persistent public health problem. *Clin Microbiol Rev* **20**, 133-63 (2007).
7. Ivanov, I.I. *et al.* Induction of intestinal Th17 cells by segmented filamentous bacteria. *Cell* **139**, 485-98 (2009).
8. Underhill, D.M. & Iliev, I.D. The mycobiota: interactions between commensal fungi and the host immune system. *Nat Rev Immunol* **14**, 405-16 (2014).
9. Hoarau, G. *et al.* Bacteriome and Mycobiome Interactions Underscore Microbial Dysbiosis in Familial Crohn's Disease. *MBio* **7**(2016).
10. Hallen-Adams, H.E. & Suhr, M.J. Fungi in the healthy human gastrointestinal tract. *Virulence* **8**, 352-358 (2017).



11. Zhang, Z. *et al.* Peripheral Lymphoid Volume Expansion and Maintenance Are Controlled by Gut Microbiota via RALDH<sup>+</sup> Dendritic Cells. *Immunity* **44**, 330-42 (2016).
12. Atarashi, K. *et al.* Th17 Cell Induction by Adhesion of Microbes to Intestinal Epithelial Cells. *Cell* **163**, 367-80 (2015).
13. Didier, E.S. Microsporidiosis: an emerging and opportunistic infection in humans and animals. *Acta Trop* **94**, 61-76 (2005).
14. Ferguson, B.A., Dreisbach, T.A., Parks, C.G., Filip, G.M. & Schmitt, C.L. Coarse-scale population structure of pathogenic *Armillaria* species in a mixed-conifer forest in the Blue Mountains of northeast Oregon. *Canadian Journal of Forest Research* **33**, 612-623 (2003).
15. Chin, V.K. *et al.* Multi-step pathogenesis and induction of local immune response by systemic *Candida albicans* infection in an intravenous challenge mouse model. *Int J Mol Sci* **15**, 14848-67 (2014).
16. Pande, K., Chen, C. & Noble, S.M. Passage through the mammalian gut triggers a phenotypic switch that promotes *Candida albicans* commensalism. *Nat Genet* **45**, 1088-91 (2013).
17. Anderson, J., Mihalik, R. & Soll, D. Ultrastructure and antigenicity of the unique cell wall pimple of the *Candida* opaque phenotype. *Journal of Bacteriology* **172**, 224-235 (1990).
18. Miller, M. & Johnson, A. White-opaque switching in *Candida albicans* is controlled by mating-type locus homeodomain proteins and allows efficient mating. *Cell* **110**, 293-302 (2002).

19. Huang, G. Regulation of phenotypic transitions in the fungal pathogen *Candida albicans*. *Virulence* **3**, 251-61 (2012).
20. Phan, Q.T. *et al.* Als3 is a *Candida albicans* invasin that binds to cadherins and induces endocytosis by host cells. *PLoS Biol* **5**, e64 (2007).
21. Carlisle, P.L. *et al.* Expression levels of a filament-specific transcriptional regulator are sufficient to determine *Candida albicans* morphology and virulence. *Proc Natl Acad Sci U S A* **106**, 599-604 (2009).
22. Nantel, A. *et al.* Transcription profiling of *Candida albicans* cells undergoing the yeast-to-hyphal transition. *Molecular Biology of the Cell* **13**, 3452-3465 (2002).
23. Moyes, D.L. *et al.* Candidalysin is a fungal peptide toxin critical for mucosal infection. *Nature* **532**, 64-8 (2016).
24. Mayer, F.L., Wilson, D. & Hube, B. *Candida albicans* pathogenicity mechanisms. *Virulence* **4**, 119-28 (2013).
25. White, S.J. *et al.* Self-regulation of *Candida albicans* population size during GI colonization. *PLoS Pathog* **3**, e184 (2007).
26. Vautier, S. *et al.* *Candida albicans* colonization and dissemination from the murine gastrointestinal tract: the influence of morphology and Th17 immunity. *Cell Microbiol* **17**, 445-50 (2015).
27. Rosenbach, A., Dignard, D., Pierce, J.V., Whiteway, M. & Kumamoto, C.A. Adaptations of *Candida albicans* for growth in the mammalian intestinal tract. *Eukaryot Cell* **9**, 1075-86 (2010).
28. Perlroth, J., Choi, B. & Spellberg, B. Nosocomial fungal infections: epidemiology, diagnosis, and treatment. *Medical Mycology* **45**, 321-346 (2007).

29. Wiesner, S.M., Jechorek, R.P., Garni, R.M., Bendel, C.M. & Wells, C.L. Gastrointestinal colonization by *Candida albicans* mutant strains in antibiotic-treated mice. *Clin Diagn Lab Immunol* **8**, 192-5 (2001).
30. Fan, D. *et al.* Activation of HIF-1alpha and LL-37 by commensal bacteria inhibits *Candida albicans* colonization. *Nat Med* **21**, 808-14 (2015).
31. Mason, K.L. *et al.* Interplay between the gastric bacterial microbiota and *Candida albicans* during postantibiotic recolonization and gastritis. *Infect Immun* **80**, 150-8 (2012).
32. Allison, D.L. *et al.* *Candida*-Bacteria Interactions: Their Impact on Human Disease. *Microbiol Spectr* **4**(2016).
33. Trunk, K. *et al.* The type VI secretion system deploys antifungal effectors against microbial competitors. *Nat Microbiol* **3**, 920-931 (2018).
34. Hogan, D. & Kolter, R. *Pseudomonas*-*Candida* interactions: an ecological role for virulence factors. *Science* **296**, 2229-2232 (2002).
35. Boon, C. *et al.* A novel DSF-like signal from *Burkholderia cenocepacia* interferes with *Candida albicans* morphological transition. *ISME J* **2**, 27-36 (2008).
36. Vilchez, R. *et al.* *Streptococcus mutans* inhibits *Candida albicans* hyphal formation by the fatty acid signaling molecule trans-2-decenoic acid (SDSF). *Chembiochem* **11**, 1552-62 (2010).
37. Bongomin, F., Gago, S., Oladele, R.O. & Denning, D.W. Global and Multi-National Prevalence of Fungal Diseases-Estimate Precision. *J Fungi (Basel)* **3**(2017).

38. Brown, G.D. *et al.* Hidden Killers: Human Fungal Infections. *Medical Mycology* **4**, 165rv113 (2012).
39. Odds, F.C. *et al.* *Candida albicans* strain maintenance, replacement, and microvariation demonstrated by multilocus sequence typing. *J Clin Microbiol* **44**, 3647-58 (2006).
40. Carlisle, P.L. & Kadosh, D. A genome-wide transcriptional analysis of morphology determination in *Candida albicans*. *Molecular Biology of the Cell* **24**, 246-260 (2012).
41. Kadosh, D. & Johnson, A. Induction of *Candida albicans* filamentous growth program by relief of transcriptional repression: a genome-wide analysis. *Molecular Biology of the Cell* **16**, 2903-2912 (2012).
42. Lane, S., Birse, C., Zhou, S., Matson, R. & Liu, H. DNA array studies demonstrate convergent regulation of virulence factors by Cph1, Cph2, and Efg1 in *Candida albicans*. *J Biol Chem* **276**, 48988-96 (2001).
43. Lu, Y., Su, C., Solis, N.V., Filler, S.G. & Liu, H. Synergistic regulation of hyphal elongation by hypoxia, CO(2), and nutrient conditions controls the virulence of *Candida albicans*. *Cell Host Microbe* **14**, 499-509 (2013).
44. Zheng, L., Kelly, C.J. & Colgan, S.P. Physiologic hypoxia and oxygen homeostasis in the healthy intestine. A Review in the Theme: Cellular Responses to Hypoxia. *Am J Physiol Cell Physiol* **309**, C350-60 (2015).
45. Kalantar-Zadeh, K. *et al.* A human pilot trial of ingestible electronic capsules capable of sensing different gases in the gut. *Nature Electronics* **1**, 79-87 (2018).

46. Tailford, L.E., Crost, E.H., Kavanaugh, D. & Juge, N. Mucin glycan foraging in the human gut microbiome. *Front Genet* **6**, 81 (2015).
47. Perez, J.C., Kumamoto, C.A. & Johnson, A.D. *Candida albicans* commensalism and pathogenicity are intertwined traits directed by a tightly knit transcriptional regulatory circuit. *PLoS Biol* **11**, e1001510 (2013).
48. Gabrielli, E. *et al.* In vivo induction of neutrophil chemotaxis by secretory aspartyl proteinases of *Candida albicans*. *Virulence* **7**, 819-25 (2016).
49. Gabrielli, E. *et al.* Induction of caspase-11 by aspartyl proteinases of *Candida albicans* and implication in promoting inflammatory response. *Infect Immun* **83**, 1940-8 (2015).
50. Pietrella, D. *et al.* Secreted aspartic proteases of *Candida albicans* activate the NLRP3 inflammasome. *Eur J Immunol* **43**, 679-92 (2013).
51. Pietrella, D. *et al.* The Inflammatory response induced by aspartic proteases of *Candida albicans* is independent of proteolytic activity. *Infect Immun* **78**, 4754-62 (2010).
52. Homann, O.R., Dea, J., Noble, S.M. & Johnson, A.D. A phenotypic profile of the *Candida albicans* regulatory network. *PLoS Genet* **5**, e1000783 (2009).
53. Noble, S.M., French, S., Kohn, L.A., Chen, V. & Johnson, A.D. Systematic screens of a *Candida albicans* homozygous deletion library decouple morphogenetic switching and pathogenicity. *Nat Genet* **42**, 590-8 (2010).
54. Pierce, J.V., Dignard, D., Whiteway, M. & Kumamoto, C.A. Normal Adaptation of *Candida albicans* to the murine gastrointestinal tract requires Efg1p-dependent regulation of metabolic and host defense genes. *Eukaryot Cell* **12**, 37-49 (2013).

55. Pierce, J.V. & Kumamoto, C.A. Variation in *Candida albicans* EFG1 expression enables host-dependent changes in colonizing fungal populations. *MBio* **3**, e00117-12 (2012).
56. Braun, B. & Johnson, A. TUP1, CPH1 and EFG1 make independent contributions to filamentation in *Candida albicans*. *Genetics* **155**, 57-67 (2000).
57. Lo, H. *et al.* Nonfilamentous *C. albicans* mutants are avirulent. *Cell* **90**, 939-949 (1995).
58. Nobile, C.J. *et al.* A recently evolved transcriptional network controls biofilm development in *Candida albicans*. *Cell* **148**, 126-38 (2012).
59. Du, H. *et al.* Roles of *Candida albicans* Gat2, a GATA-type zinc finger transcription factor, in biofilm formation, filamentous growth and virulence. *PLoS One* **7**, e29707 (2012).
60. Schweizer, A., Rupp, S., Taylor, B., Rollinghoff, M. & Schroppel, K. The TEA/ATTS transcription factor CaTec1p regulates hyphal development and virulence in *Candida albicans*. *Molecular Microbiology* **38**, 435-445 (2000).
61. Lassak, T. *et al.* Target specificity of the *Candida albicans* Efg1 regulator. *Mol Microbiol* **82**, 602-18 (2011).
62. Leng, P., Lee, P.R., Wu, H. & Brown, A.J. Efg1, a morphogenetic regulator in *Candida albicans*, is a sequence-specific DNA binding protein. *J Bacteriol* **183**, 4090-3 (2001).
63. Nobile, C.J. & Mitchell, A.P. Regulation of cell-surface genes and biofilm formation by the *C. albicans* transcription factor Bcr1p. *Curr Biol* **15**, 1150-5 (2005).

64. Banerjee, M. *et al.* UME6, a novel filament-specific regulator of *Candida albicans* hyphal extension and virulence. *Molecular Biology of the Cell* **19**, 1354-1365 (2008).
65. Earle, K.A. *et al.* Quantitative Imaging of Gut Microbiota Spatial Organization. *Cell Host Microbe* **18**, 478-88 (2015).
66. Johansson, M.E. & Hansson, G.C. Preservation of mucus in histological sections, immunostaining of mucins in fixed tissue, and localization of bacteria with FISH. *Methods Mol Biol* **842**, 229-35 (2012).
67. Bohm, L. *et al.* The yeast form of the fungus *Candida albicans* promotes persistence in the gut of gnotobiotic mice. *PLoS Pathog* **13**, e1006699 (2017).
68. Xu, W. *et al.* Activation and alliance of regulatory pathways in *C. albicans* during mammalian infection. *PLoS Biol* **13**, e1002076 (2015).
69. Woolford, C.A. *et al.* Bypass of *Candida albicans* Filamentation/Biofilm Regulators through Diminished Expression of Protein Kinase Cak1. *PLoS Genet* **12**, e1006487 (2016).
70. De Bernardis, F., Muhlschlegel, F., Cassone, A. & Fonzi, W. The pH of host niche controls gene expression in and virulence of *Candida albicans*. *Infection and Immunity* **66**, 3317-3325 (1998).
71. Azadmanesh, J., Gowen, A.M., Creger, P.E., Schafer, N.D. & Blankenship, J.R. Filamentation Involves Two Overlapping, but Distinct, Programs of Filamentation in the Pathogenic Fungus *Candida albicans*. *G3 (Bethesda)* **7**, 3797-3808 (2017).

72. Jackson, B.E., Wilhelmus, K.R. & Hube, B. The role of secreted aspartyl proteinases in *Candida albicans* keratitis. *Invest Ophthalmol Vis Sci* **48**, 3559-65 (2007).
73. Bailey, D., Feldmann, P., Bovey, M., Gow, N. & Brown, A. The *Candida albicans* HYR1 gene, which is activated in response to hyphal development, belongs to a gene family encoding yeast cell wall proteins. *Journal of Bacteriology* **178**, 5353-5360 (1996).
74. Chen, Y., Wu, C., Chung, W. & Lee, F. Differential secretion of Sap4-6 proteins in *Candida albicans* during hyphae formation. *Microbiology* **148**, 3743-3754 (2002).
75. Davis, D., Wilson, B. & Mitchell, A.P. Rim101-dependent and -independent pathways govern pH responses in *Candida albicans*. *Molecular and Cellular Biology* **20**, 971-978 (2000).
76. Gomez-Raja, J. & Davis, D.A. The beta-arrestin-like protein Rim8 is hyperphosphorylated and complexes with Rim21 and Rim101 to promote adaptation to neutral-alkaline pH. *Eukaryot Cell* **11**, 683-93 (2012).
77. Li, M., Martin, S., Bruno, V.M., Mitchell, A.P. & Davis, D. *Candida albicans* Rim13p, a protease required for Rim101p processing at acidic and alkaline pHs. *Eukaryotic Cell* **3**, 741-751 (2004).
78. Wolf, J.M., Johnson, D.J., Chmielewski, D. & Davis, D.A. The *Candida albicans* ESCRT pathway makes Rim101-dependent and -independent contributions to pathogenesis. *Eukaryot Cell* **9**, 1203-15 (2010).



79. Xu, X.L. *et al.* Bacterial peptidoglycan triggers *Candida albicans* hyphal growth by directly activating the adenylyl cyclase Cyr1p. *Cell Host Microbe* **4**, 28-39 (2008).
80. Bockmuhl, D., Krishnamurthy, S., Gerads, M., Sonnenburn, A. & Ernst, J.F. Distinct and redundant roles of the two protein kinase A isoforms Tpk1p and Tpk2p in morphogenesis and growth of *Candida albicans*. *Molecular Microbiology* **42**, 1243-1257 (2001).
81. Castilla, R., Passeron, S. & Cantore, M. N-acetyl-D-Glucosamine induces germination in *Candida albicans* through a mechanism sensitive to inhibitors of cAMP-dependent protein kinase. *Cell Signaling* **10**, 713-719 (1998).
82. Klengel, T. *et al.* Fungal adenylyl cyclase integrates CO<sub>2</sub> sensing with cAMP signaling and virulence. *Curr Biol* **15**, 2021-6 (2005).
83. Leberer, E. *et al.* Ras links cellular morphogenesis to virulence by regulation of the MAP kinase and cAMP signalling pathways in the pathogenic fungus *Candida albicans*. *Molecular Microbiology* **42**, 673-687 (2001).
84. Rocha, C. *et al.* Signaling through adenylyl cyclase is essential for hyphal growth and virulence in the pathogenic fungus *Candida albicans*. *Molecular Biology of the Cell* **12**, 3631-3643 (2001).
85. Childers, D.S., Mundodi, V., Banerjee, M. & Kadosh, D. A 5' UTR-mediated translational efficiency mechanism inhibits the *Candida albicans* morphological transition. *Mol Microbiol* **92**, 570-85 (2014).
86. Tso, G. *et al.* Experimental evolution of a fungal pathogen into a gut symbiont. *Science* **362**, 589-595 (2018).

87. Naglik, J., Albrecht, A., Bader, O. & Hube, B. *Candida albicans* proteinases and host/pathogen interactions. *Cell Microbiol* **6**, 915-26 (2004).
88. Parra-Ortega, B., Cruz-Torres, H., Villa-Tanaca, L. & Hernandez-Rodriguez, C. Phylogeny and evolution of the aspartyl protease family from clinically relevant *Candida* species. *Mem Inst Oswaldo Cruz* **104**, 505-512 (2009).
89. Chen, C., Pande, K., French, S.D., Tuch, B.B. & Noble, S.M. An iron homeostasis regulatory circuit with reciprocal roles in *Candida albicans* commensalism and pathogenesis. *Cell Host Microbe* **10**, 118-35 (2011).
90. Langmead, B., Trapnell, C., Pop, M. & Salzberg, S. Ultrafast and memory-efficient alignment of short DNA sequences to the human genome. *Genome Biology* **10**, R25 (2009).
91. Noble, S.M. & Johnson, A.D. Strains and strategies for large-scale gene deletion studies of the diploid human fungal pathogen *Candida albicans*. *Eukaryot Cell* **4**, 298-309 (2005).
92. Carette, J.E. *et al.* Global gene disruption in human cells to assign genes to phenotypes by deep sequencing. *Nat Biotechnol* **29**, 542-6 (2011).
93. Rohland, N. & Reich, D. Cost-effective, high-throughput DNA sequencing libraries for multiplexed target capture. *Genome Res* **22**, 939-46 (2012).
94. Schindelin, J. *et al.* Fiji: an open-source platform for biological-image analysis. *Nat Methods* **9**, 676-82 (2012).
95. Skrzypek, M.S. *et al.* The *Candida* Genome Database (CGD): incorporation of Assembly 22, systematic identifiers and visualization of high throughput sequencing data. *Nucleic Acids Res* **45**, D592-D596 (2017).

96. Turnbaugh, P. *et al.* The effect of diet on the human gut microbiome: a metagenomic analysis in humanized gnotobiotic mice. *Science Translational Medicine* **1**, 6ra14 (2009).
97. Bray, N.L., Pimentel, H., Melsted, P. & Pachter, L. Near-optimal probabilistic RNA-seq quantification. *Nat Biotechnol* **34**, 525-7 (2016).
98. Ritchie, M.E. *et al.* limma powers differential expression analyses for RNA-sequencing and microarray studies. *Nucleic Acids Res* **43**, e47 (2015).
99. Banerjee, M. *et al.* Expression of UME6, a key regulator of *Candida albicans* hyphal development, enhances biofilm formation via Hgc1- and Sun41-dependent mechanisms. *Eukaryot Cell* **12**, 224-232 (2013).
100. Zeidler, U. *et al.* UME6 is a crucial downstream target of other transcriptional regulators of true hyphal development in *Candida albicans*. *FEMS Yeast Res* **9**, 126-42 (2009).
101. Childers, D.S. & Kadosh, D. Filament condition-specific response elements control the expression of NRG1 and UME6, key transcriptional regulators of morphology and virulence in *Candida albicans*. *PLoS One* **10**, e0122775 (2015).
102. Sardi, J.C., Scorzoni, L., Bernardi, T., Fusco-Almeida, A.M. & Mendes Giannini, M.J. *Candida* species: current epidemiology, pathogenicity, biofilm formation, natural antifungal products and new therapeutic options. *J Med Microbiol* **62**, 10-24 (2013).
103. Nash, A.K. *et al.* The gut mycobiome of the Human Microbiome Project healthy cohort. *Microbiome* **5**, 153 (2017).

104. Miranda, L.N. *et al.* Candida colonisation as a source for candidaemia. *J Hosp Infect* **72**, 9-16 (2009).
105. Limon, J.J., Skalski, J.H. & Underhill, D.M. Commensal Fungi in Health and Disease. *Cell Host Microbe* **22**, 156-165 (2017).
106. Koh, A.Y. Murine models of Candida gastrointestinal colonization and dissemination. *Eukaryot Cell* **12**, 1416-22 (2013).
107. Sam, Q.H., Chang, M.W. & Chai, L.Y. The Fungal Mycobiome and Its Interaction with Gut Bacteria in the Host. *Int J Mol Sci* **18**(2017).
108. Manzoni, P. *et al.* Oral Supplementation with Lactobacillus casei subspecies rhamnosus prevents enteric colonization by Candida species in preterm neonates: a randomized study. *Clinical Infectious Diseases* **42**, 1735-1742 (2006).
109. Hatakka, K. *et al.* Probiotics reduce the prevalence of oral Candida in the elderly- a randomized controlled trial. *Journal of Dental Research* **86**, 125-130 (2007).
110. Hillman, E.T., Lu, H., Yao, T. & Nakatsu, C.H. Microbial Ecology along the Gastrointestinal Tract. *Microbes Environ* **32**, 300-313 (2017).
111. Heeney, D.D., Gareau, M.G. & Marco, M.L. Intestinal Lactobacillus in health and disease, a driver or just along for the ride? *Curr Opin Biotechnol* **49**, 140-147 (2018).
112. Gu, S. *et al.* Bacterial community mapping of the mouse gastrointestinal tract. *PLoS One* **8**, e74957 (2013).

113. Allonsius, C.N. *et al.* Interplay between *Lactobacillus rhamnosus* GG and *Candida* and the involvement of exopolysaccharides. *Microb Biotechnol* **10**, 1753-1763 (2017).
114. Rossoni, R.D. *et al.* Antifungal activity of clinical *Lactobacillus* strains against *Candida albicans* biofilms: identification of potential probiotic candidates to prevent oral candidiasis. *Biofouling* **34**, 212-225 (2018).
115. Payne, S. *et al.* In vitro studies on colonization resistance of the human gut microbiota to *Candida albicans* and the effects of tetracycline and *Lactobacillus plantarum* LPK. *Current Issues Intestinal Microbiology* **4**, 1-8 (2003).
116. Shankar, J. *et al.* Using Bayesian modelling to investigate factors governing antibiotic-induced *Candida albicans* colonization of the GI tract. *Sci Rep* **5**, 8131 (2015).
117. Pepoyan, A. *et al.* Probiotic *Lactobacillus acidophilus* Strain INMIA 9602 Er 317/402 Administration Reduces the Numbers of *Candida albicans* and Abundance of Enterobacteria in the Gut Microbiota of Familial Mediterranean Fever Patients. *Front Immunol* **9**, 1426 (2018).
118. Vila, T. *et al.* Targeting *Candida albicans* filamentation for antifungal drug development. *Virulence* **8**, 150-158 (2017).
119. Liang, W. *et al.* Lactic acid bacteria differentially regulate filamentation in two heritable cell types of the human fungal pathogen *Candida albicans*. *Mol Microbiol* **102**, 506-519 (2016).

120. Trejo-Hernandez, A., Andrade-Dominguez, A., Hernandez, M. & Encarnacion, S. Interspecies competition triggers virulence and mutability in *Candida albicans*-*Pseudomonas aeruginosa* mixed biofilms. *ISME J* **8**, 1974-88 (2014).
121. Tachedjian, G., Aldunate, M., Bradshaw, C.S. & Cone, R.A. The role of lactic acid production by probiotic *Lactobacillus* species in vaginal health. *Res Microbiol* **168**, 782-792 (2017).
122. Mayeur, C. *et al.* Faecal D/L lactate ratio is a metabolic signature of microbiota imbalance in patients with short bowel syndrome. *PLoS One* **8**, e54335 (2013).
123. Morales, D.K. *et al.* Control of *Candida albicans* metabolism and biofilm formation by *Pseudomonas aeruginosa* phenazines. *MBio* **4**, e00526-12 (2013).
124. Hogan, D.A., Vik, A. & Kolter, R. A *Pseudomonas aeruginosa* quorum-sensing molecule influences *Candida albicans* morphology. *Mol Microbiol* **54**, 1212-23 (2004).
125. Cruz, M.R., Graham, C.E., Gagliano, B.C., Lorenz, M.C. & Garsin, D.A. *Enterococcus faecalis* inhibits hyphal morphogenesis and virulence of *Candida albicans*. *Infect Immun* **81**, 189-200 (2013).
126. Demuyser, L., Jabra-Rizk, M.A. & Van Dijck, P. Microbial cell surface proteins and secreted metabolites involved in multispecies biofilms. *Pathog Dis* **70**, 219-30 (2014).
127. Nobile, C.J., Nett, J.E., Andes, D.R. & Mitchell, A.P. Function of *Candida albicans* adhesin Hwp1 in biofilm formation. *Eukaryot Cell* **5**, 1604-10 (2006).
128. Nobile, C.J. *et al.* Critical role of Bcr1-dependent adhesins in *C. albicans* biofilm formation in vitro and in vivo. *PLoS Pathog* **2**, e63 (2006).

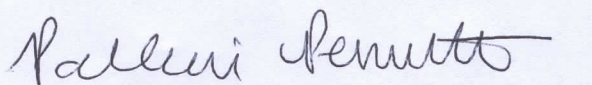
129. Lee, S.M. *et al.* Bacterial colonization factors control specificity and stability of the gut microbiota. *Nature* **501**, 426-9 (2013).
130. Sigal, M. *et al.* Helicobacter pylori Activates and Expands Lgr5(+) Stem Cells Through Direct Colonization of the Gastric Glands. *Gastroenterology* **148**, 1392-404 e21 (2015).
131. Roux, K.J., Kim, D.I., Raida, M. & Burke, B. A promiscuous biotin ligase fusion protein identifies proximal and interacting proteins in mammalian cells. *J Cell Biol* **196**, 801-10 (2012).
132. Chen, A.L. *et al.* Novel components of the Toxoplasma inner membrane complex revealed by Bioid. *MBio* **6**, e02357-14 (2015).

**Publishing Agreement**

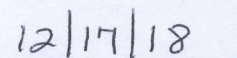
*It is the policy of the University to encourage the distribution of all theses, dissertations, and manuscripts. Copies of all UCSF theses, dissertations, and manuscripts will be routed to the library via the Graduate Division. The library will make all theses, dissertations, and manuscripts accessible to the public and will preserve these to the best of their abilities, in perpetuity.*

**Please sign the following statement:**

*I hereby grant permission to the Graduate Division of the University of California, San Francisco to release copies of my thesis, dissertation, or manuscript to the Campus Library to provide access and preservation, in whole or in part, in perpetuity.*



Author Signature



Date